Optimization of a cold-transfer system

Upperman, J.M.

Award date:
1986

OPTIMIZATION
OF A
COLD-TRANSFER SYSTEM

J.M. UPPERMAN

dec. 1985

De uitwerking van een
AFSTUDEEROPDRACHT,
van sept. 1984 tot okt. 1985 uitgevoerd bij
PHILIPS I&E (Industrial and Electro-acoustical Systems Division),
CRYOGENIC DEPARTMENT

TH EINDHOVEN,
AFDELING DER TECHNISCHE NATUURKUNDE,
VAKGROEP VASTE STOF,
SUBGROEP KRYOGENE TECHNIEKEN

Afstudeerbegeleider: dr. A.Th.A.M. de Waele
Afstudeerhoogleraar: dr. H.M. Gijsman

Woord vooraf

Philips I&E Ontwikkeling Koudetechniek heeft een jaar achter de rug dat vele malen turbulenter was dan de gasstroming in het te optimaliseren koude-transportsysteem. De verhuizing van Eindhoven naar Acht en de begeleiding van nieuw aangetrokken personeel vergden nogal wat van de "oudgedienden". Daarom hecht ik eraan mijn waardering uit te spreken voor de wijze waarop men mij in de groep ontvangen heeft en terzijde heeft gestaan, ook al kon niet voorkomen worden dat de drukte enige sporen naliet op de voortgang van mijn afstudeerwerk.

Ir. G. Huijgen en ing. E. Slot wil ik danken voor het in mij gestelde vertrouwen en voor de vrijheid die ik kreeg om verschillende benodigdheden te bestellen. Samen met dhr. P. van den Berk en ing. L. Hamers maakte ing. A. Castelijns me wegwijs in het koude-transportgebeuren. Verder heeft hij, samen met dhr. H. Sleumer van het Constructiebureau, een belangrijk aandeel gehad in de totstandkoming van de nieuwe meetunit. De meetopstellingen werden grotendeels gerealiseerd door de heren R. Hendriks en W. Roelofs. Evenals de heren B. de Beijer, A. Duisters en A. Slenders hebben ze mij, door hun praktische inzicht en hun goede humeur in drukke tijden, zeer veel geleerd. De afdeling Logistiek heeft, in de persoon van de heren C. van den Berk en J. Wagemakers, de bestellingen met zorg afgewikkeld, terwijl secretaresse mej. E. Louwers par.4.1.2 en hoofdstuk 5 van het verslag uittypte en me inwijdde in de geheimen van haar tekstverwerker.

Op de T.H. ontving ik waardevolle hulp van dhr. L. Penders bij het opstarten van een digitale teller en kon ik altijd terecht bij mijn afstudeerbegeleider dr. A. de Waele. Laatstgenoemde heeft door zijn suggesties mijn aandacht meerdere keren gericht op essentiële eigenschappen van het te optimaliseren koude-transportsysteem. Ook ben ik hem erkentelijk voor de nauwgezette wijze waarop hij mijn afstudeerverslag corrigeerde, ondanks het feit dat dit als een feuilleton met vele afleveringen tot hem kwam.

Terugblikkend is mijn laatste T.H.-studiejaar niet gemakkelijk, maar wel boeiend en leerzaam geweest. Mede door de inzet van bovengenoemde personen heb ik mijn afstudeerfase met plezier en voldoening kunnen beëindigen.

Veldhoven 1985 J.M.U.

Contents

1. SYMBOLS

symbol	quantity	SI-unit
A	area	m^2
B	blade height	m
c	specific heat	J/(kg K)
D	diameter	m
e	2.71828...	-
F	circulation factor	-
g	acceleration of free fall = 9.81	m/s^2
h	specific enthalpy	J/kg
H	stage height	m
ΔH	pressure head	m
k	curvature	m^{-4}
K	constant	
l,L	length	m
m	mass	kg
$\dot{m}$	mass flow rate	kg/s
M	molar mass	kg/mol
n	number of layers	-
N	number of bends	-
Nu	Nusselt's number	-
p	1. pressure	$Pa=10^{-5}bar$
	2. average circuit pressure	Pa
P	power	W
$\dot{Q}$	heat flow rate	W
r	radius	m
R	1. Rydberg's universal gas constant = 8.314	J/(mol K)
	2. resistance	Ω
Re	Reynold's number	-
S	wall thickness	m
t	time	s
Δt	cool-down time	s
T	1. temperature	K
	2. gas temperature	K

symbol	quantity	SI-unit
u	1. rotation speed	m/s
	2. impeller tip speed	m/s
v	absolute gas velocity	m/s
V	volume	m^3
$\dot{V}$	volume flow rate	m^3/s
w	relative gas velocity	m/s
x	distance	m
z	number of blades	-
α (alfa)	heat transfer coefficient	$W/(m^2K)$
β (bèta)	blade angle	-
Δ (delta)	difference	
ζ (zèta)	resistance coefficient	-
η (èta)	1. dynamic viscosity	Pa s
	2. efficiency	%
ϑ (thèta)	rotation angle	-
λ (lambda)	thermal conductivity	W/(m K)
λ'	friction factor	-
λ_p	power coefficient	-
Λ (lambda)	heat transfer number	-
ν (nu)	rotation frequency	Hz
ξ (xi)	dimensionless distance	-
π (pi)	3.14159...	-
ρ (rho)	density	kg/m^3
σ (sigma)	1. Boltzmann's constant = $5.67\ 10^{-8}$	$W/(m^2K^4)$
	2. maximum stress	N/m^2
τ (tau)	dimensionless temperature	-
φ (fi)	volume coefficient	-
ψ (psi)	pressure coefficient	-

index	meaning
a	application
b	beginning
c	1.coil
	2.cylinder
ch	characteristic
ci	circulation
con	conduction
e	end
f	1.fan
	2.impeller
h	fenolhardpaper
he	heat exchanger
i	in
m	1.meridional or radial
	2.molar
max	maximum
myl	mylar
o	1.out
	2.outer
opt	optimal
p	at constant pressure
r	radiative
s	1.shield
	2.stage
sh	shaft
sp	specific
st	static
t	1.transfer line
	2.tube circuit
tl	transfer line
th	theoretical
u	tangential
w	tube wall
1	1.impeller: inlet
	2.circulation: fan behind the stage
2	1.impeller: outlet
	2.circulation: fan in front of the stage
20	20K-circuit
70	70K-circuit
∞	infinite number of blades

2. SUMMARY

The cold-transfer system, developed at the Philips Research Laboratories between 1960 and 1970, consists of two separate circuits through each of which helium gas is circulated by a centrifugal fan. In addition, both circuits contain two helium transfer lines and two heat exchangers.
In order to optimize the circuits, their behaviour has been described by a set of 23 equations, which was solved numerically. In cooperation with Philips I&E (Industrial & Electro-acoustic Systems Division) Development Cryogenics a measuring unit has been designed and built, with which the behaviour of the circuits can be analysed experimentally.
The most important changes, proposed to optimize the transfer system, are an increase of the heat exchanger diameters, a fan impeller with curved blades instead of straight ones, a spirally shaped fan casing instead of a circular one, a reduction of the impeller rotation frequency, a separation of the helium gas pressure inside the transfer system into two different circuit pressures and an enlargement of these pressures.
It is expected that these changes will lead to a significant increase of the cooling power at the application site. Their effect will have to be investigated by future experiments.

3. INTRODUCTION

In low-temperature technology it is often desirable to separate the site, where a certain cooling power is needed, from the cold source or cooling machine. In these cases a cold-transfer system is necessary.
At the Philips Research Laboratories a cold-transfer system has been developed, which consists of two separate circuits. According to their mean temperature during normal operation, they are called the 20K-circuit and the 70K-circuit. Each transports cold from a cooling machine over a distance of usually 7 m towards the place where the cold is needed. Presently the transfer system is used by Philips Medical Systems in order to cool the shields around a superconducting magnet. This magnet is used to achieve nuclear magnetic resonance, a phenomenon by which it is possible to scan tissues inside the human body.
Calculations on the transfer system have been carried out by Mulder (MUL67) and Peters (PET83). The latter calculated the cool-down time of the magnet mentioned above by using mean volume flows. Mulder, who designed the system, presented calculations on the 20K-circuit. In his design he maximized the cooling power at the end of the transfer system at a fixed temperature of the object to be cooled.
Mulder's approach was rather rough and did not include the 70K-circuit, while both authors based their calculations on the behaviour of the presently used fans and neglected cold losses over the transfer lines. In order to optimize the transfer system (including the fans), it was therefore necessary to carry out new calculations. Mass flows were used instead of mean volume flows, and the temperature of the object to be cooled was minimized at a fixed value of the cooling power.
When reading this report, the following points should be noted.
1. In the text references have been labeled by codes of the form (LLLFF) where the L's are letters and the F's figures. Via these codes the references can be looked up in chapter 9. Equations are referred to by codes of the form (N-N) where the N's are numbers. The first number indicates the chapter where the equation can be found.
2. Some of the equations contain constants that are not dimensionless. Unless stated otherwise, all quantities should then be expressed in SI-units.
3. In this report the gas velocity and the gas temperature inside the cold-transfer system are defined as the mean velocity and the mean temperature across the area, perpendicular to the direction of the flow.

The cold-transfer system, which will be analysed in this chapter, conveys cold from a cold source over a certain distance to one or more objects to be cooled. From now on the cold recipients will be referred to as "the application". In our case the cold source is a Philips A20 cryogenerator,a two-stage cooling machine based on the Stirling cycle (see Fig.4.1).

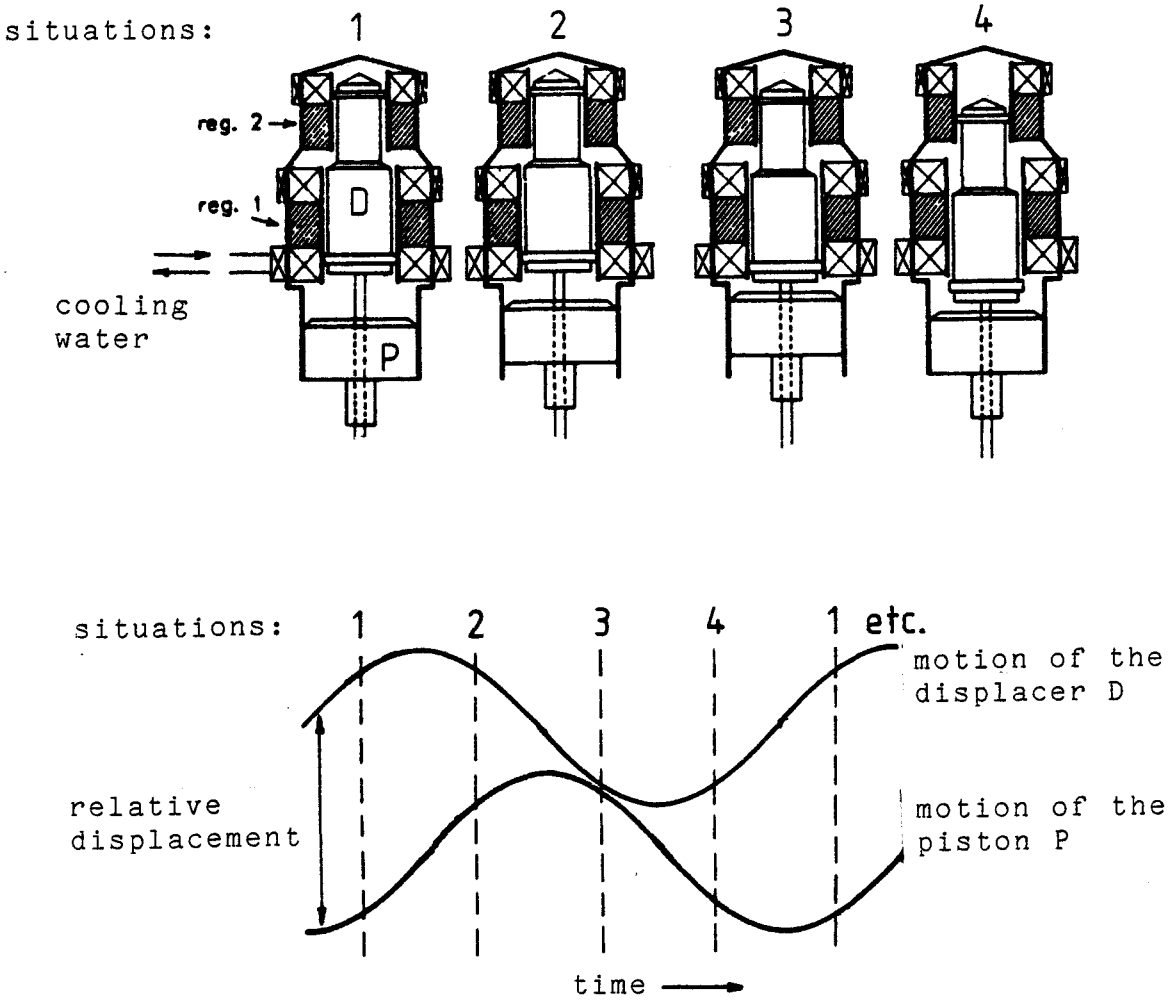

Fig.4.1 Schematic cross-sectional view of the head of the Philips A20 cryogenerator. Within an ideal Stirling cycle four changes of state can be distinguished: 1->2 isothermal compression, 2->3 isochoric cooling, 3->4 isothermal expansion and 4->1 isochoric warming. In reality these processes are gradually changing into each other by the harmonic oscillations of the displacer and the piston, the phase difference between the two being 90 degrees. The regenerators are heat reservoirs. Helium is used as working gas.

The A20 cryogenerator produces cold on two levels: the 70K-stage (first or middle stage) and the 20K-stage (second or end stage). The cold production of each stage ($\dot{Q}_{s20}$,$\dot{Q}_{s70}$) varies with the stage temperatures T_{s20} and T_{s70} as shown in Fig.4.2.

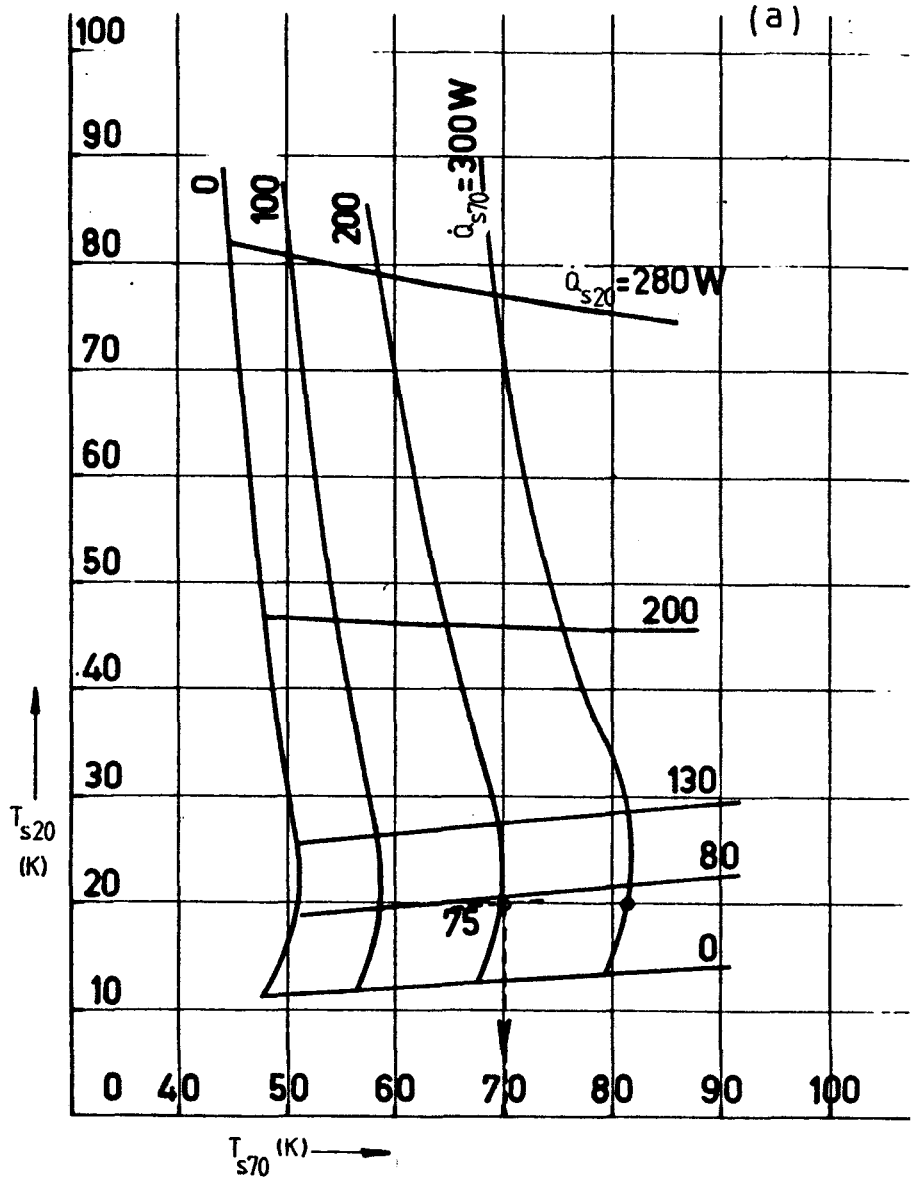

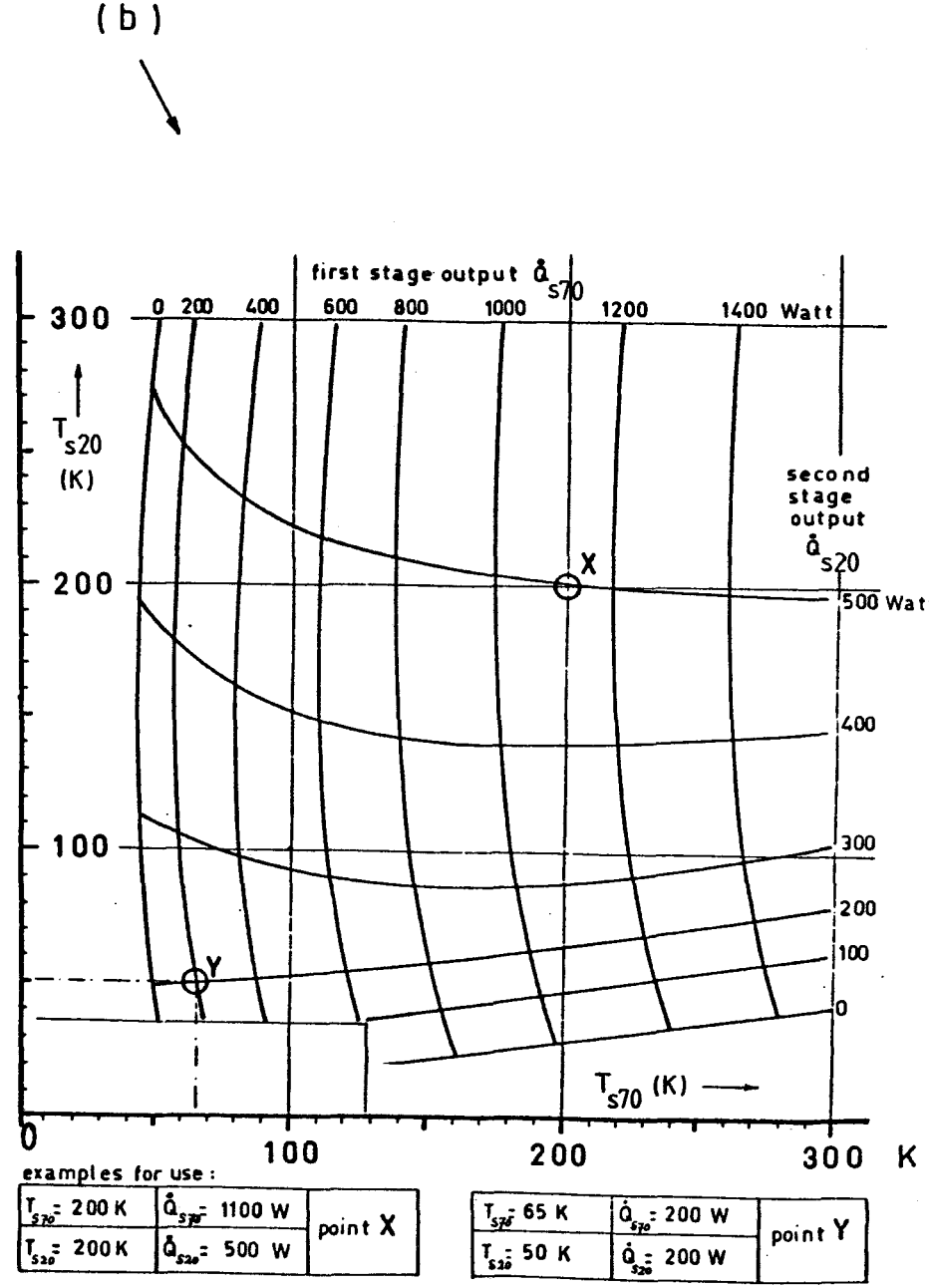

Fig.4.2 Cooling power field of the Philips A20 cryogenerator.
(a) stage temperatures below 100K
(b) stage temperatures up to 300K

The two stages owe their names to the usual working-point of the machine which lies near T_{s20}=20K and T_{s70}=70K (see Fig.4.2(a)). Note the following aspects of the cooling power field:

1. T_{s70} can be lower then T_{s20}
2. T_{s70} decreases when $\dot{Q}_{s20}$ is increased from 100 W to 300 W while $\dot{Q}_{s70}$ has a fixed value
3. T_{s20} decreases when $\dot{Q}_{s70}$ is increased from 0 W to 800 W while $\dot{Q}_{s20}$ has a fixed value higher than 200 W
4. If the two stages behaved independently, the lines of constant $\dot{Q}_{s20}$ and of constant $\dot{Q}_{s70}$ would run parallel to the T_{s70}- and the T_{s20}-axis respectively.

4.1 The cold-transfer system and its components

In order to transport cold from the A20 cryogenerator to the application, a cold-transfer system has been developed at the Philips Research Laboratories (MUL67). It consists of two separate tube systems which contain helium-gas with a pressure of ca. 25 bar.

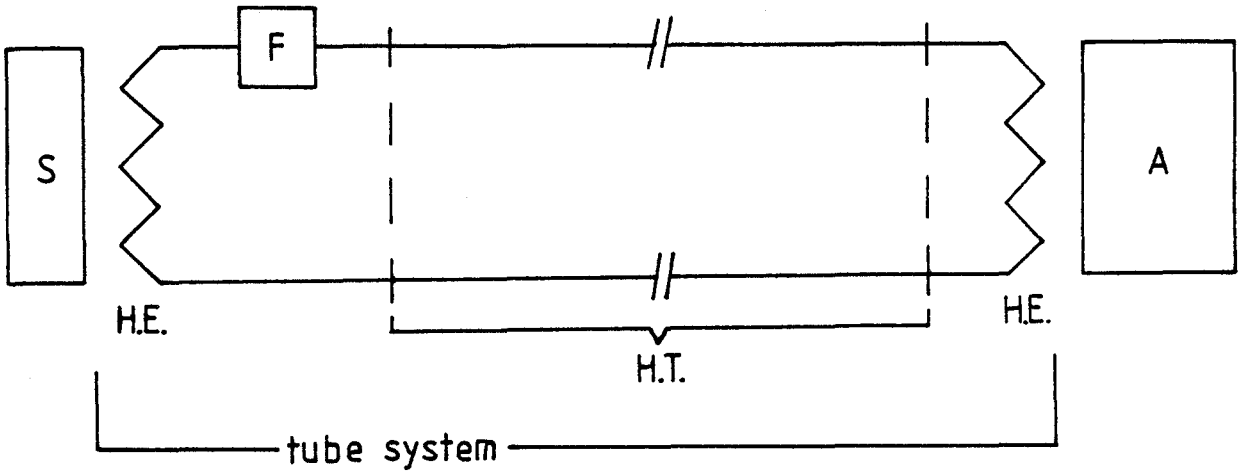

Fig.4.3 Tube system with which cold can be transferred from a stage S of the A20 cryogenerator to the application A. It is filled with He-gas and consists of one centrifugal fan F, two heat exchangers H.E. and two helium transfer lines H.T.

Each tube system forms a closed loop in which a centrifugal fan has been incorporated. This fan circulates the helium-gas through the loop. The gas is cooled by a heat exchanger around a stage of the A20 cryogenerator and is transported towards the application through a helium transfer line with a length of usually 7 m. The gas then absorbs heat from the application while flowing through another heat exchanger, after which it is transported back towards the A20 cryogenerator through a second helium transfer line (see Fig.4.4).

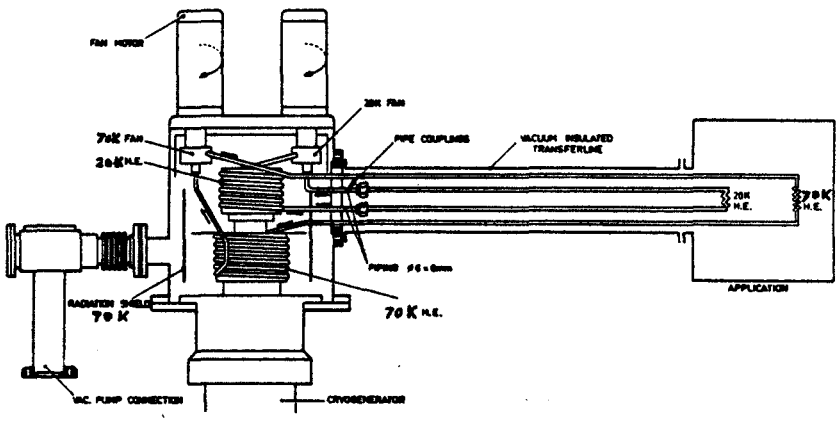

Fig.4.4 Cold-transfer system in connection with the A20 cryogenerator

In the next four paragraphs we will have a closer look at He-gas as a cold-transfer medium and at each component of the cold-transfer system.

4.1.1 Helium gas as a cold-transfer medium

The medium which acts as a heat- or cold-carrier between cooling machine and application is helium gas with a pressure between 20 bar and 30 bar. Helium follows the ideal-gas law in good approximation, even if the pressure p=30 bar and the temperature T=20 K:

$$p\ V_m = R\ T \qquad (4\text{-}1)$$

in which V_m stands for the molar volume (m^3/mol) and R for Rydberg's universal gas constant: R=8.314 J/(mol K). We will use the ideal-gas law mostly in the form

$$\varrho = M/V_m = Mp/RT: \qquad (4\text{-}2)$$

$M=4.003\ 10^{-3}$ kg/mol, which is the molar mass of He and ϱ is its density. Deviations from real values of ϱ are shown in Table 4.1.
In the kinetic theory of gases it is shown that the specific heat capacity at constant pressure

$$c_p = (\partial h/\partial T)_p \quad \text{where h is the specific enthalpy} \qquad (4\text{-}3)$$

becomes for an ideal monoatomic gas

$$c_p = dh/dT = (5/2)\ (R/M) \qquad (4\text{-}4)$$

which in the case of helium is equal to 5192 J/(kg K). The difference with real values of c_p is shown in Table 4.1.

T (K)	20		70		150		300	
p (atm)	20	30	20	30	20	30	20	30
$\varrho_{i.g.}$ (kg/m^3)	48.79	73.18	13.94	20.91	6.505	9.757	3.252	4.879
ϱ_{real} (kg/m^3)	48.40	69.44	13.42	19.77	6.378	9.470	3.221	4.808
$(\varrho_{i.g.}-\varrho_{real})/\varrho_{real}$ (%)	+0.81	+5.4	+3.9	+5.8	+2.0	+3.0	+1.0	+1.5
$c_{p,i.g.}$ (J/kg K)	5192	5192	5192	5192	5192	5192	5192	5192
$c_{p,real}$ (J/kg K)	6044	6088	5268	5301	5204	5210	5194	5194
$(c_{p,i.g.}-c_{p,real})/c_{p,real}$ (%)	-14	-15	-1.4	-2.1	-0.23	-0.35	-0.04	-0.04

Table 4.1 ϱ and c_p of He: ideal-gas values (i.g.) in comparison with real values

For describing the viscosity η of He-gas as a function of temperature and pressure there exist several expressions.
Conte (CON70) gives for T between 4K and 1100K

$$\eta = 5.02\ 10^{-7}\ T^{0.647}. \qquad (4\text{-}5)$$

Peters (PET83) writes

$$\eta = 5\ 10^{-7}\ T^{0.65} + 6.8\ 10^{-7}\ p/T \qquad (4\text{-}6)$$

with p in bar, T in K and η in Pa.s. However, the pressure dependent term can be neglected in our calculations.
Fitting experimental data given in appendix 10.1 with p=25atm and T between 20K and 300K, we find

$$\eta = 8.3\ 10^{-7}\ T^{0.55} \qquad (4\text{-}7)$$

which is accurate within 5%.

The last property to which we will pay attention in this paragraph is the thermal conductivity λ. It varies with temperature (and pressure) in nearly the same way as η. Applying the same fitting procedure as for η we find

$$\lambda = 6.4\ 10^{-3}\ T^{0.55} \qquad (4\text{-}8)$$

which is accurate within 7%.

T-S-diagrams and further details on thermophysical properties of He are presented in appendix 10.1.

4.1.2 The centrifugal fan

As mentioned in paragraph 4.1.1, the helium gas is in each tube system circulated by means of a centrifugal fan. Such a fan consists at the moment of a twelve-bladed impeller running in a cylindrical casing. Helium gas enters the centre of the impeller in an axial direction and is discharged at the periphery, the impeller rotation being towards the casing outlet (Fig.4.5).

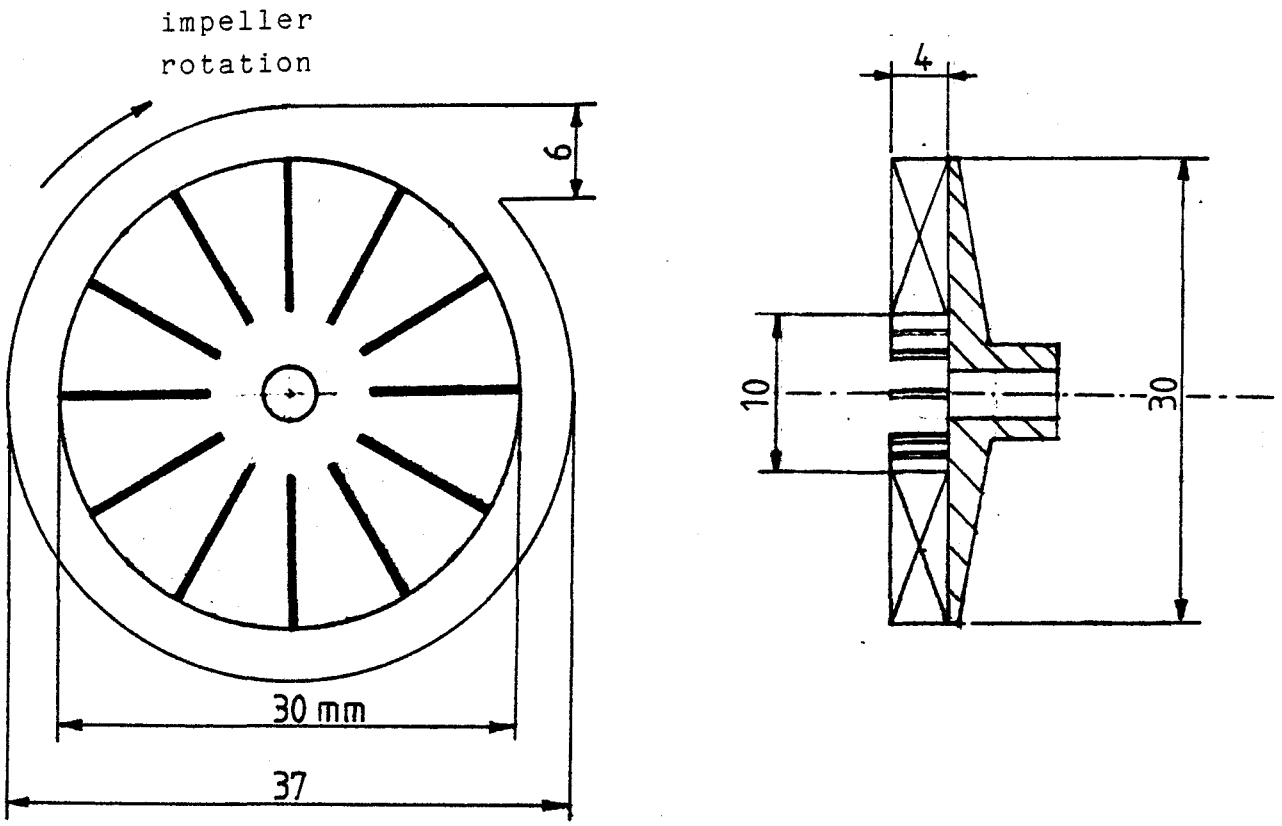

Fig.4.5 (a) Impeller together with casing and outlet
(b) Cross-sectional view of impeller

The fan characteristics are usually presented in a ΔH_f - $\dot{V}$ - diagram. The static pressure head ΔH_f is related to the static pressure difference Δp_f over the fan by

$$\Delta H_f = \Delta p_f / (\rho\, g). \qquad (4\text{-}9)$$

A gas column with height ΔH_f in the field of gravity would exert a static pressure $\Delta p_f = \rho \cdot g \cdot \Delta H_f$ on its base. ΔH_f is expressed in meters and is independent of the helium gas density ρ (see Fig.4.6).

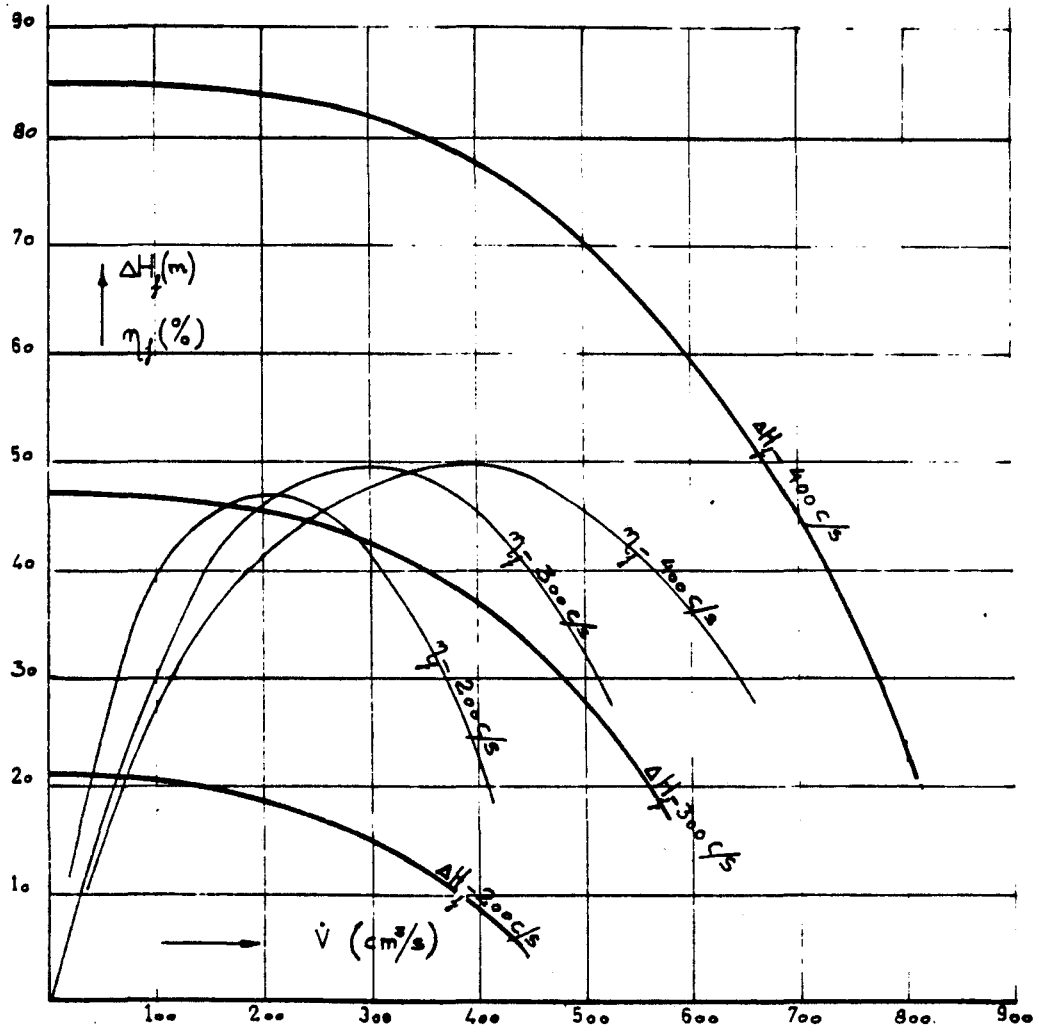

Fig. 4.6 Fan characteristics of the centrifugal fan as measured by Mulder (MUL 67).
The static pressure head ΔH_f and the fan efficiency η_f are given as functions of the volume flow $\dot{V}$ and the rotation frequency of the impeller ν.

The characteristics may be described roughly by parabolas:

$$\Delta H_f = \Delta H_{max} \, (1-(\dot{V}/\dot{V}_{max})^2) \qquad (4\text{-}10)$$

where ΔH_{max} is the maximum pressure head (obtained at $\dot{V}=0$) and $\dot{V}_{max}$ the maximum volume flow (obtained at $\Delta H_f=0$).
For all centrifugal fans may be written

$$\Delta H_{max} = \Delta p_{max}/\varrho g = \text{constant } \varrho u^2/\varrho g = \text{constant } u^2/g \qquad (4\text{-}11)$$

where the constant is the same for geometrically similar fans and has a value between 0.5 and 0.7 , and where u is equal to the tip speed of the impeller:

$$u = \pi D_f \nu . \tag{4-12}$$

D_f and ν are the impeller diameter and the rotation frequency respectively. According to Osborne (OSB77) $\dot{V}_{max}$ is proportional to u and the "impeller area" $(\pi/4)D_f^2$, yielding

$$\dot{V}_{max} = \text{constant } D_f^3 \nu \tag{4-13}$$

for geometrically similar fans.
In our case the fan diameter D_f= 30 mm
(see Fig. 4.5). It follows from Fig. 4.6 that

$$\Delta H_{max} = 0.58 \pi^2 D_f^2 \nu^2/g \tag{4-11a}$$

and

$$\dot{V}_{max} = 0.084 \quad D_f^3 \nu . \tag{4-13a}$$

In Fig. 4.6 is also shown the fan efficiency η_f, which is equal to the amount of work exerted on the gas P_f, divided by the mechanical shaft power P_{sh}:

$$\eta_f = P_f/P_{sh} \tag{4-14}$$

where

$$P_f = \int_{\text{fan inlet}}^{\text{fan outlet}} \dot{V} \, dp. \tag{4-15}$$

The maximum fan efficiency of centrifugal fans lies usually between 50% and 80%: Fig. 4.6 shows a maximum efficiency of 50%. The difference

$$P_{sh} - P_f = (1-\eta_f) P_{sh} \tag{4-16}$$

is due to friction losses occurring along the impeller blades and the fan casing, and is supplied to the gas as heat.

As shown in Fig. 4.4, the impellers are driven by fan motors which are placed on top of the head of the A20. At the moment these are a.c. (alternating current)-motors. They are in normal operation when connected to a 50Hz three phase supply with 220V between the phases, yielding a maximum power of 21W at a rotation frequency of 2600 cycles/minute ≈ 43 Hz. However, before mounting the motors on the A20, they are "upgraded" in order to operate them via a frequency converter at 18000 cycles/minute=300 Hz, being the present rotation frequency of the impellers.

Each impeller is fixed to a shaft of stainless steel (length $L_{sh} \approx 60$ mm, mean diameter $D_{sh} \approx 4$ mm) of which the end leaving the motor is at room temperature, while the other end assumes the temperature of the gas passing through the impeller (see Fig. 4.7).

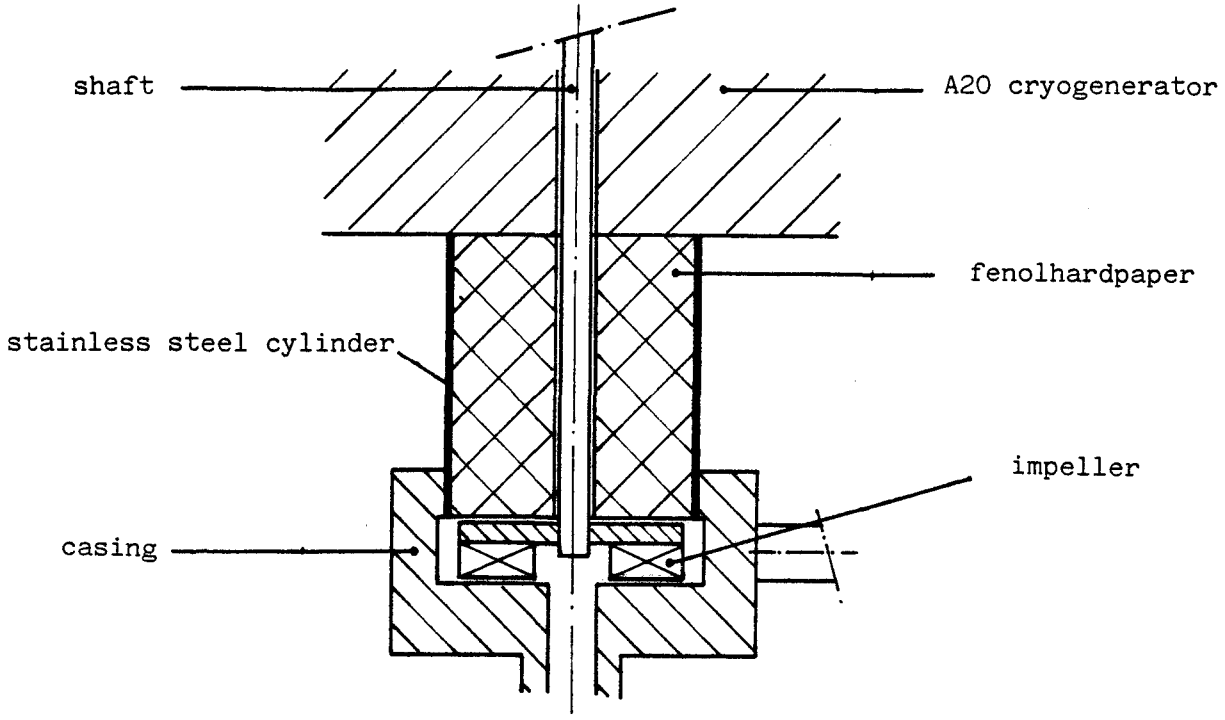

Fig. 4.7 The way in which the impeller and its casing are connected to the fan motor and the head of the A20 (scale 1 to 1)

The impeller casing is fixed to the head of the A20 by means of a thin-walled cylinder of stainless steel, of which the temperature decreases from room temperature to impeller temperature over a length $L_c \approx 33$ mm. It has an inner diameter which is somewhat larger than the impeller diameter $D_f = 30$ mm, so that one can remove the impeller from its casing without having to disconnect it from the shaft. The cylinder wall has a thickness $S_c = 0.3$ mm.
The He-gas spreads itself from the impeller casing upward around the fan motor. In order to prevent cold losses by convection the space between the shaft and the thin-walled cylinder is filled with fenolhardpaper which at room temperature has a thermal conductivity $\lambda_h \approx 0.3$ W/m.K (FAS70).
The cold loss by conduction in the 20K-fan $\dot{Q}_{f,con20}$ can be estimated from the data given above by

$$\dot{Q}_{f,con20} = (\dot{Q}_{sh} + \dot{Q}_c + \dot{Q}_h)_{20} = (1/L_{sh}) \left(\tfrac{\pi}{4} D_{sh}^2\right) \int_{20K}^{300K} \lambda_s \, dT$$

$$+ (1/L_c) \left(\tfrac{\pi}{4}(D_f + 2S_c)^2 - \tfrac{\pi}{4} D_f^2\right) \int_{20K}^{300K} \lambda_s \, dT$$

$$+ (1/L_c) \left(\tfrac{\pi}{4} D_f^2 - \tfrac{\pi}{4} D_{sh}^2\right) \int_{20K}^{300K} \lambda_h \, dT =$$

$$= 0.6 \text{ W} + 2.6 \text{ W} + 1.8 \text{ W} = 5.0 \text{ W}, \qquad (4\text{-}17)$$

where $\dot{Q}_{sh}, \dot{Q}_c$ and $\dot{Q}_h$ are the heat flows through the shaft, the cylinder and the hardpaper respectively.
(See appendix 10.2 for thermal conductivity integrals of stainless steel.)

For the 70K-fan we find accordingly

$$\dot{Q}_{f,con70} = (\dot{Q}_{sh} + \dot{Q}_c + \dot{Q}_h)_{70} =$$
$$= 0.6\ W + 2.4\ W + 1.5\ W = 4.5\ W, \qquad (4\text{-}18)$$

which shows that the thin-walled cylinder is the main cause of cold loss by conduction.
The fans are normally operating at ν = 300Hz, $\dot{V}$ = 200cm^3/s and ΔH_f= 45m (see Fig.4.6), while p = 25bar. The static pressure differences Δp_{f20} and Δp_{f70} across the 20K- and the 70K-fan respectively can therefore be estimated from (4-9) and (4-2):

$$\Delta p_f = (Mp/RT)\ g\ \Delta H_f, \qquad (4\text{-}19)$$

yielding Δp_{f20}=2.7 10^4 Pa =270 mbar and Δp_{f70}=7.6 10^3 Pa =76 mbar.
Because in both cases Δp_f is small in comparison with the average transfer system pressure of 25 bar, (4-15) may be rewritten as

$$P_f = \dot{V}\ \Delta p_f, \qquad (4\text{-}20)$$

giving P_{f20}=5.4 W and P_{f70}=1.5 W. With η_f=46% (see Fig.4.6) we find via (4-14) the shaft powers P_{sh}. When passing through a fan the gas receives per second an energy of

$$\begin{aligned} (\dot{Q}_{f,con} + P_{sh})_{20} &= 5.0\ W + 11.7\ W \approx 17\ W \\ (\dot{Q}_{f,con} + P_{sh})_{70} &= 4.5\ W + \ 3.3\ W \approx \ 8\ W. \end{aligned} \qquad (4\text{-}21)$$

We will now pass on to the calculation of the temperature difference between inlet and outlet of each fan. According to the first law of thermodynamics for an open system, the increase of the specific enthalpy Δh_f across a fan is given by

$$\dot{m}\ \Delta h_f = \dot{Q}_{f,con} + P_{sh}, \qquad (4\text{-}22)$$

where the mass flow

$$\dot{m} = \rho\dot{V} = (Mp/RT)\ \dot{V} \qquad (4\text{-}23)$$

with $\dot{m}_{20}$=12 10^{-3} kg/s and $\dot{m}_{70}$=3.4 10^{-3} kg/s. From (4-21) to (4-23) it follows that

$$\Delta h_{f20} = 1.6\ 10^3\ J/kg \text{ and } \Delta h_{f70} = 2.6\ 10^3\ J/kg. \qquad (4\text{-}24)$$

By writing

$$\Delta h = (\partial h/\partial T)_p \, \Delta T + (\partial h/\partial p)_T \, \Delta p \qquad (4\text{-}25)$$

we may compare the terms

$$(\partial h/\partial p)_{20K} \, \Delta p_{f20} = -4.1 \; 10^{-2} \text{ J/kg}$$
$$\text{and} \qquad (\partial h/\partial p)_{70K} \, \Delta p_{f70} = 1.5 \; 10^{-2} \text{ J/kg} \qquad (4\text{-}26)$$

with (4-24). They can clearly be ignored (again showing that the ideal gas approximation for He is valid), so that for all enthalpy calculations on the transfer system we may write

$$dh = (\partial h/\partial T)_p \, dT = c_p \, dT. \qquad (4\text{-}27)$$

With c_p(25 bar,20 K)=6,0 10^3 J/(kg K) and
c_p(25 bar,70 K)=5.2 10^3 J/(kg K) it follows from (4-24) and (4-27) that the temperature differences across the fans are

$$\Delta T_{f20} = 0.3 \text{ K and } \Delta T_{f70} = 0.5 \text{ K}. \qquad (4\text{-}28)$$

These results justify, together with (4-19), the change from (4-15) to (4-20). When flowing through the impeller the gas may indeed be considered as having a constant density.

4.1.3 The heat exchangers

The cold transfer system contains a 20K and a 70K tube system. Each tube system possesses two heat exchangers consisting of coiled copper tubes. One is wrapped around a stage of the cooling machine and the other around (a part of) the application (see Fig.4.3). The heat exchangers around the two stages are shown in Fig.4.8.

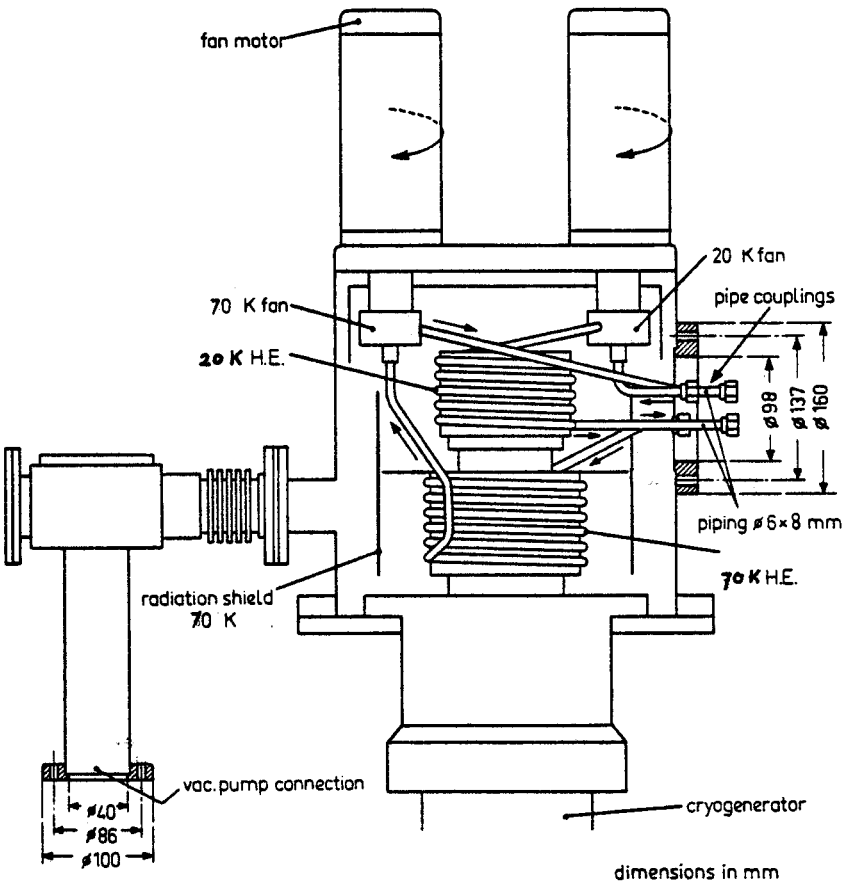

Fig.4.8 The heat exchangers inside the A20 cryogenerator in connection with the stages and the centrifugal fans.

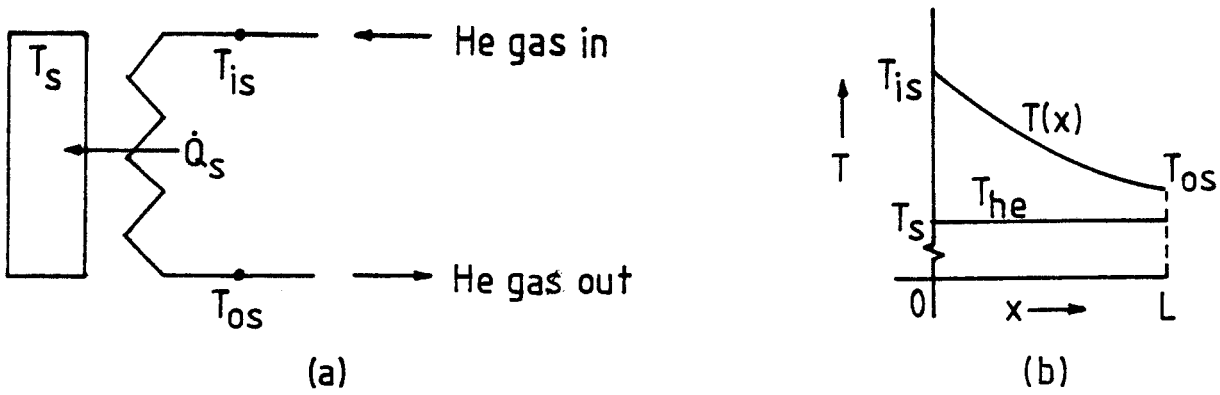

Fig.4.9 (a)Heat flow $\dot{Q}_s$ from the helium gas inside a heat exchanger to a stage of the cooling machine. The temperature of the He gas decreases from T_{is} at the stage inlet to T_{os} at the stage outlet.
(b)T-x-diagram: x is the distance over which the gas has traveled in the heat exchanger, L is the length of the heat exchanger, T_{he} is the temperature of the heat exchanger which is equal to the stage temperature T_s and T(x) is the gas temperature.

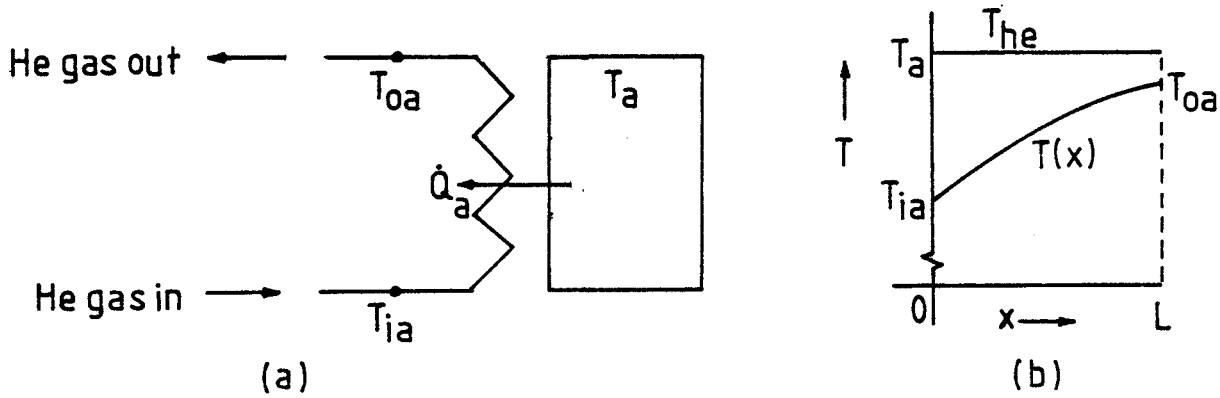

Fig.4.10 (a)Heat flow $\dot{Q}_a$ from (a part of) the application to the helium gas inside a heat exchanger. The temperature of the gas increases from T_{ia} at the application inlet to T_{oa} at the application outlet.
(b)T-x-diagram: see Fig.4.9(b). The temperature of the heat exchanger T_{he} is equal to the application temperature T_a.

In the stationary state the mass flow $\dot{m}$ has the same value everywhere in the tube system:

$$\dot{m} = \text{constant}. \tag{4-29}$$

The first law of thermodynamics becomes for the gas inside a heat exchanger

$$d\dot{Q} = \dot{m}\, dh \tag{4-30}$$

as kinetic and potential energy differences are neglegable. The infinitesimal heat flow $d\dot{Q}$ takes place over a part dx of the heat exchanger length. Together with (4-27) we find

$$d\dot{Q} = \dot{m}\, c_p\, dT. \qquad (4\text{-}31)$$

Assume that a small volume of the gas has moved a distance x along a heat exchanger with length L, inner diameter D and temperature T_{he} and that it has a temperature T(x). The heat flow $d\dot{Q}$ at position x is caused by the temperature difference $(T_{he} - T(x))$ and flows through the ring-shaped surface π D dx. We write

$$d\dot{Q} = \alpha\, (T_{he} - T(x))\, \pi\, D\, dx \qquad (4\text{-}32)$$

where α is the heat transfer coefficient. In appendix 10.3 it is shown that it is weakly temperature dependent ($\alpha = 11.4\ T(x)^{0.11}\ m^{0.8}/D^{1.8}$) and, combining (4-31) and (4-32), that

$$\frac{T(x)-T_{he}}{T_i-T_{he}} = e^{-\Lambda x/L} \qquad (4\text{-}33)$$

where T_i is the temperature of the gas entering the heat exchanger (see Fig. 4.9(b) and Fig.4.10(b)). The heat transfer number Λ characterises the quality of the heat exchanger and is given by

$$\Lambda = \frac{\alpha\, \pi DL}{\dot{m} c_p} = \frac{11.4\ \pi}{c_p}\ \frac{T_{he}^{0.11}\ L}{\dot{m}^{0.2}\ D^{0.8}} \qquad . \qquad (4\text{-}34)$$

Λ is a dimensionless parameter. In deriving (4-34) it is assumed that T_{he} is homogeneous.
The inner diameters of the heat exchangers of the cooling machine both are D=6mm, while their lengths are L_{20}=1.9m and L_{70}=1.7m respectively. Using (4-23) and taking c_p(25bar,20K)=6.0 kJ/(kg K) and c_p(25bar,70K)=5.2 kJ/(kg K) their heat transfer numbers can be evaluated:

$$\Lambda_{s20} = 2.3 \text{ and } \Lambda_{s70} = 3.5. \qquad (4\text{-}35)$$

According to (4-33), the temperature difference between the gas and the heat exchanger at the outlet is related to the difference at the inlet by

$$\frac{T_o-T_{he}}{T_i-T_{he}} = e^{-\Lambda}, \qquad (4\text{-}36)$$

which is 0.10 for the 20K stage and 0.030 for the 70K stage.
When gas is flowing turbulently through a heat exchanger with coil diameter D_c (20K stage: D_c=0.10 m, 70K stage: D_c=0.12 m) the static pressure drop dp in a distance dx is given by

$$dp = \lambda'(Re)\,\frac{1}{2}\rho v^2\,(1+3.74\,\frac{D}{D_c})\,\frac{dx}{D}$$

$$= \frac{16}{\pi^2}\,\lambda'(Re)\,\frac{dx}{D^5}\,(1+3.74\,\frac{D}{D_c})\,\frac{1}{2}\rho\dot{V}^2, \qquad (4\text{-}37)$$

where λ' is the friction factor (see Fig.4.11) and the average flow velocity $v = \dot{V}/(\frac{\pi}{4}D^2)$.

(k is the dimension of the inegalities on the tube wall)

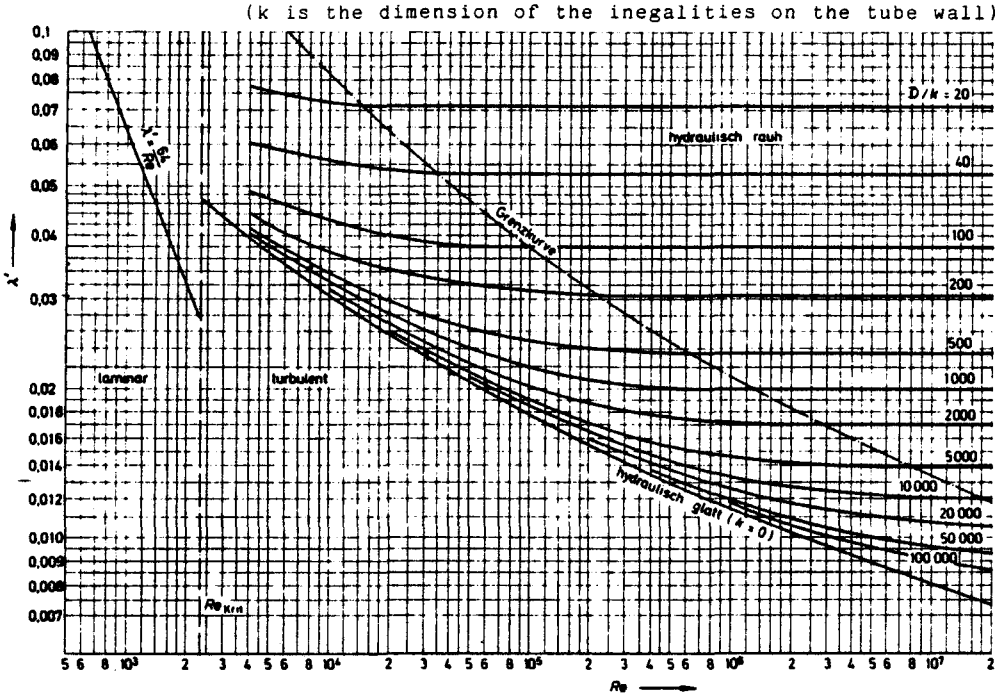

Fig.4.11 Friction factor for tube flow as a function of Reynold's number Re (BOH71)

Reynold's number Re is defined by

$$Re := \rho v D/\eta = \rho\dot{V}D/(\eta\,\frac{\pi}{4}D^2) = \frac{4}{\pi}\,\dot{m}/(\eta D) \qquad (4\text{-}38)$$

From (4-7),(4-23) and D=6 mm, Re can be calculated for the heat exchangers around the stages:

$$Re_{s20} = 5.9\ 10^5 \quad \text{and} \quad Re_{s70} = 8.4\ 10^4. \qquad (4\text{-}39)$$

These values are both well above Re=2300 so that the He-flow inside the heat exchangers is turbulent. Regarding the heat exchangers as smooth tubes, their friction factor may be written as

$$\lambda'(Re) = 0.32\ Re^{-0.25}. \qquad (4\text{-}40)$$

which is known as Blasius' equation for turbulent tube flow (see Fig.4.11).

4.1.4 The helium transfer lines

The four helium transfer lines which run between the cryogenerator and the application are bellows with a length L of 7m and an inner diameter D of 12.7 mm. Because of their corrugated surface they must be regarded as rough tubes (see Fig.4.12).

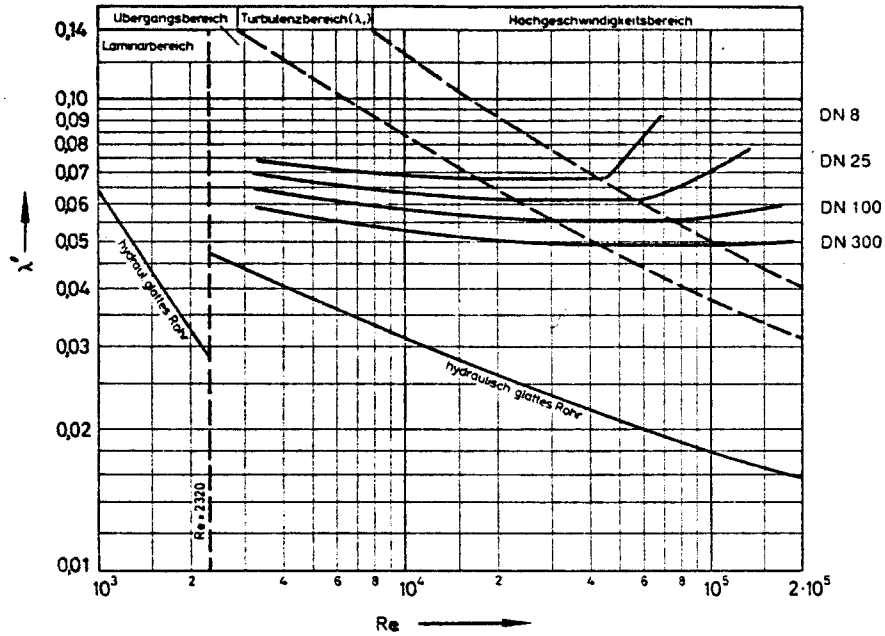

Fig.4.12 Friction factor λ' for several bellows as a function of Reynold's number Re. A helium transfer line has type number DN12: its characteristic falls in between DN8 and DN25.

The static pressure drop dp occurring along a part dx of a transfer line is given by

$$dp = \lambda'(Re)\ \frac{1}{2}\rho v^2\ \frac{dx}{D}$$

$$= \frac{16}{\pi^2}\ \lambda'(Re)\ \frac{dx}{D^5}\ \frac{1}{2}\rho \dot{V}^2. \qquad (4\text{-}41)$$

The helium transfer lines are enclosed in an evacuated transfer hose with an inner diameter of 0.1m. Fig.4.13 provides a cross-sectional view of their position.

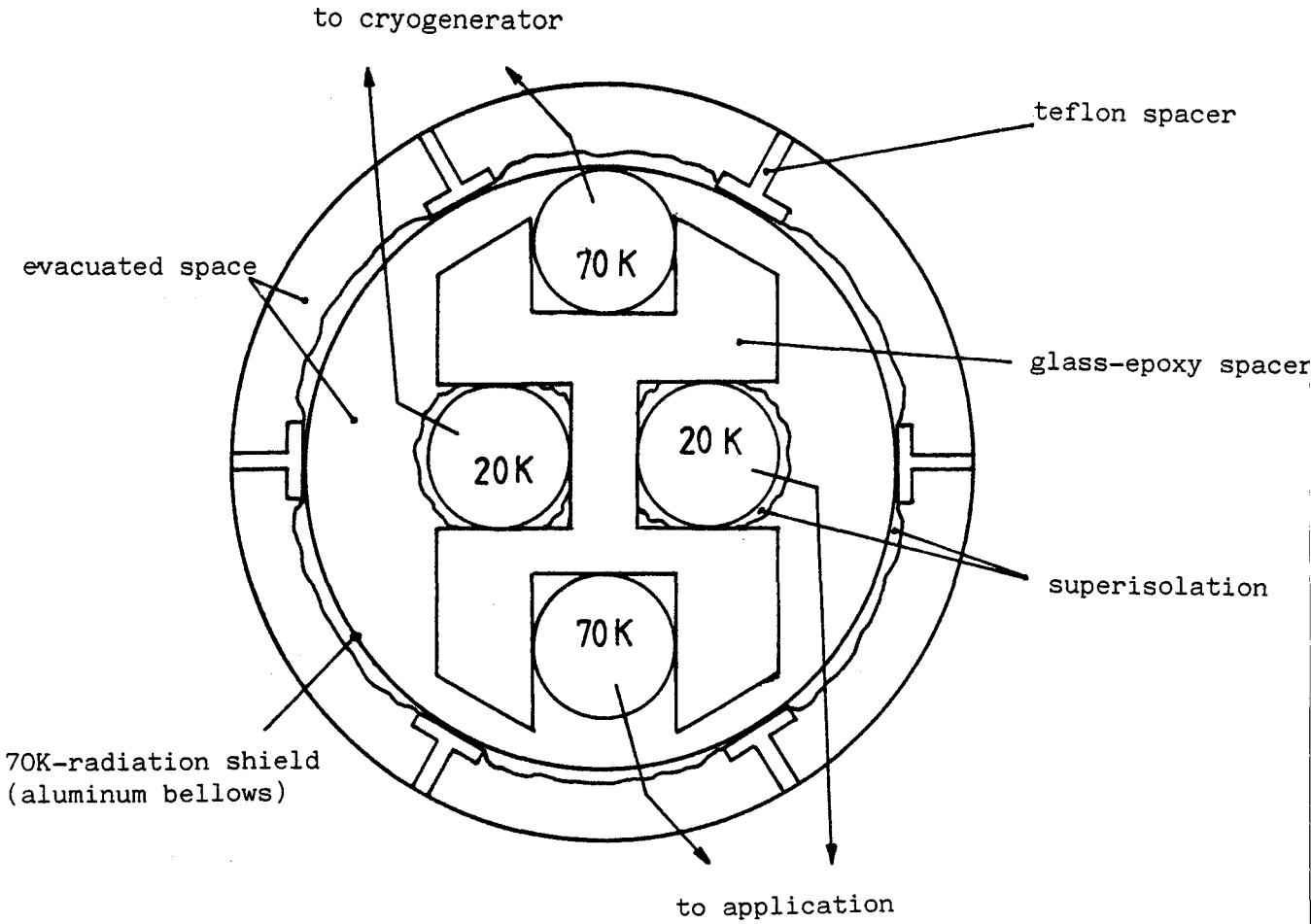

Fig.4.13 Cross-sectional view of transfer hose, showing how the helium transfer lines are positioned and shielded from the room temperature

The transfer lines are separated from each other by glass-epoxy spacers. The 20K-lines are surrounded by 5 layers of superisolation, while the 70K-line returning to the cryogenerator cools an aluminum bellows. This bellows, which is surrounded by 10 layers of superisolation, acts as a 70K radiation shield between room temperature and the 20K-lines. It is separated from the transfer hose by teflon spacers. The spacer configuration as shown in Fig.4.13 repeats itself at each 0.2m along the axis of the transfer hose.

The superisolation layers mentioned above are polyester foils (thickness ca. 10μm), covered on both sides with a layer of aluminum (thickness ca. 0.2μm). The foils are of the Mylar type and have an emission coefficient $e_{myl} \approx 0.04$. By wrapping them loosely around each other in order to avoid heat conduction between the foils, they behave as separate radiation shields. When placed between two surfaces of a different temperature they may reduce heat transfer considerably, the reduction factor being ca. 1/n when using n foils.

We will now estimate the magnitude of the heat flows towards the 70K radiation shield and the transfer lines in two extreme situations. In the first situation it is supposed that the superisolation functions ideally and that there is an ideal thermal coupling between the radiation shield and the 70K-line returning to the cryogenerator (see Fig. 4.14(a)). In the second situation it is supposed that there is no mechanical contact between the radiation shield and the 70K-line, and that the superisolation behaves as one layer with the same temperature as the surface around which it has been wrapped (see Fig.4.14(b)).

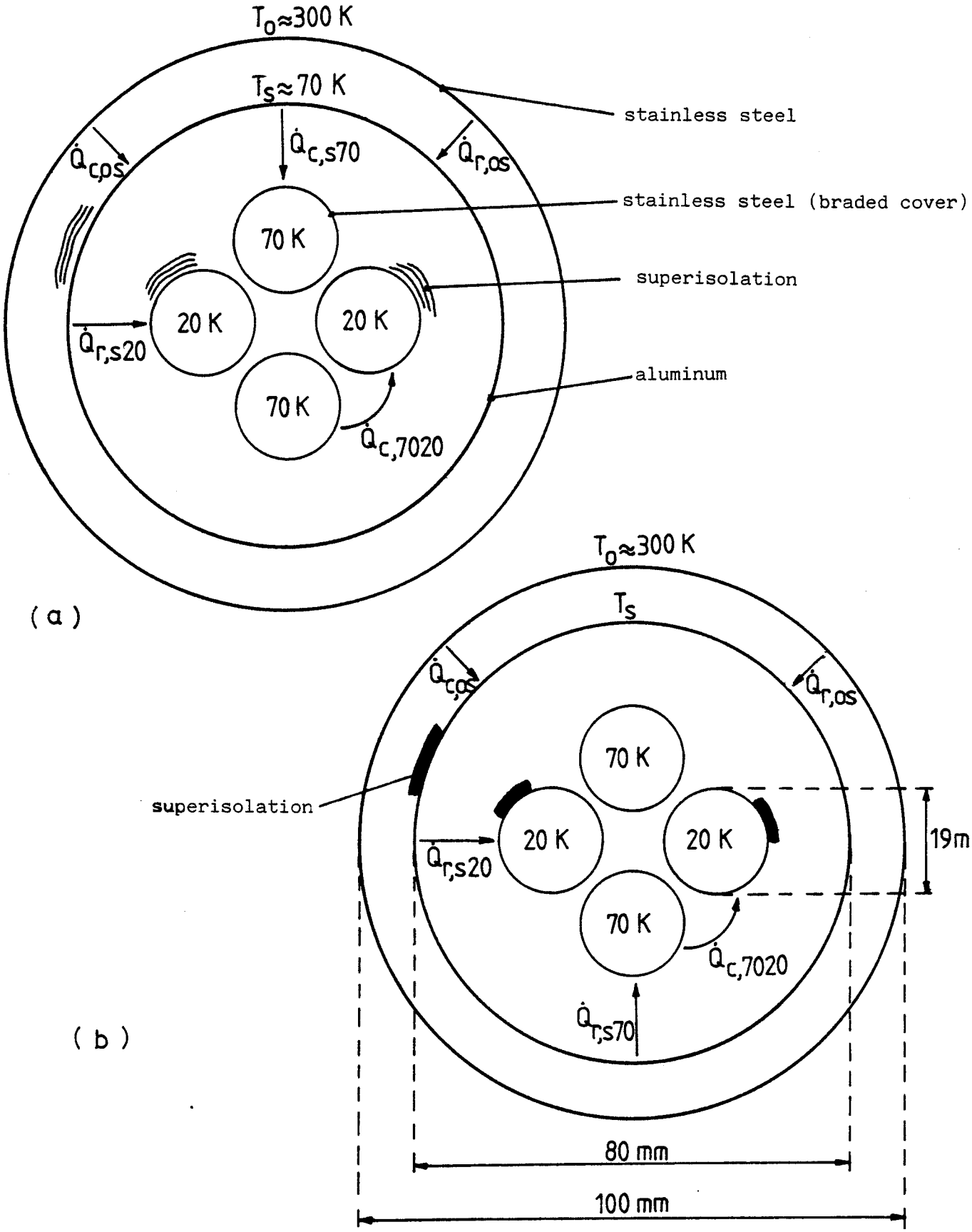

Fig. 4.14 Conductive ($\dot{Q}_c$) and radiative heat flows ($\dot{Q}_r$) from the outer transfer hose (temperature T_o) towards the 70K radiation shield (temperature T_s) and the four helium transfer lines. Two cases are distinguished:

a) ideally functioning superisolation and ideal thermal coupling between the radiation shield and one of the 70K lines

b) isothermal superisolation and no mechanical contact between the radiation shield and the 70K circuit.

The conductive heat flows $\dot{Q}_c$ will be calculated with

$$\dot{Q}_c = (A/l) \int_{T_1}^{T_2} \lambda(T)\, dT \qquad (4\text{-}42)$$

(compare (4-17) and see appendix 10.2), where λ is the thermal conductivity of teflon. A is the area through which and l the distance along which $\dot{Q}_c$ is flowing.
The radiative heat flow $\dot{Q}_r$ between two coaxial cylindrical surfaces is given by

$$\dot{Q}_r = \sigma\, E\, A_1\, (T_2^4 - T_1^4) \qquad (4\text{-}43)$$

where $\frac{1}{E} = \frac{1}{e_1} + \frac{A_1}{A_2}\left(\frac{1}{e_2} - 1\right)$ and

Stefan-Boltzmann's constant $\sigma = 5.67\ 10^{-8} W/(m^2 K^4)$

(CON70): see Fig. 4.15 for clarification of the symbols.

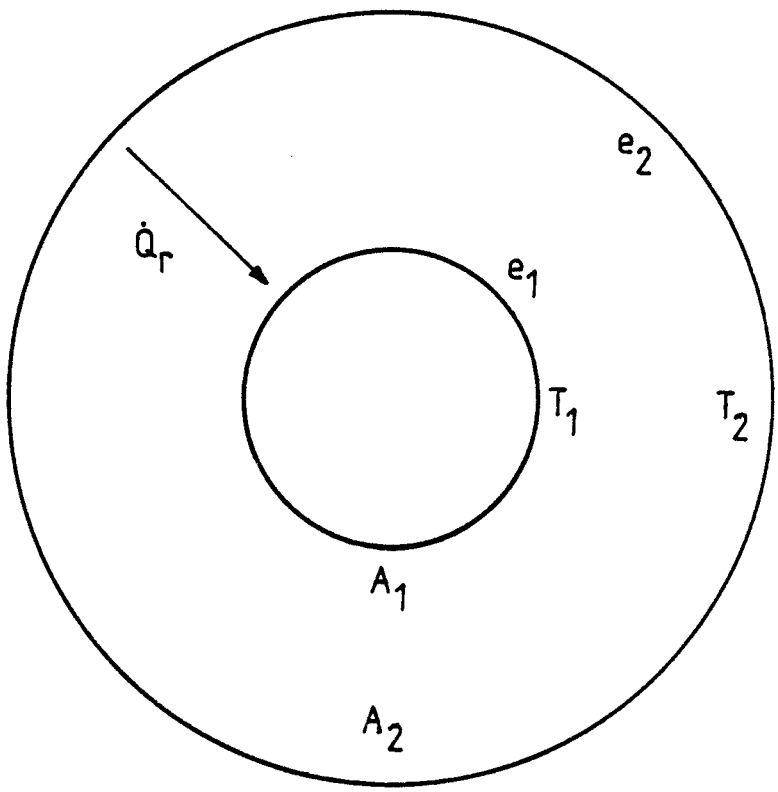

Fig. 4.15 Net radiative heat flow $\dot{Q}_r$ from surface A_2 to surface A_1 with temperatures T_2 and T_1 and emission coefficients e_1 and e_2.

Because the pressure inside the transfer hose is about 10^{-5}mbar, the heat conduction through the residual gas is molecular. The heat flows resulting from this process are about 0.1W or less and will be neglected in the now following calculations.

Situation 1 (see Fig. 4.14 (a))

Every 0.2 m along the axis of the transfer hose there are 6 teflon spacers to center the 70K radiation shield. Since the hose is 7 m long there are 210 teflon spacers, of which about the half will make a thermal contact between the transfer hose and the radiation shield. Using (4-42) gives

$$\dot{Q}_{c,os} = \frac{210}{2} \frac{(15\ 10^{-3})\ (2\ 10^{-3})}{10\ 10^{-3}} \int_{70K}^{300K} \lambda(T)\, dT = 18\ W.$$

When n Mylar foils are wrapped around A_1 (Fig.4.15), all having approximately the same area A_1, it follows from (4-43) that

$$\dot{Q}_r = \sigma\, E' A_1\, (T_2^4 - T_1^4)$$

$$\text{where } \frac{1}{E'} = \frac{1}{E} + n \left(\frac{2}{e_{myl}} - 1 \right) \qquad (4\text{-}44)$$

and where 1/E is given in (4-43).

Taking e_1=0.1 (aluminum), e_2=0.15 (stainless steel), e_{myl}=0.04 and n=10, (4-44) yields $1/E'$=505 and since A_1=1.7m^2

$$\dot{Q}_{r,os} = 1.6\ W.$$

Each 20K- (and 70K-) transfer line has a braded cover of stainless steel with e_1=0.3. Taking e_2=0.1 (aluminum) and n=5, we find $1/E'$ = 250 and

$$\dot{Q}_{r,s20} = 2.4\ 10^{-3}\ W.$$

Since $\dot{Q}_{r,s20}$ is neglegibly small, $\dot{Q}_{c,s70}$ may be written as

$$\dot{Q}_{c,s70} = \dot{Q}_{c,os} + \dot{Q}_{r,os} = 20\ W.$$

Situation 2 (see Fig.4.14(b))

In this case the radiation shield assumes an equilibrium temperature T_s satisfying

$$\dot{Q}_{c,os}(T_s) + \dot{Q}_{r,os}(T_s) = 2\,(\dot{Q}_{r,s20}(T_s) + \dot{Q}_{r,s70}(T_s)) \qquad (4\text{-}45).$$

The factor 2 is due to the fact that there are two 20K and two 70K transfer lines. $\dot{Q}_{c,os}(T_s)$ follows from (4-42). Using (4-43) with e_1=0.04 (Mylar) and e_2=0.15 (stainless steel),

$$\dot{Q}_{r,os}(T_s) = 3.38\ 10^{-9}\ (300^4 - T_s^4).$$

Taking e_1=0.04 (Mylar) and e_2=0.1 (aluminum)

$$2\ \dot{Q}_{r,s20}(T_s) = 1.83\ 10^{-9}(T_s^4 - 20^4)$$

and with e_1=0.3 (braded cover of stainless steel) and e_2=0.1 (aluminum) we find

$$2\ \dot{Q}_{r,s70}(T_s) = 8.93\ 10^{-9}(T_s^4 - 70^4).$$

The solution of (4-45) is given by the point P in Fig.4.16:

T_s = 220 K while

$\dot{Q}_{c,os} + \dot{Q}_{r,os}$ = 6 W + 20 W = 26 W

$2\dot{Q}_{r,s20} + 2\dot{Q}_{r,s70}$ = 4 W + 22 W = 26 W.

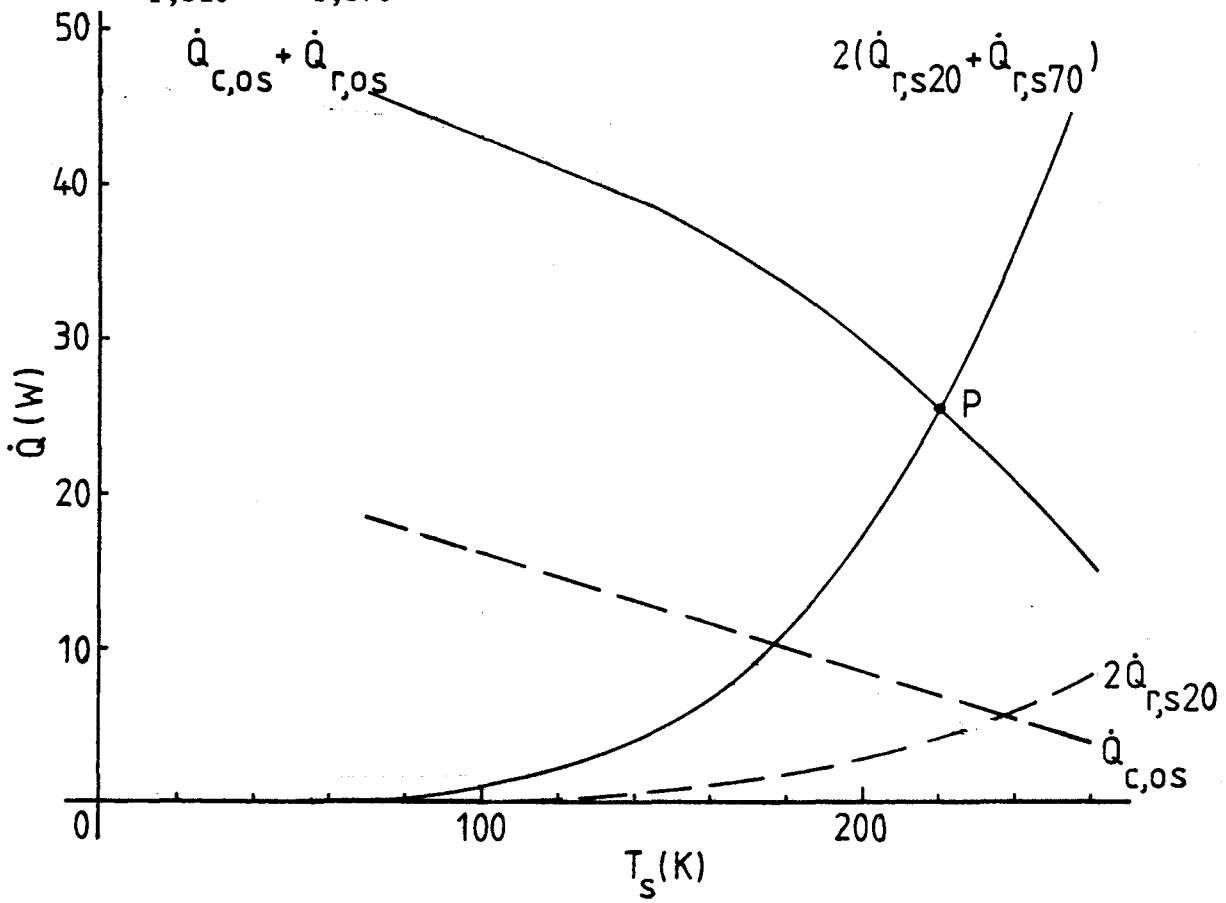

Fig.4.16 The heat flows $\dot{Q}_{c,os}$, $\dot{Q}_{r,os}$, $2\dot{Q}_{r,s20}$ and $2\dot{Q}_{r,s70}$ of Fig.4.14(b), given as functions of the radiation shield temperature T_s. The solution of equation (4-45) is given by the point P.

The heat flow $\dot{Q}_{c,7020}$ between a 70K- and a 20K-transfer line is established by 35 glass-epoxy spacers (thickness 2mm). Its order of magnitude may be estimated by supposing that the conduction paths are 3mm wide and 15mm long (see Fig.4.17).

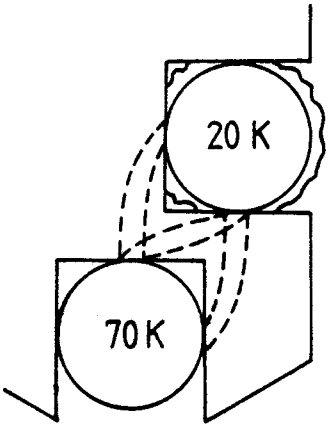

Fig.4.17 Three conduction paths in a glass-epoxy spacer separating a 20K and a 70K transfer line (compare Fig.4.13)

Using (4-42) with λ=0.2W/(m K), it is found that $\dot{Q}_{c,7020}$=0.4W. Since each 20K line receives heat from both 70K lines, the 20K circuit will receive from the 70K circuit $4\dot{Q}_{c,7020}\approx$2W.

Comparing the situations 1 and 2 we see that there is virtually no difference in the amount of heat received by the 70K circuit (ca. 20 W). The situations differ from each other where the 20K circuit is concerned. In situation 1 the heat flow towards this circuit is about 2 W, whereas cold losses on the 20K circuit tend to be larger in situation 2: 2 W + 4 W = 6 W.

4.2 The cold transfer system in the stationary state

When the A20 cryogenerator is put in operation, the applications are cooled by the 20K stage and the 70K stage. The cool-down period results in the stationary state when the heat extracted from the application $\dot{Q}_a$ equals the heat flowing towards the application from its surroundings. Typical stationary state values of $\dot{Q}_a$ are 10 W in the 20K circuit and 60 W in the 70K circuit. In the paragraphs 4.2.1 and 4.2.2 we will study several characteristics of the steady operation. In paragraph 4.2.3 a model is proposed to describe this operation and paragraph 4.2.4 contains an outline of the optimization process.

4.2.1 Situating the centrifugal fans

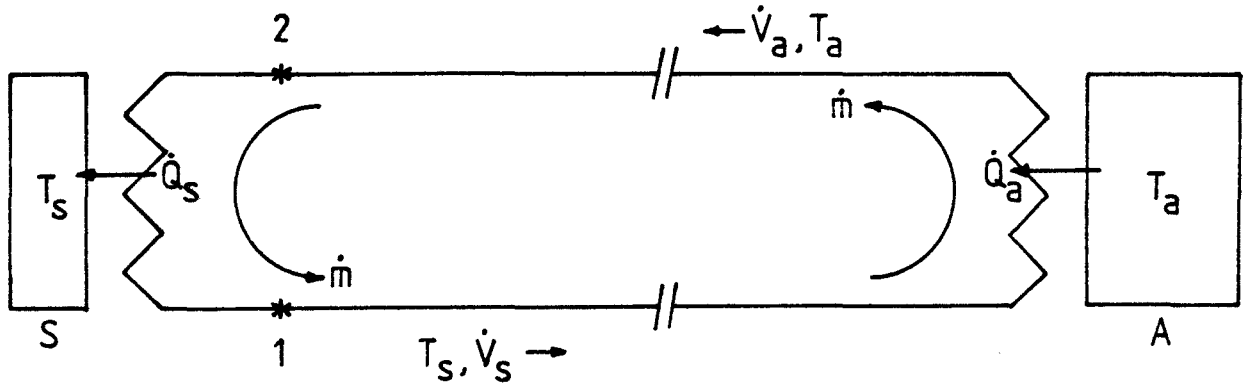

Fig.4.18 Working principle of the cold transfer system. The heat flow $\dot{Q}_a$ is transported via the mass flow $\dot{m}$ from the application A to the stage S. The fan may be placed behind the stage, which is presently the case in the 70K circuit and will be referred to as situation 1. The fan may also be placed in front of the stage, which is presently the case in the 20K circuit and will be referred to as situation 2 (compare Fig.4.3).

Neglecting cold losses and the mechanical shaft power of the fan P_{sh} (see (4-21)) $\dot{Q}_s = \dot{Q}_a$ (see Fig.4.18). When the temperature difference between a heat exchanger and the gas leaving it may be neglected as well, the gas in the upper transfer line has the application temperature T_a and the gas in the lower transfer line has the stage temperature T_s.
The centrifugal fan circulating the He gas through a tube system may be placed in the cold gas stream leaving the stage (Fig.4.18, situation 1) or in the warmer gas stream leaving the application (Fig.4.18, situation 2). As the fans are volume transporters, the largest mass flow may be expected in situation 1. This is important because the temperature difference between the application and the stage is given by (see (4-31))

$$\Delta T := T_a - T_s \approx \dot{Q}_a/(\dot{m}\, c_p) \qquad (4\text{-}46)$$

and should be as small as possible. We will now estimate ΔT_1 (situation 1) and ΔT_2 (situation 2) for the present transfer system geometry and for various values of $\dot{Q}_a$. The helium pressure p in the tube system will be regarded as a constant. Using (4-2),(4-29),(4-46) and Fig.4.18 we find

$$\dot{V}_a = \frac{\rho(p,T_s)}{\rho(p,T_a)}\,\dot{V}_s = \frac{T_a}{T_s}\,\dot{V}_s = \left(1 + \frac{\Delta T}{T_s}\right)\dot{V}_s = \dot{V}_s + \frac{\dot{Q}_a}{\rho(p,T_s)\; c_p\; T_s}$$

which yields together with (4-4)

$$\dot{V}_a = \dot{V}_s + (2/5)\;(\dot{Q}_a/p) =: \dot{V}_s + \Delta\dot{V}. \qquad (4\text{-}47)$$

Assuming that in Fig.4.18 the heat exchangers as well as the transfer lines are identical and taking their friction factors to be $\lambda'_{he}=0.02$ and $\lambda'_{tl}=0.07$, the static pressure drop over the tubes of the circuit may be written via (4-37) and (4-41) as

$$\Delta p_t = k_t\;(1/2)\;\overline{(\rho \dot{V}^2)}_{circuit} = k_t\;(1/2)\;\dot{m}^2\;\overline{(1/\rho)}_{circuit}$$

$$= k_t\,\frac{1}{2}\,\frac{\dot{m}^2}{\rho(p,\overline{T})} \qquad \text{with } k_t = 2\;10^{10}\;m^{-4} \qquad (4\text{-}48)$$

while $\overline{T} := (T_a + T_s)/2.$ (4-49)

Hence, in the situations 1 and 2 the static pressure head which is lost over the tubes of the circuit will be

$$\Delta H_{t,1} = \Delta p_t/[\rho(p,T_s)\; g] = [k_t/(2g)]\;\dot{V}_s^{\,2}\;(\overline{T}/T_s)$$

with $$\overline{T}/T_s = 1 + (1/2)(\Delta T/T_s) = 1 + (1/2)(\Delta\dot{V}/\dot{V}_s) \qquad (4\text{-}50a)$$

and $$\Delta H_{t,2} = \Delta p_t/[\rho(p,T_a)\; g] = [k_t/(2g)]\;\dot{V}_a^{\,2}\;(\overline{T}/T_a)$$

with $$\overline{T}/T_a = 1 - (1/2)(\Delta T/T_a) = 1 - (1/2)(\Delta\dot{V}/\dot{V}_a). \qquad (4\text{-}50b)$$

Writing $\Delta H_{max}=u^2/(2g)$ (see (4-11)), the fan static pressure head is given by (4-10):

$$\Delta H_f = (u^2 - k_f\;\dot{V}^2)/(2\;g)$$

where $$k_f := u^2/\dot{V}_{max}^{\,2} = 1.7\;10^9\;m^{-4}. \qquad (4\text{-}51)$$

The constant k_f is a measure for the curvature of the fan characteristic and is independent of the rotation frequency ν (see Fig.4.6, (4-12) and (4-13a)). Equating (4-50) and (4-51) the volume flows $\dot{V}_{s1}$ and $\dot{V}_{a2}$ are found:

$$\dot{V}_{s1} = [a - (1/2)\, k_t\, \Delta\dot{V}]/b$$

and $$\dot{V}_{a2} = [a + (1/2)\, k_t\, \Delta\dot{V}]/b \qquad (4\text{-}52)$$

where $a = [4u^2(k_t+k_f) + (k_t \Delta\dot{V}/2)^2]^{1/2}$ and $b = 2(k_t+k_f)$.

Using (4-47),(4-52) yields

$$\dot{V}_{s1} - \dot{V}_{s2} = \Delta\dot{V}\,(k_t+2k_f)/(2k_t+2k_f) \approx 0.5\,\Delta\dot{V}. \qquad (4\text{-}53)$$

For a given value of $\dot{Q}_a$ the stage temperature T_s has a fixed value. Therefore

$$\Delta T_2/\Delta T_1 = \dot{m}_1/\dot{m}_2 = \dot{V}_{s1}/\dot{V}_{s2}. \qquad (4\text{-}54)$$

With a transfer system pressure p=20bar and a fan rotation frequency ν=300Hz the following results are obtained (see Table 4.3).

$\dot{Q}_a$ (W)	$\Delta\dot{V}$ (cm^3/s)	$\dot{V}_{s1}$ (cm^3/s)	$\dot{V}_{a1}$ (cm^3/s)	$\dot{V}_{s2}$ (cm^3/s)	$\dot{V}_{a2}$ (cm^3/s)	$\Delta T_2/\Delta T_1$
800	160	160	320	80	240	2.0
600	120	170	290	110	230	1.5
400	80	180	260	140	220	1.3
300	60	180	240	150	210	1.2
200	40	180	220	160	200	1.0
100	20	190	210	180	200	1.0
50	10	190	200	190	200	1.0

Table 4.3 The volume flow $\dot{V}_s$ leaving the stage and the volume flow $\dot{V}_a$ leaving the application as functions of the cooling power $\dot{Q}_a$ at the application for the situations 1 and 2 in Fig.4.18. ΔT is the temperature difference between the application and the stage, and $\Delta\dot{V}$ is the difference between $\dot{V}_{s1}$ and $\dot{V}_{a1}$.

The stages are assumed to behave independently. Their cooling powers $\dot{Q}_s$ are written as

$$\dot{Q}_{s20} = K_1 \ln(T_s/K_2) \qquad \text{with } K_1=160 \text{ W and } K_2=14 \text{ K}$$

and

$$\dot{Q}_{s70} = K_1 (T_s^2-K_2)^{1/2}-K_0 \qquad (4\text{-}55)$$

$$\text{with } K_0=55 \text{ W}, \; K_1=5.0 \text{ W/K and } K_2=2.9\ 10^3 \text{ K}^2.$$

Calculating T_s for the values of $\dot{Q}_a=\dot{Q}_s$ in Table 4.3, ΔT_1 is obtained via (4-46) with $\dot{m}=\rho(p,T_s)\ \dot{V}_{s1}$, while $\Delta T_2=(\Delta T_2/\Delta T_1)\ \Delta T_1$. The results are shown in Fig.4.19.

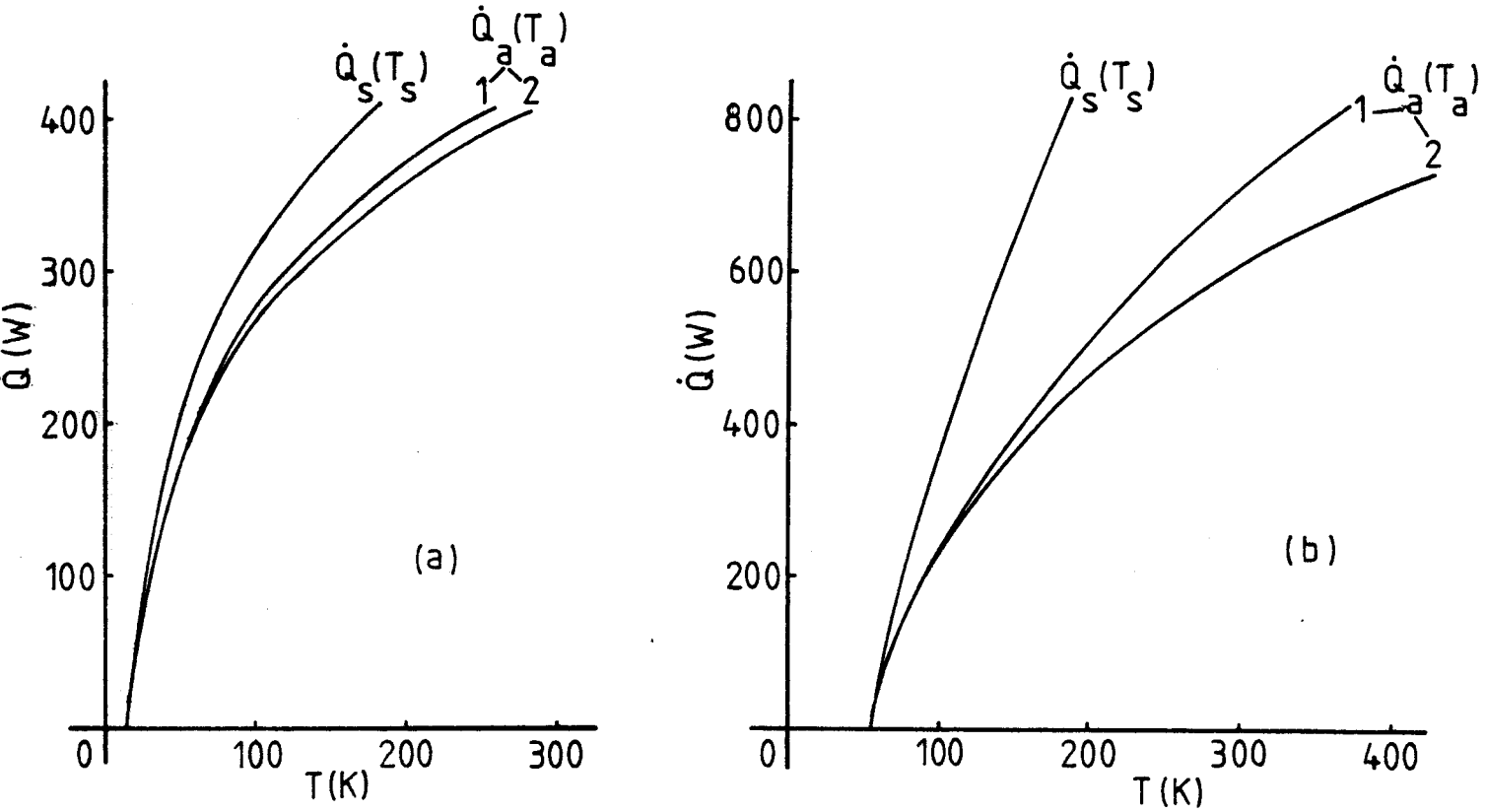

Fig.4.19 Temperature differences between the stage and the application at a given cooling power $\dot{Q}_s=\dot{Q}_a$. The indices 1 and 2 are related to situation 1 (the fan behind the stage) and situation 2 (the fan in front of the stage).
(a) 20K circuit (b) 70K circuit

Apparently the situations 1 and 2 are equally satisfying for normal stationary state operation ($\dot{Q}_a$<100W). In order to minimize the cool-down period situation 1 is preferable, especially in the 70K circuit.

4.2.2 Optimal impeller tip speed for an ideally isolated transfer system

A fan produces three effects. By creating a mass flow $\dot{m}$ it reduces the temperature difference $T_a - T_s$ between the application and the stage. However, due to the shaft power P_{sh} and the heat flow by conduction $\dot{Q}_{f,con}$ (see (4-21)), this positive effect is accompanied by two negative ones: a temperature difference ΔT_f over the fan and an increase of the stage temperature. These effects lead to an optimal impeller tip speed u_{opt}, which we will estimate for the situations 1 and 2 in Fig.4.18.

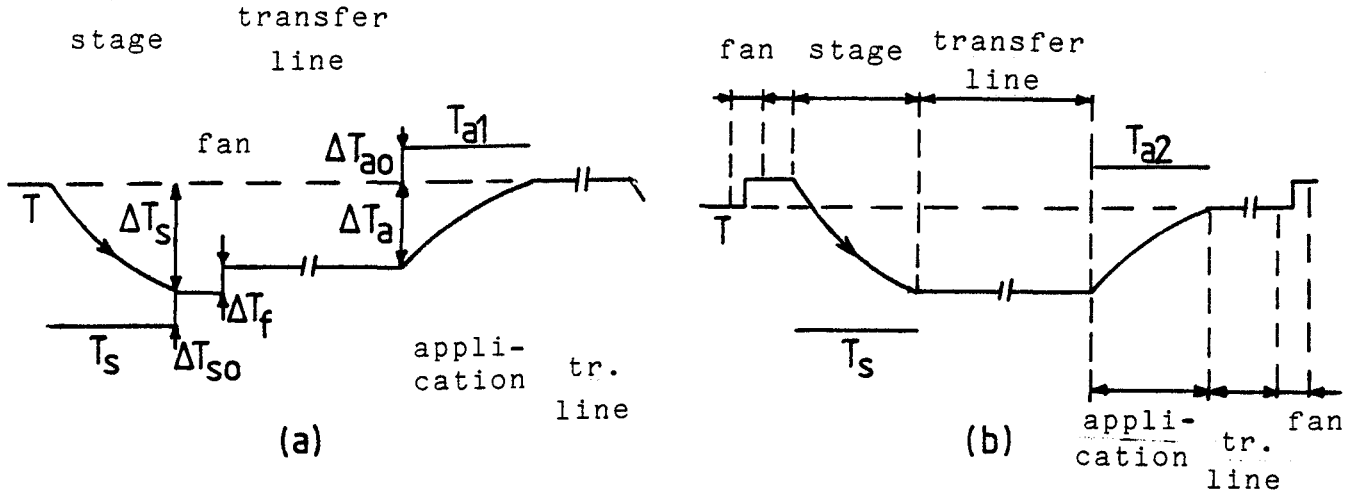

Fig.4.20 Variation of the temperature T of the helium gas when it flows through a tube system. Cold losses on the transfer lines are neglected. (a) Fig.4.18, situation 1 (b) Fig.4.18, situation 2

Ignoring cold losses on the transfer lines, the application temperature is given by (see Fig.4.20)

$$T_{a1} = T_s + \Delta T_{so} + \Delta T_f + \Delta T_a + \Delta T_{ao} \qquad \text{(sit.1)} \qquad (4\text{-}56a)$$

$$T_{a2} = T_s + \Delta T_{so} \qquad + \Delta T_a + \Delta T_{ao} \qquad \text{(sit.2).} \qquad (4\text{-}56b)$$

With $\Delta T_{so} = (\Delta T_s + \Delta T_{so}) e^{-\Lambda_s}$ and $\Delta T_{ao} = (\Delta T_a + \Delta T_{ao}) e^{-\Lambda_a}$ (see (4-36)) (4-56) may be rewritten as

$$T_{a1} = T_s + \Delta T_a [1 + (e^{\Lambda_s} - 1)^{-1} + (e^{\Lambda_a} - 1)^{-1}] + \Delta T_f [1 + (e^{\Lambda_s} - 1)^{-1}]$$

$$\approx T_s + \Delta T_a + \Delta T_f \qquad (4\text{-}57a)$$

and $$T_{a2} \approx T_s + \Delta T_a \qquad (4\text{-}57b)$$

when $\Lambda > 2$ (see (4-35)). (4-57) shows the reason why situation 2 has been preferred in the 20K circuit in spite of the smaller mass flow during the cool-down period.
Assuming that $T_a - T_s \ll (T_a + T_s)/2$, the helium density and the volume flow may be regarded as constants. Equating (4-48) and (4-51) we find (see Fig.4.21)

$$\dot{V} = u \,/\, (k_t + k_f)^{1/2}. \qquad (4\text{-}58)$$

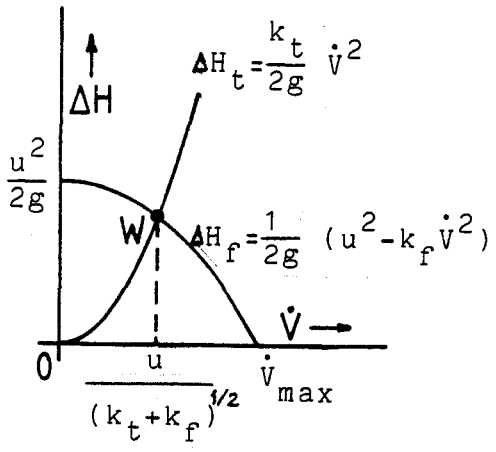

Fig.4.21 ΔH-$\dot{V}$-diagram, in which the fan characteristic $\Delta H_f(\dot{V})$ and the tube system characteristic $\Delta H_t(\dot{V})$ intersect at the working point W

In order to obtain the maximum fan efficiency, $\dot{V}$ should be about $(1/2)\dot{V}_{max} = (1/2)u/k_f^{1/2}$ (see Fig.4.6), which yields for a properly designed fan

$$\dot{V} = u \,/\, [k_t + (1/3)k_t]^{1/2} = u \,/\, [(4/3)k_t]^{1/2}. \qquad (4\text{-}59)$$

Taking η_f=50%, the mechanical shaft power is given by

$$P_{sh} = \dot{V}\,\Delta p/\eta_f = 2\,\dot{V}\,k_t\,(1/2)\rho\dot{V}^2 = \rho\,k_t\,\dot{V}^3. \qquad (4\text{-}60)$$

Neglecting $\dot{Q}_{f,con}$, ΔT_f is given by

$$\Delta T_f = P_{sh}/(\dot{m}c_p) = (k_t/c_p)\,\dot{V}^2 = (3/4)\,u^2/c_p. \qquad (4\text{-}61)$$

ΔT_a is given by

$$\Delta T_a = \dot{Q}_a/(\dot{m}c_p) = [(4/3)k_t]^{1/2}\,\dot{Q}_a/(\rho u c_p). \qquad (4\text{-}62)$$

Using (4-57) and (4-55) with $\dot{Q}_s = \dot{Q}_a + P_{sh}$, Fig.4.22 is obtained.

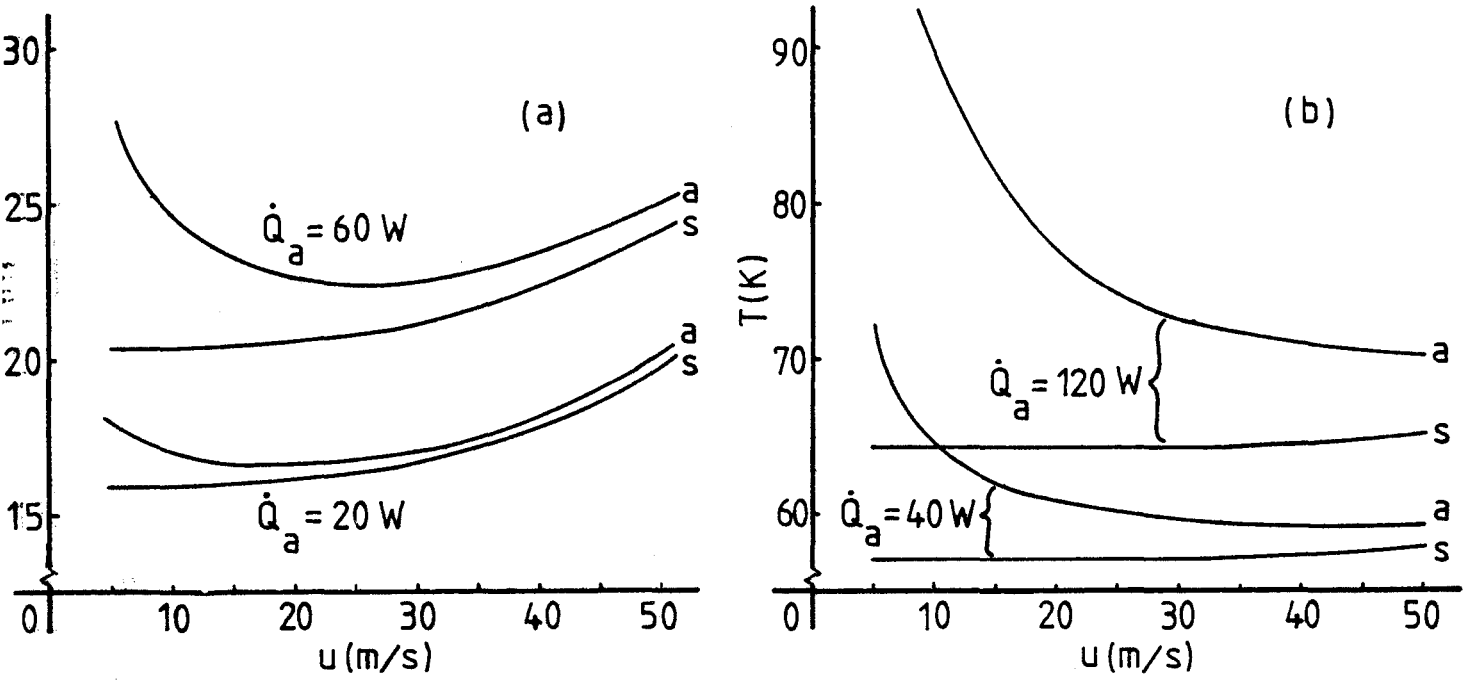

Fig.4.22 The application temperature T_a and the stage temperature T_s as functions of the impeller tip speed u for the present tube system geometry (k_t=2 10^{10} m^{-4})
(a) 20K circuit (b) 70K circuit

The value of u for which T_a is smallest is the optimum value u_{opt}. Fig.4.22(a) shows that u_{opt} varies with $\dot{Q}_a$. By differentiating (4-57b) with respect to u, this variation in the 20K circuit is given by

(4-63)

$$u_{opt}^4 = (16/27)\ (K_1^2/K_2)\ [(\dot{Q}_a/K_1)/e^{\dot{Q}_a/K_1}]\ [k_t/(\rho^2 c_p)]$$

(see (4-55)). For the 20K circuit 15m/s < u_{opt} < 30m/s, while for the 70K circuit $u_{opt} \approx$ 50m/s. The present impeller tip speed u=28m/s.

4.2.3 Model describing the stationary state operation

In this paragraph a set of equations will be presented which describe the stationary state operation of a tube system (see Fig.4.23).

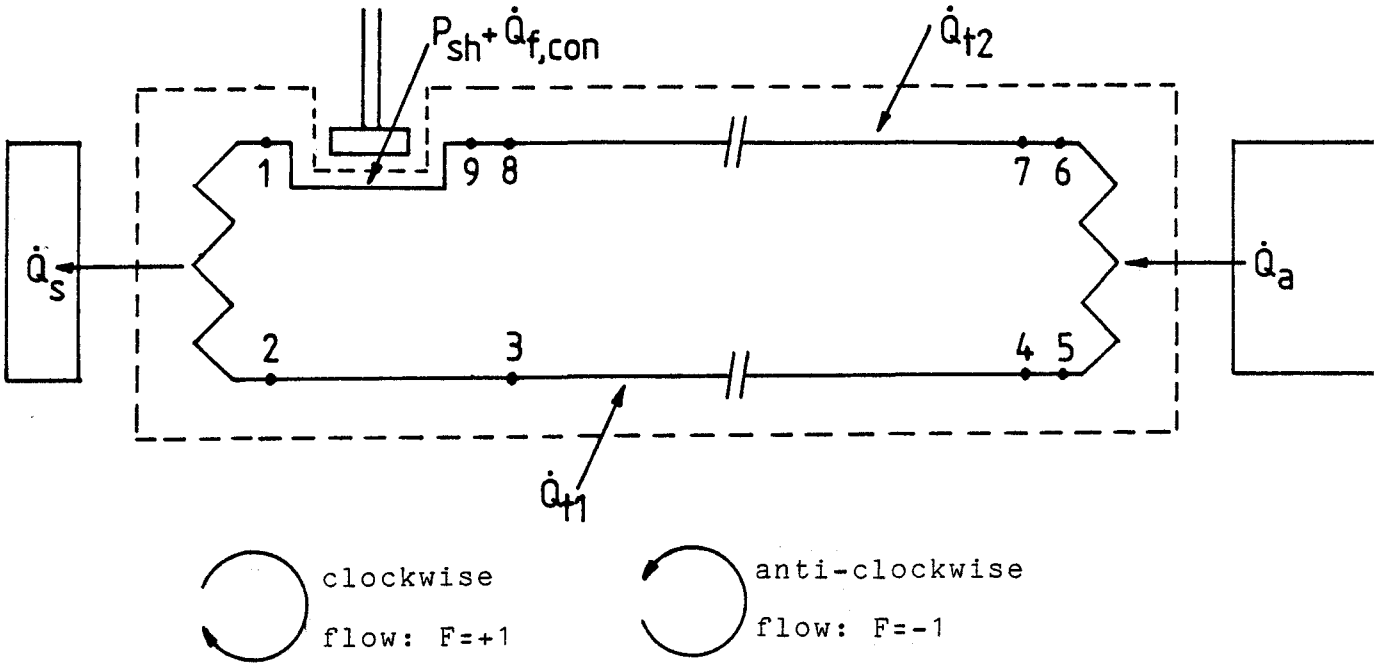

Fig.4.23 Helium gas inside a tube system (surrounded by dashed line) divided into nine parts.
1-2, 5-6: gas inside the heat exchangers
3-4, 7-8: gas inside the transfer lines
1-9: gas inside the centrifugal fan
2-3, 4-5, 6-7, 8-9: gas inside bends, enlargements, contractions
According to the first law of thermodynamics for a closed system
$\dot{Q}_s = \dot{Q}_a + \dot{Q}_{t1} + \dot{Q}_{t2} + P_{sh} + \dot{Q}_{f,con}$.

The unknown variables are the pressures p_1 to p_9, the temperatures T_1 to T_9, T_s and T_a, the mechanical shaft power P_{sh}, the heat flow $\dot{Q}_s$ and the mass flow $\dot{m}$. As there are 23 unknown variables, 23 equations will be needed to describe the stationary state. $\dot{Q}_a$, $\dot{Q}_{t1}$, $\dot{Q}_{t2}$, $\dot{Q}_{f,con}$, c_p and the average pressure p in the tube system will be given fixed values, as well as the fan efficiency η_f and the fan static pressure head ΔH_f.
In Fig.4.23 the flow may be either clockwise or anti-clockwise. In coming equations this possibility will be accounted for by a factor F:

F = +1 for clockwise flow (fan behind the stage) (4-64)
and F = -1 for anti-clockwise flow (fan in front of the stage).

Using the first law of thermodynamics for an open system

$$\dot{Q}_s = F\,\dot{m}c_p\,(T_2-T_1), \tag{4-65}$$

$$\dot{Q}_a = F\,\dot{m}c_p\,(T_5-T_6), \tag{4-66}$$

$$\dot{Q}_{t1} = F\,\dot{m}c_p\,(T_3-T_4), \tag{4-67}$$

$$\dot{Q}_{t2} = F\,\dot{m}c_p\,(T_7-T_8), \tag{4-68}$$

$$P_{sh} + \dot{Q}_{f,con} = F\,\dot{m}c_p\,(T_9-T_1), \tag{4-69}$$

$$0 = T_2-T_3, \tag{4-70}$$

$$0 = T_4-T_5, \tag{4-71}$$

$$0 = T_6-T_7 \tag{4-72}$$

and

$$0 = T_8-T_9. \tag{4-73}$$

The cooling power of the 20K stage and the 70K stage is given as a function of the stage temperature by (4-55):

$$\dot{Q}_s = \dot{Q}_s(T_s). \tag{4-74}$$

The shaft power follows from (4-14), (4-20) and (4-9):

$$P_{sh} = (\dot{V}\,\Delta p)_f/\eta_f = \dot{m}\,g\,\Delta H_f\,/\,\eta_f. \tag{4-75}$$

The heat exchanger equation (4-36) yields

$$T_1-T_s = (T_2-T_s)\,e^{-F\Lambda_s} \tag{4-76}$$

and

$$T_5-T_a = (T_6-T_a)\,e^{-F\Lambda_a}\ , \tag{4-77}$$

where Λ is given by (4-34).
Nine more equations are found by regarding the pressure differences in the circuit. Using the ideal gas law (4-2), the pressure difference across the fan is given by

$$F\,(p_9-p_1) = \varrho g\,\Delta H_f = (Mp/R)\,[2/(T_1+T_9)]\,g\,\Delta H_f. \tag{4-78}$$

The static pressure drop Δp_t over a transfer line with length L_t and inner diameter D_t is given by (4-41):

$$p_t = (16/\pi^2)\,(\lambda_t'/D_t^5)\,(\dot{m}^2/2)\,(R/Mp)\int_0^{L_t} T(x)dx$$

where the friction factor λ_t' is regarded as a constant (see Fig.4.12).

Assuming that T(x) is proportional to x we find

$$F\,(p_4-p_3) = \\ = (16/\pi^2)\,(\lambda'_t/D_{t1}^5)\,(\dot{m}^2/2)\,(R/Mp)\,[(T_3+T_4)/2]\,L_t \qquad (4\text{-}79)$$

and

$$F\,(p_8-p_7) = \\ = (16/\pi^2)\,(\lambda'_t/D_{t2}^5)\,(\dot{m}^2/2)\,(R/Mp)\,[(T_7+T_8)/2]\,L_t. \qquad (4\text{-}80)$$

The pressure drop over a heat exchanger follows from (4-37), (4-40), (4-38) and (4-7):

$$\Delta p_{he} = (16/\pi^2)(1/D_{he}^5)(1+3.74D_{he}/D_c)(\dot{m}^2/2)(R/Mp)\int_0^{L_{he}} \lambda'_{he}(T)\,T(x)dx$$

where $\lambda'_{he} \sim T^{0.14}$. In order to calculate the integral, where T(x) is given by (4-33), it is useful to approximate $T^{0.14}$ by $(2.60\ 10^{-3}T + 1.54)$, which is accurate within 5% for 20K < T < 300K. The integral follows from

$$\int_0^{L_{he}} T(x)dx = L_{he}T_{he} + L_{ch}(T_i-T_{he})\,(1-e^{-L_{he}/L_{ch}})$$

and

$$\int_0^{L_{he}} T^2(x)dx = L_{he}T_{he}^2 + L_{ch}(T_i-T_{he})\,(1-e^{-L_{he}/L_{ch}}) \cdot \\ \cdot [2T_{he} + (T_i+T_{he})\,(1+e^{-L_{he}/L_{ch}})\,/\,2]$$

where the characteristic length $L_{ch} := (L/\Lambda)_{he} = \dot{m}c_p/(\alpha\pi D_{he})$: see (4-34). Thus

$$F\,(p_2-p_1) \sim 1.54\int_0^{L_s} T(x)dx + 2.60\ 10^{-3}\int_0^{L_s} T^2(x)dx \qquad (4\text{-}81)$$

where $T_i = T_{(1.5+F/2)}$

and

$$F\,(p_6-p_5) \sim 1.54\int_0^{L_a} T(x)dx + 2.60\ 10^{-3}\int_0^{L_a} T^2(x)dx \qquad (4\text{-}82)$$

where $T_i = T_{(5.5+F/2)}$.

When the diameters of the transfer lines differ from those of the heat exchangers, it is necessary to use enlargements and contractions in order to connect them. Their total irreversible static pressure drops are about $(0.14\ 10^{10}m^{-4})\,(1/2)\,\rho\,\dot{V}^2$. Because this is small in comparison with $\Delta p_t = (2\ 10^{10}m^{-4})\,(1/2)\,\rho\,\dot{V}^2$ (see (4-48)), the effect of enlargements and contractions will be neglected. The static pressure drops across the parts 2-3, 4-5, 6-7 and 7-8 in Fig.4.23 are mainly caused by straight and bended (90°) tube pieces with the same diameter as the heat exchangers to which they have been fixed. The static pressure drop over a bend of 90° is given by

$$p_b = \zeta\,(1/2)\rho v^2 = (16/\pi^2)(\zeta/D^4)\,(1/2)\rho\dot{V}^2 \text{ with } 0.4<\zeta<0.8.$$

This yields together with (4-41)

$$F\,(p_3-p_2) = (16/\pi^2)\,D_s^{-4}\,(\dot{m}^2/2)\,(RT_2/Mp)\cdot \cdot(\lambda'(T_2)\,L_{23}/D_s + N_{23}\zeta_{23}), \tag{4-83}$$

$$F\,(p_5-p_4) = (16/\pi^2)\,D_a^{-4}\,(\dot{m}^2/2)\,(RT_5/Mp)\cdot \cdot(\lambda'(T_5)\,L_{45}/D_a + N_{45}\zeta_{45}), \tag{4-84}$$

$$F\,(p_7-p_6) = (16/\pi^2)\,D_a^{-4}\,(\dot{m}^2/2)\,(RT_6/Mp)\cdot \cdot(\lambda'(T_6)\,L_{67}/D_a + N_{67}\zeta_{67}) \tag{4-85}$$

and

$$F\,(p_9-p_8) = (16/\pi^2)\,D_s^{-4}\,(\dot{m}^2/2)\,(RT_9/Mp)\cdot \cdot(\lambda'(T_9)\,L_{89}/D_s + N_{89}\zeta_{89}), \tag{4-86}$$

where λ' is given by (4-40) and N is the number of bends. Of the 23 required equations 22 have been given ((4-65) to (4-86)). The last one is needed to establish the average system pressure p:

$$(p_1+p_9)/2 = p. \tag{4-87}$$

The set of 23 equations is solved by means of an Algol computer program which is given in appendix 10.4.

4.2.4 Optimization of the cold transfer system

The model given in the last paragraph will be used to optimize the heat exchangers and the centrifugal fans.
In all calculations the optimum will be defined as the situation at which the application temperature T_a is minimal for a given value of the cooling power at the application, $\dot{Q}_a$.
The calculations are divided into two tasks. The first is to analyse the influence of placing the fan behind the stage or in front of it (situation 1 or 2 in Fig.4.18, F=+1 or F=-1 in Fig.4.23). Our second task is to analyse how the avarage transfer system pressure, the static pressure head of the fan, the inner diameter and the coil diameter of the two heat exchangers in the circuit influence the efficiency of the transfer system. The most important reason for carrying out the second task is the following reason. The quality of a heat exchanger is given by the heat transfer number Λ, which is roughly proportional to L_{he}/D_{he} (4-34), whereas the pressure drop over a heat exchanger is roughly proportional to L_{he}/D_{he}^5 (4-37). When the area on which the heat exchanger is mounted has a fixed value, as is the case with the two stages of the cryogenerator, there should be a length L_{he} and an inner diameter D_{he} at which the heat exchanger functions optimally. In calculations it will be supposed that the two heat exchangers within a circuit have the same dimensions.
The optimization of the helium transfer lines with respect to thermal insulation will be carried out via measurements.

At the moment the centrifugal fans have a rotation frequency of 300 Hz. As this is undesirably high for the presently used fan motors, a new fan design will aim at a reduction of the rotation frequency.
In designing and comparing fans dimensionless coefficients are used. The most important of these are the pressure coefficient

$$\psi := \Delta p \,/\, [(1/2)\rho u_2^2] = 2\, g\, \Delta H_f \,/\, u_2^2, \qquad (4\text{-}88)$$

the volume coefficient

$$\varphi := \dot{V} \,/\, [u_2\, (\pi/4) D_2^2] \qquad (4\text{-}89)$$

and the power coefficient

$$\begin{aligned} \lambda_P &:= P_{sh} \,/\, [u_2\, (\pi/4) D_2^2\, (1/2)\rho u_2^2] = \\ &= [\dot{V}\, \Delta p/\eta_f] \,/\, [u_2\, (\pi/4) D_2^2\, (1/2)\rho u_2^2] = \\ &= \varphi\, \psi \,/\, \eta_f \end{aligned} \qquad (4\text{-}90)$$

(see (4-14)). In (4-88) to (4-90) u_2 and D_2 represent the impeller tip speed u and the outer impeller diameter D_f respectively. For convenience, the notations u_2 and D_2 will be used in the rest of this paragraph.

The impeller of a centrifugal fan belongs to one of three groups: it can have blades that curve backward or forward with respect to the direction of rotation, or it can have blades of which the tips end in a radial direction. In Fig.4.24 is shown how ψ and λ_p vary with φ for fans with a different impeller type. Their physical significance follows from the fact that they are the same for geometrically similar fans and independent of their size and rotation frequency. For the radial bladed fan used till now (ΔH=45 m, $\dot{V}$=200 cm^3/s, $D_f=D_2$=3 cm, ν=300 Hz, η_f=50%) we find ψ=1.1, φ=0.010 and λ_p=0.022.

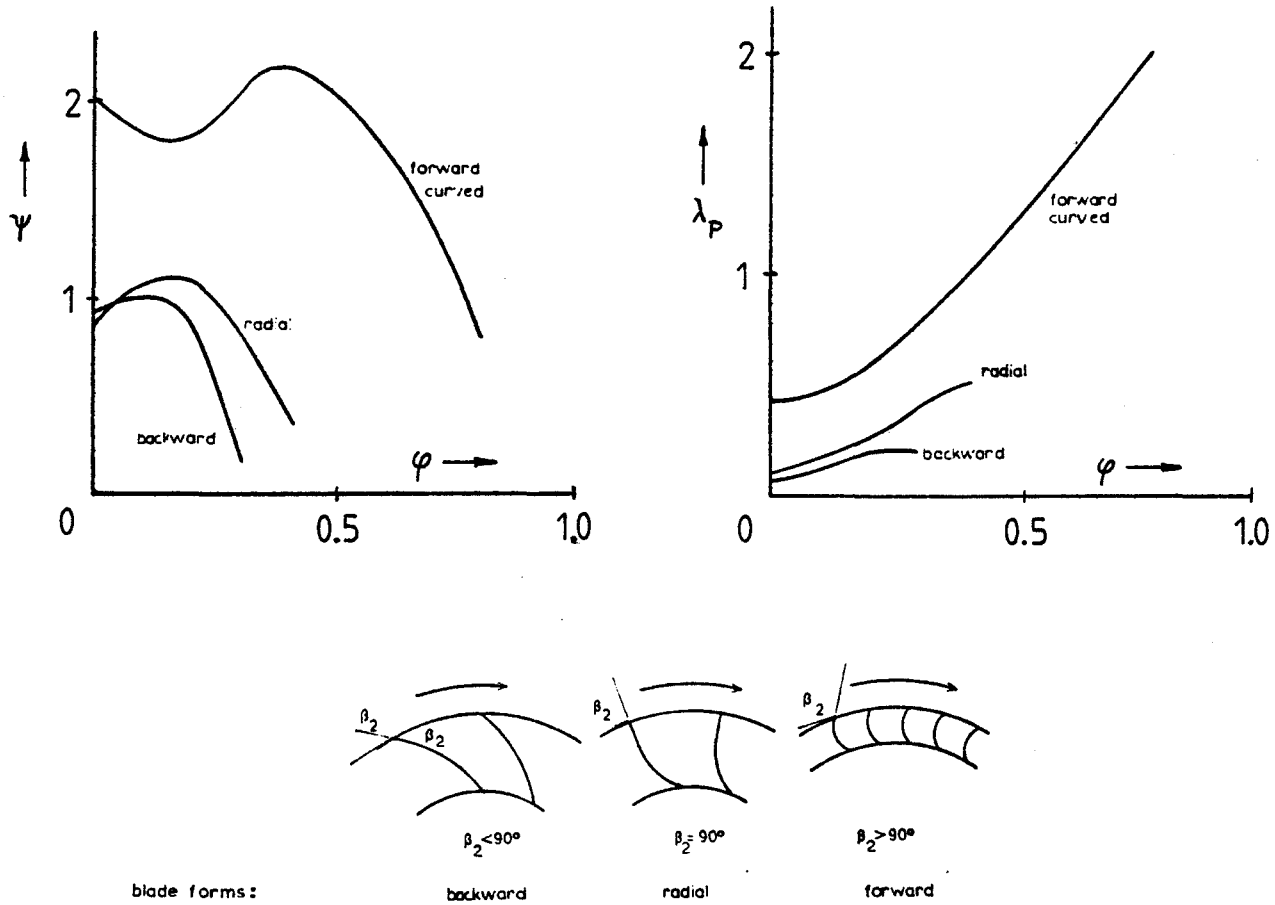

Fig.4.24 The approximate behaviour of the pressure coefficient ψ and the power coefficient λ_p as functions of the volume coefficient φ for centrifugal fans with a forward, radial or backward bladed impeller.

The essential angles and velocities inside an impeller are shown in Fig.4.25.

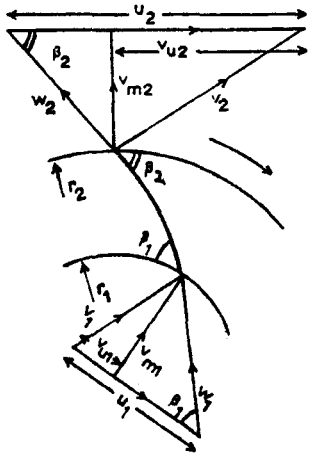

Fig.4.25 The impeller speeds u, the absolute gas velocities v with their tangential components v_u and their radial (or meridional) components v_m, the relative gas velocities w and the blade angles β at the impeller inlet (index 1) and at the impeller outlet (index 2) for a backward bladed impeller.

Ideally, the gas should follow the direction of the blades while passing through an impeller (w_1 in the direction of β_1 and w_2 in the direction of β_2). This can only happen when the impeller consists of an infinite (∞) number of blades with zero thickness. When it is supposed in addition that no friction losses occur, it can be shown by using Bernoulli's equation that the total theoretical pressure difference across an impeller is given by

$$\Delta p_{th\infty} = (1/2)\rho(u_2^2-u_1^2) + (1/2)\rho(v_2^2-v_1^2) + (1/2)\rho(w_1^2-w_2^2) = \rho\, u_2\, v_{u2} - \rho\, u_1\, v_{u1} \qquad (4\text{-}91)$$

(see Fig.4.25 for the clarification of the symbols).
The term $(1/2)\rho(u_2^2-u_1^2)$ is an increase of the static pressure due to the centrifugal forces acting on the gas. It is the most valuable term of (4-91), as it does not have any connection with possible friction losses.
The term $(1/2)\rho(v_2^2-v_1^2)$ is an increase of the dynamic pressure. It can become available as an increase of the static pressure only after the gas has been led through gradually enlarging ducts (e.g. a fan casing).
The term $(1/2)\rho(w_1^2-w_2^2)$ is an increase of the static pressure due to the fact that the space between adjacent blades becomes larger towards the outer diameter of the impeller, so that $w_2 < w_1$.
As the gas enters a centrifugal fan usually in a radial direction, the second part of (4-91) is reduced to

$$\Delta p_{th\infty} = \rho u_2 v_{u2} = \rho u_2^2 - \dot{V}\rho u_2/(\pi D_2 B_2 \tan\beta_2) \qquad (4\text{-}92)$$

or, expressed in ψ and φ,

$$\psi_{th\infty} = 2 - \varphi\, D_2/(2B_2\tan\beta_2) \tag{4-93}$$

where B_2 is the blade height at the outer impeller diameter D_2. The straight characteristics of (4-93) have been derived for the impeller without the fan casing, while Fig.4.24 presents characterictics of complete fans. In reality the characteristics of (4-93) are bent downwards by friction losses, which are proportional to $\dot{V}^2$ and there fore to φ^2.
The theoretical static pressure increase across the impeller follows from (4-91) (see Fig.4.25 for the clarification of the symbols):

$$\begin{aligned}\Delta p_{st,th\infty} &= (1/2)\rho(u_2^2-u_1^2) + (1/2)\rho(w_1^2-w_2^2) = \\ &= (1/2)\rho(u_2^2-w_2^2+v_1^2) \approx \\ &\approx (1/2)\rho(u_2^2-w_2^2+v_{2m}^2).\end{aligned} \tag{4-94}$$

With $w_2=v_{2m}/\sin\beta_2$ and using $\dot{V}=\pi D_2 B_2 v_{2m}$, the corresponding pressure coefficient takes the form

$$\psi_{st,th} = 1 - \varphi^2\,[D_2/(4B_2\tan\beta_2)]^2 \tag{4-95}$$

and reaches its maximum value 1 for radial bladed impellers: $\beta_2=90^\circ$.
Therefore it is proposed to use such an impeller in the new fan design.
Eck (ECK72) shows that, in order to minimize friction losses inside the impeller that are proportional to $(1/2)\rho w_1^2$,

$$\beta_1 < 35^\circ \quad \text{and} \quad D_1/D_2 > 1.194\,\varphi^{1/3} \tag{4-96}$$

where β_1 is the blade angle at the impeller inlet and D_1/D_2 the ratio of the impeller diameters at the inlet and at the outlet. The blade height B_1 at the impeller inlet is usually equal to $D_1/2$. With

$$\dot{V} = \pi D_1 B_1 v_{m1} = (\pi D_1^2/2)\, v_{m1} \tag{4-97}$$

β_1 can be calculated from

$$\beta_1 = \arctan\,(v_{m1}/u_1) = \arctan\,[(\varphi/2)\,(D_2/D_1)^3]. \tag{4-98}$$

The optimum number of blades z is approximately given by

$$z \approx 10\,\sin\beta_2\,/\,(1 - D_1/D_2). \tag{4-99}$$

In a fan design it is usually proposed that $v_1=v_{1m}$ is equal to v_{2m} (see (4-94)). Combining $\dot{V}=\pi D_2 B_2 v_{m2}$ with (4-97) yields the blade height B_2 at the impeller outlet:

$$B_2 = (D_1/D_2)\ B_1. \qquad (4\text{-}100)$$

In order to minimize friction losses, the profile of a fan casing should follow a streamline of a free vortex. In a free vortex the angular momentum of a mass element remains constant:

$$v_u\ r = \text{constant} \qquad (4\text{-}101)$$

where v_u is the tangential velocity and r the distance from the impeller rotation axis. As the free vortex flow takes place outside the impeller, r is larger than $D_2/2=r_2$. The height B of the fan casing is usually taken larger than B_2 in order to reduce the absolute velocity v_2 (see (4-91)). Usually $B\approx 2B_2$ as is shown in Fig.4.26.

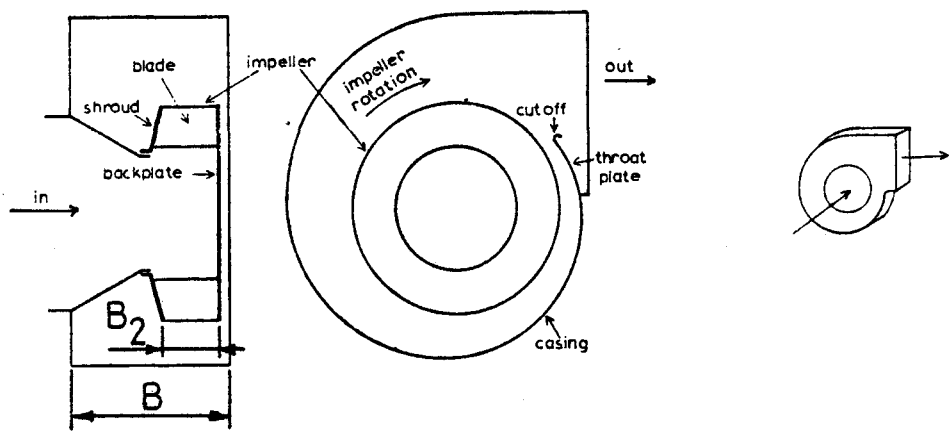

Fig.4.26 The way in which an impeller and a casing are combined to yield a centrifugal fan. The impeller blades are always fixed to the backplate and are usually covered at the other side by a conical plate, called the shroud.

Mass conservation demands that

$$2\pi r_2\ B_2\ v_{m2} = \dot{V} = 2\pi r\ B\ v_m \qquad (4\text{-}102)$$

and as $v_{u2}r_2=v_u r$ according to (4-101), it follows that

$$v_m/v_u = (B_2/B)\ (v_{m2}/v_{u2}). \qquad (4\text{-}103)$$

As $v_m := dr/dt$ and $v_u := r\, d\vartheta/dt$ where ϑ is the rotation angle and t the time, the casing profile is given by

$$\vartheta(r) = (v_u/v_m)\ \ln(r/r_2) \text{ or } r(\vartheta) = r_2\ e^{(v_m/v_u)\vartheta}. \tag{4-104}$$

This profile is called a logarithmic spiral (see Fig.4.26(b)). It intersects each circle around the origin at the same angle $\arctan(v_m/v_u)$ because v_m/v_u is a constant (4-103). For radial bladed fans $v_{u2}=u_2$. Combining (4-103), (4-102) and (4-89) in this case, it follows that

$$v_m/v_u = (\varphi/4)\ (D_2/B). \tag{4-105}$$

5. MEASURING METHODS

5.1 Measurements

The first quantities of interest are the rotation frequencies ν of the fans as functions of the variable resistance inside the frequency converter by which the fan motors are driven. At a fixed resistance, ν may decrease with increasing gas density.
Other important quantities are the cold losses in each fan ($P_{sh}+\dot{Q}_{f,con}$) and the cold losses along the transfer lines ($\dot{Q}_{t1}$ and $\dot{Q}_{t2}$, see Fig. 4.23). By measuring the temperature difference ΔT_a over the heat exchanger at the application and the temperature differences ΔT across the fans and the transfer lines, these quantities follow via (4-4), (4-29) and (4-31) from

$$\text{cold loss} = \dot{Q}_a \, \Delta T \, / \, \Delta T_a \qquad (5\text{-}1)$$

when the heat flow at the application, $\dot{Q}_a$, is known.
In order to analyse the behaviour of the cryogenerator and the transfer lines a special unit was built. It will be referred to as the measuring unit and it contains for both circuits the part on the right hand side of the points 4 and 7 in Fig.4.23. In the measuring unit a known heat flow $\dot{Q}_a$ is supplied to the gas, and by measuring the temperature difference over the heat exchanger the cold losses are obtained via (5-1). The mass flow follows from (4-66).
Each fan generates a static pressure difference which equals the pressure drop over the rest of the circuit. In order to know which part causes the largest pressure drop, the static pressure differences 1-3, 3-4, 4-7, 7-8 and 8-1 are measured (See Fig. 4.23).

5.2 The dimensions of the measuring unit

In determining the dimensions of the heat exchangers it was argued that in order to assure proper heat transfer Re should be larger than 2300, even at T_a = 300K. This results via (4-38), (4-6), (4-2), p=20 bar and V=200 cm^3/s in an inner diameter D < 27 mm. Other requirements were $\Lambda > 2$ at room temperature (see (4-34)) and a small pressure drop with respect to the pressure difference over the fan. In the actual design copper tube heat exchangers were used with D = 8 mm and a length L = 1.6 m.
Each heat exchanger has been soldered around a hollow copper cylinder with a wall thickness of 10 mm. Between them lies a 3 m long heating resistance with R = 18 Ω.
The coil diameter D_c of the heat exchangers is 70mm. Each end of a heat exchanger tube has been fixed to a hollow copper block (25 mmx30mmx70mm) via a thin-walled (0.3 mm) tube of stainless steel (inner diameter 7.4 mm, length 100 mm). The blocks assume the temperature of the gas which flows through them when entering or leaving a heat exchanger. Thermometers, mounted on them, measure the gas temperature. The tubes of stainless steel prohibit heat flowing from the heat exchangers towards the blocks. This heat flow would be especially disastrous when trying to measure the temperature of the "cold" gas entering the "warm" heat exchanger. In appendix 10.5 the dimensions of the stainless steel tubes have been derived.
The 20K heat exchanger is surrounded by a 70K radiation shield, which is fixed to the 70K-heat exchanger.
The heat exchangers are mounted on an aluminum flange (diameter 0.35 m). A stainless steel kettle (height 0.3 m) is placed over them and fixed to the flange. After mounting the flange on the A20 cryogenerator or on the end of the outer transfer hose, the measuring unit can be evacuated.

5.3 Sensors and measuring instruments

The rotation frequencies of the fans are measured by using opto-couplers. They consist of a photo diode emitting infrared radiation and a transistor which functions as a detector. When a rotating disk with a slit is placed partially between the diode and the transistor, the transistor will only receive radiation from the diode when the slit passes by. By this process an alternating collector voltage is generated, which is supplied to a digital counter. In our case the disk (aluminum, thickness 1 mm, diameter 25 mm) has been fixed to the impeller shaft, which is just sticking out above the motor house.
The digital counter possesses several terminals supplying 5V over 100 Ω. It has been connected to the opto-couplers as shown in Fig. 5.1.

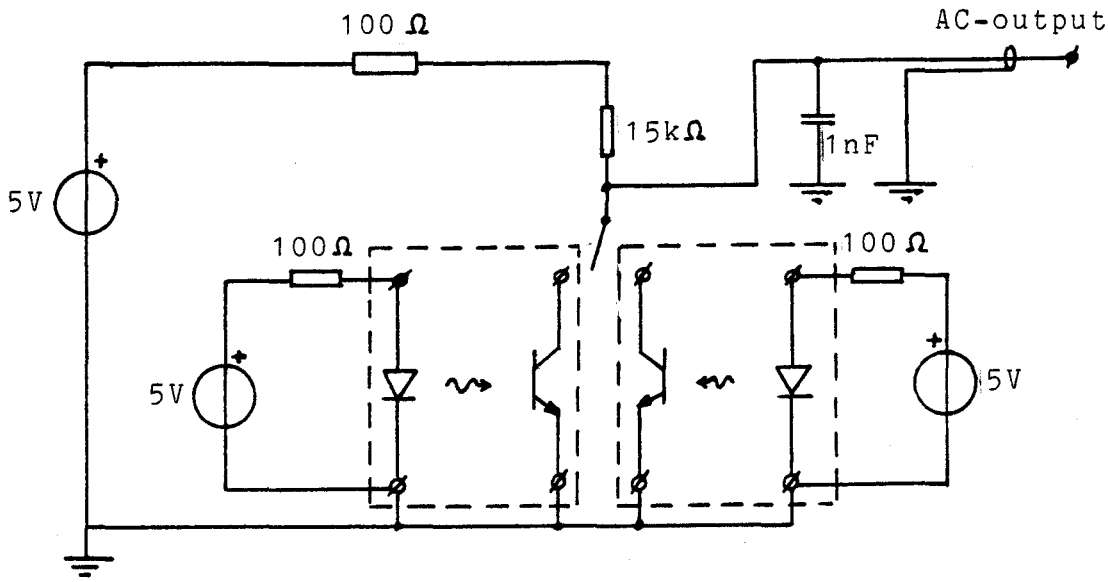

Fig. 5.1 Connection of the opto-couplers (surrounded by dashed lines, mounted on the 20K- and the 70K-fan respectively) via a switch and a coax cable to the AC-input of the digital counter.

The temperatures in the circuits are measured by using H_2 - and N_2 - vapour pressure bulbs, Allen-Bradley carbon resistances of 100 Ω, 470 Ω, and 15kΩ and by Pt100 resistances. The places at which temperatures are measured have been indicated with an asterisk in Fig.5.2.

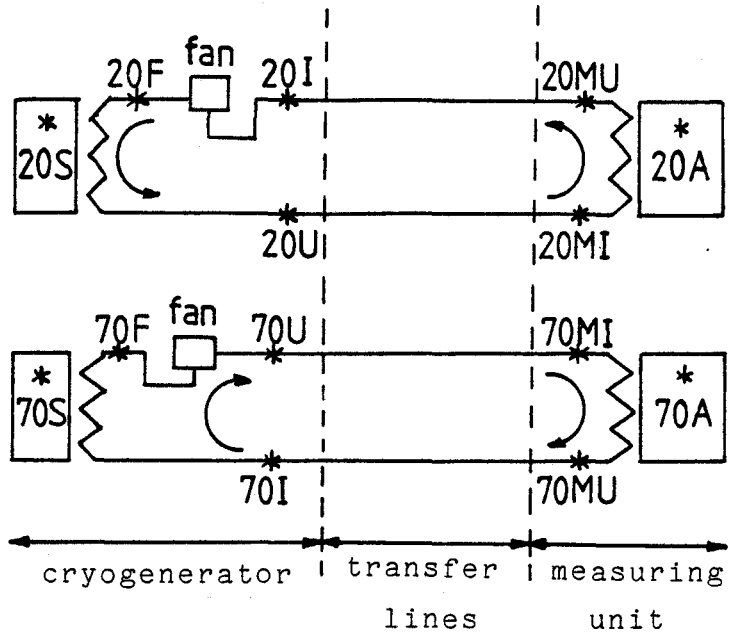

Fig. 5.2 Places at which temperatures can be measured have been marked with an asterisk (*). Clarification of the symbols: S=stage, A=application, I=cryogenerator in, F=between fan and stage, U=cryogenerator out, MI=measuring unit in, MU=measuring unit out

Table 5.1 shows where the thermometers have been placed.

	20							70						
	S	I	F	U	MI	MU	A	S	I	F	U	MI	MU	A
H_2-bulb	X				X	X								
N_2-bulb												X	X	
Allen-Bradley(Ω)	15k	15k	15k	15k	100	100	100	15k	15k	15k	15k	470	470	470
Pt100	X				X	X	X	X				X	X	X

Table 5.1 Thermometer types and the places where they are situated. See also Fig. 5.2.

The vapour pressure bulbs are compact cylinders enclosing a volume of about 1 cm^3.
The bulbs in the measuring unit have been connected to Leybold manometers (full scale 2000 mbar) via stainless steel capillaries (1x2 mm) inside and via copper tubes (4x6 mm) outside the measuring unit. They function as accurate thermometers when there is liquid in them. Therefore they can only be used between the triple point and the critical point of the gas.
With a maximum pressure of 2000 mbar we find for normal H_2 $14K \leq T \leq 23K$ and for N_2 $63K \leq T \leq 85K$.
In order to measure temperatures higher than 70K, Pt100 resistances are used in combination with a programmable Philips multi-point data recorder, type PM8237A. This instrument registers the resistance value via a four wire measurement and plots or prints the temperature in °C.
The Pt100 resistances of the measuring unit have been placed in the copper blocks (MI and MU) and in the copper cylinders (A) mentioned in paragraph 5.2. To insure a good thermal contact with the copper they were covered beforehand with Apiezon grease. The Pt100 resistances in the cryogenerator were clamped on the stage surfaces after having been covered with aluminum paste to improve the thermal contact.

The temperature gap between 20K and 70K is covered by Allen-Bradley carbon resistances (See Fig. 5.3). They are measured by an IT resistance bridge, which has a range of 20 Ω to 2 MΩ.
In order to prevent self heating of a resistance, the bridge supplies to it a small excitation voltage (10 μV to 1 mV, 25 Hz).
Therefore it is necessary to screen the cables connecting the Allen-Bradleys to the IT-bridge.

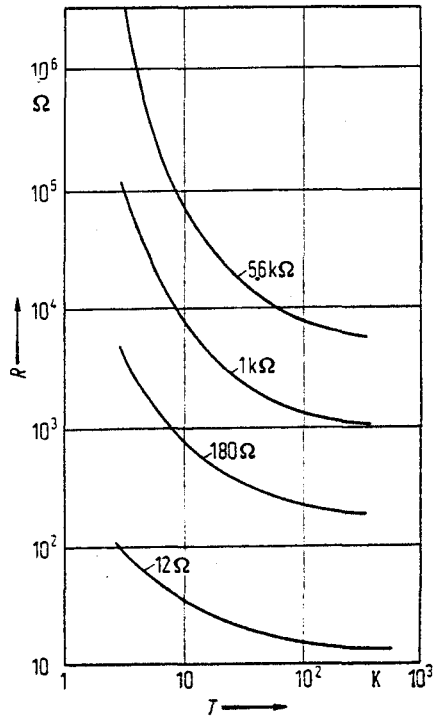

Fig. 5.3 R-T-characteristics of four Allen-Bradley resistances (EDE81)

Before an Allen-Bradley is used as a thermometer it should be immersed in liquid nitrogen (77K) between ten and twenty times. After each immersion it should have time to assume the room temperature again. This thermal treatment results in an improved reproducibility.

The Allen-Bradleys inside the measuring unit have been mounted on copper plates as shown in Fig. 5.4.

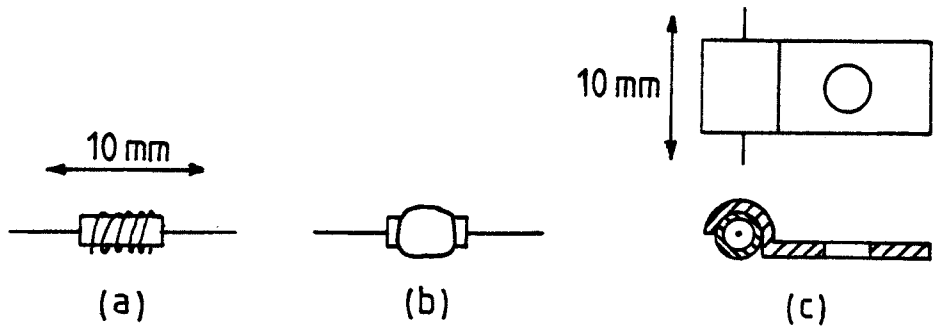

Fig. 5.4 Fixation of an Allen-Bradley resistance inside the measuring unit to a copper plate.

Step 1) Copper wire (Ø 0.1 mm to 0.3 mm) is wrapped around the body of an Allen-Bradley

Step 2) The copper wire and the Allen-Bradley are covered by a "drop" of tin solder

Step 3) The body of the Allen-Bradley is soldered to a copper plate.

Each copper plate can be screwed to the surface of which the temperature has to be measured. The thermal contact is improved by aluminum paste.

The Allen-Bradleys inside the cryogenerator have been mounted directly on the tubes by means of tie-wraps. Thermal contact has again been achieved by aluminum paste.
The measuring leads of the Allen-Bradleys are 100µm manganine wires (see Fig. 5.5). They were used instead of copper wires in order to minimize conductive heat flows towards the thermometers.

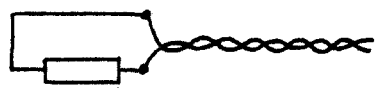

Fig. 5.5 Allen-Bradley resistance soldered to twined manganine wires

By twining the manganine wires the possibility of inducted voltages influencing the measurements is kept to a minimum. The wires are led over the surface of which the temperature will be measured, just before they reach the thermometer. This action, which is called thermal grounding, prevents conductive heat flows in the wires from entering the thermometer.
The R-T-characteristic of an Allen-Bradley can be written as

$$1/T = \sum_{i=1}^{n} a_i \, (\ln R)^i . \qquad (5\text{-}2)$$

The constants a_i are calculated after calibrating the Allen-Bradleys with the vapour pressure bulbs and the Pt100 resistances inside the measuring unit.
The IT resistance bridge has two input canals, which are called A and B respectively. As there are fourteen Allen-Bradleys to be measured, a switching unit has been built (see Fig. 5.6).

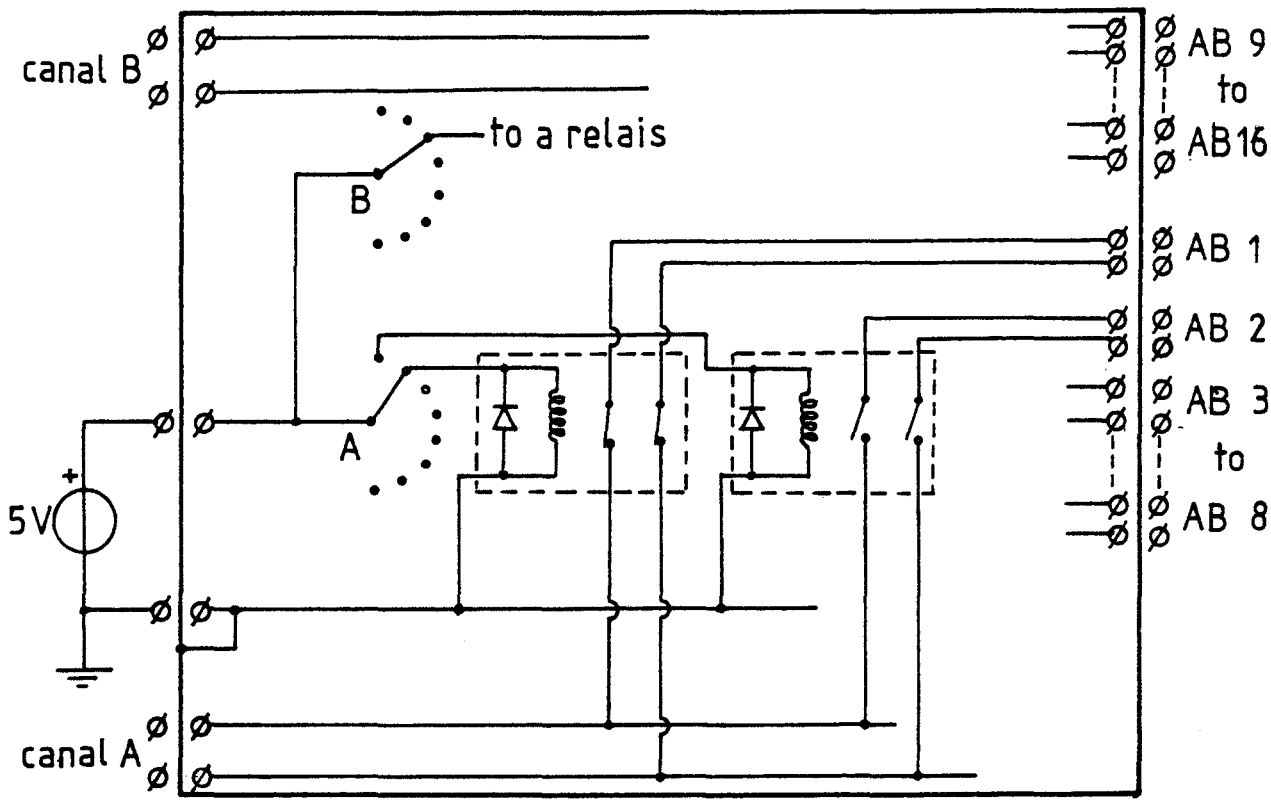

Fig. 5.6 Switching unit with which 16 Allen Bradleys can be measured on the canals A and B of the IT resistance bridge. The parts surrounded by dashed lines are reed relais.

The switching unit is fed by a 5V d.c. power supply, which has been connected to two switches, A and B. Each terminal of a switch has been connected to a reed relais. As soon as a terminal receives 5V, the corresponding relais closes its two switches and thereby connects a resistance to canal A or B of the IT-bridge. Example: in Fig. 5.6 the Allen-Bradley AB1 is measured on canal A. In building up the switching unit a print was used which has been designed by J. Keltjens (KEL82). Reed relais were used in order to keep contact resistances, occurring in the switches after a few years use, from influencing the measurements. Therefore the switching unit is also reliable when measuring resistances lower than 100 Ω. By connecting the relais to a central processing unit, it would be possible to carry out automatic temperature measurements.

The Allen-Bradleys inside the measuring unit have been connected to switch A of the switching unit via one screened computer cable. Via another screened computer cable the Allen-Bradleys inside the cryogenerator have been connected to switch B. All screening has been fixed to the aluminum-walled switching unit, which is grounded via the external 5V supply.

In order to measure the static pressure differences in each circuit, holes have been made through the tube walls at the places I, F, U, MI and MU (See Fig. 5.2). In each hole a stainless steel capillary (1x2 mm) has been soldered, through which the local static pressure is supplied to a measuring instrument (see Fig. 5.7).

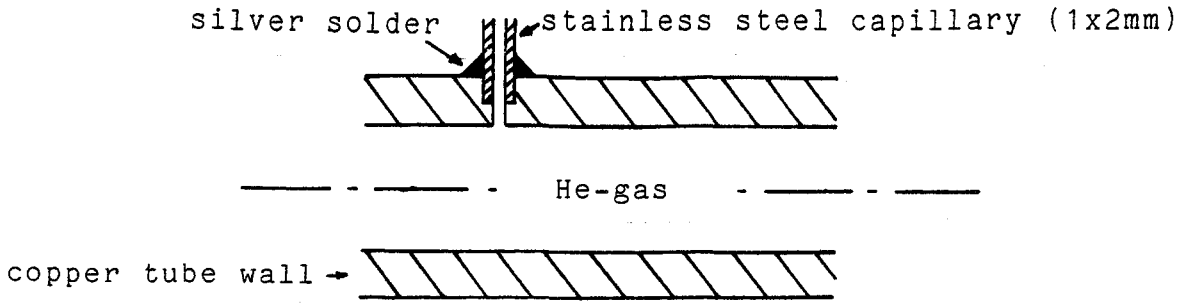

Fig. 5.7 Stainless steel capillary fixed to the tube system in order to conduct the local static pressure to a measuring instrument.

As the pressure differences over the 20K-fan and the 70K-fan could be expected to be 300 mbar and 100 mbar respectively (see (4-19)) two differential pressure transducers were used with a full scale value of 10 psi = 689 mbar and 175 mbar respectively. Each supplies a voltage, proportional to the measured pressure difference, to the PM8237A recorder mentioned before, the full scale values being 50mV and 25mV respectively.
The average tube system pressures are registered by two 35 bar pressure transducers. The voltages which they supply to the PM8237A recorder have a full scale value of 100mV.

The stainless steel capillaries (see Fig. 5.7) have been connected to the transducers outside the cryogenerator and the measuring unit via 4x6 mm copper tubes and via three-way valves. The pressure difference over a fan is measured continuously by the 689 mbar-transducer, while the other interesting pressure differences (I-MU, MU-MI, MI-U, 20U-20F and 70I-70F, see Fig. 5.2) are measured via the 175 mbar-transducer by setting the three-way valves in the right positions.
In Fig. 5.8 all the essential connections have been shown.

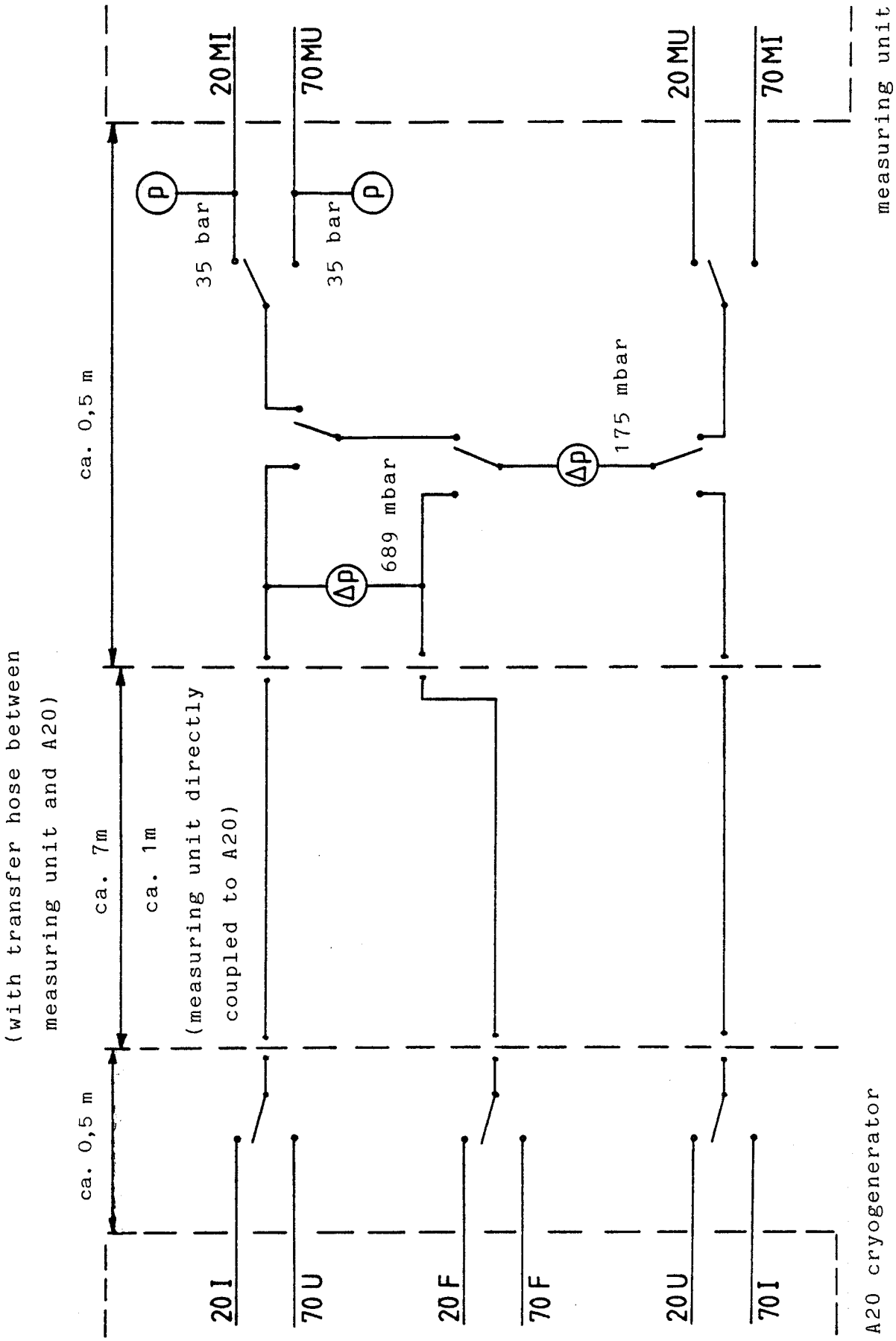

Fig.5.8 Measurement of static pressure differences in the 20K- and the 70K-circuit as shown in Fig.5.2. The external connections to the pressure transducers (Δp,p) have been made by 4x6mm copper tubes and 8 three-way valves.

6.1 Results of the computer calculations

6.1.1 The influence of the fan position on the application temperature and the cool-down time

Task 1, which was mentioned at the beginning of paragraph 4.2.4, has been carried out to investigate the behaviour of the transfer system when the fan is placed behind the stage or in front of it. All the printed results of the corresponding computer calculations have been presented in appendix 10.4. Only the most important of them will be given in this paragraph.
The following input data were used: F=1 or -1, $\dot{Q}_a$=0 W to 400 W (20K-circuit) and 0 to 800 W (70K-circuit), $\dot{Q}_{t1}=\dot{Q}_{t2}=\dot{Q}_{f,con}$=0 W, p=20 bar, c_p=5.2 kJ/(kg K), ΔH_f=45 m, η_f=46%, the heat exchanger lengths $L_s=L_a$=1.8 m, their inner diameters $D_s=D_a$=6 mm, their coil diameters $D_{sc}=D_{ac}$=0.11 m, the lengths of the transfer lines L_t=7 m and their diameters $D_{t1}=D_{t2}$=12.7 mm. The influence of bends etc. has been neglected (see Fig.4.23).

		20K-circuit					70K-circuit				
fan behind the stage (F=1)	$\dot{Q}_a$(W)	0	100	200	300	400	0	200	400	600	800
	$\Delta\dot{V}$(cm³/s)	0	20	40	60	80	0	40	80	120	160
	$\dot{m}_1$(g/s)	14.47	8.050	4.176	2.036	0.9261	3.970	2.686	1.676	1.089	0.7277
	$\dot{V}_{f1}$ (cm³/s)	231	232	219	197	165	228	209	186	161	136
	T_{s1} (K)	15.27	27.45	50.10	92.41	171.5	55.12	74.52	106.0	141.8	179.4
	T_{a1} (K)	15.47	30.34	60.11	121.7	255.5	55.31	89.61	153.1	249.2	392.3
fan in front of the stage (F=-1)	$\dot{Q}_a$(W)	0	100	200	300	400	0	200	400	600	
	$\Delta\dot{V}$(cm³/s)	0	20	40	60	80	0	40	80	120	
	$\dot{m}_2$(g/s)	14.50	7.698	3.761	1.679	0.6489	3.975	2.396	1.246	0.5388	
	$\dot{V}_{f2}$ (cm³/s)	232	241	237	222	196	228	226	218	200	
	T_{s2} (K)	15.27	27.39	49.98	92.22	171.2	55.12	74.49	105.9	141.7	
	T_{a2} (K)	15.29	30.21	60.84	127.4	290.5	55.13	91.13	168.7	356.9	
	$\frac{T_{a2}-T_{s2}}{T_{a1}-T_{s1}}$	0.1	0.98	1.08	1.20	1.42	0.05	1.10	1.33	2.00	

Table 6.1 The dependency of the theoretical volume flow difference $\Delta\dot{V}$ (defined by (4-47), see also Table 4.3), the mass flow $\dot{m}$, the volume flow through the fan $\dot{V}_f$, the stage temperature T_s and the application temperature T_a on the cooling power at the application $\dot{Q}_a$, when the fan is placed behind the stage (index 1) or in front of it (index 2). The lowest line corresponds with the values of $\Delta T_2/\Delta T_1$ in Table 4.3.

We will now estimate the influence of the place of the fan on the cool-down time, that is the time needed to cool the application from an initial temperature (usually 300 K) to a certain end temperature. It is assumed that the application temperature is homogeneous, that the heat capacity of the application is large with respect to those of the stages, the heat exchangers and the transfer lines, and that the heat leaks are small in comparison with $\dot{Q}_a$. The rate dT_a/dt is then given by

$$\dot{Q}_a(T_a) = -m_a\, c_{p,a}(T_a)\, dT_a/dt \qquad (6\text{-}1)$$

where m_a and $c_{p,a}$ are the mass and the specific heat capacity of the application respectively.
As the application usually consists of metal parts (made of Al, Cu etc.) the specific heats of aluminum and copper have been presented in appendix 10.2. For $T_a<50$ K they are proportional to T_a^3, whereas they approximate their maximum value 3R/M when T>300 K (R is Rydberg's universal gas constant and M is the molar mass of the metal). In order to use $\dot{Q}_a(T_{a1})$ and $\dot{Q}_a(T_{a2})$ as given by Table 6.1, it has to be assumed that the decrease of the application temperature during one circulation of the helium gas through the tube system is small with respect to T_a. Applying (6-1), this means that

$$m_a \gg \dot{Q}_a(T_a)\, \Delta t_{ci} \,/\, [c_{p,a}(T_a)\, T_a] \qquad (6\text{-}2)$$

where $\Delta t_{ci}\approx 10$ s is the gas circulation period ($\Delta t_{ci} \approx V/\bar{\dot{V}}$ where V is the volume of the heat exchangers and the transfer lines, and $\bar{\dot{V}}=200$ cm^3/s). Regarding the 20K-circuit with $T_a=30$ K, $\dot{Q}_a=100$ W and $c_{p,Al}=31.5$ J/(kg K) it follows from (6-2) that $m_a \gg 1$ kg, which condition is usually fulfilled. This means that the changes of state in the transfer system are quasi-static and that the stationary state values of Table 6.1 provide valid information with respect to the cool-down time. The cool-down time Δt follows from (6-1):

$$\Delta t/m_a = \int_{T_{ae}}^{T_{ab}} [c_{p,a}(T_a) \,/\, \dot{Q}_a(T_a)]\, dT_a \qquad (6\text{-}3)$$

where T_{ab} and T_{ae} are the application temperatures at the beginning and at the end of the cool-down time respectively. The specific cool-down time Δt_m is estimated by linearizing $c_{p,a}(T_a)$ and $Q_a(T_a)$:

$$\Delta t_m := \Delta t/m_a \approx \int_{T_{ae}}^{T_{ab}} (C_1 T_a + C_2)/(C_3 T_a + C_4)\, dT_a$$

$$= (C_1/C_3)(T_{ab}-T_{ae}) + [(C_2/C_3)-(C_1C_4/C_3^2)]\cdot$$

$$\cdot \ln[(C_3T_{ab}+C_4)/(C_3T_{ae}+C_4)] \qquad (6\text{-}4)$$

where C_1 to C_4 are constants. In Table 6.2 several values of Δt_m have been given for aluminum and copper.

	circuit	20K		70K	
	T_{ab}(K)	300	120	300	160
	T_{ae}(K)	120	60	160	90
Al	Δt_{m1}(s/kg)	378	96.4	212	131
	Δt_{m2}(s/kg)	392	98.9	255	141
Cu	Δt_{m1}(s/kg)	173	52.2	93.7	65.4
	Δt_{m2}(s/kg)	179	53.5	112	70.3

Table 6.2 Specific cool-down times Δt_m of the application when it consists of aluminum (Al) or copper (Cu). The fan may be placed behind the stage (index 1) or in front of it (index 2). T_{ab} and T_{ae} are the application temperatures before and at the end of the cool-down time respectively.

When the application is cooled by the 20K-circuit from 300K to 60K, Δt_{m2} may be expected to be 3% larger than Δt_{m1} according to Table 6.2. The same table shows that Δt_{m2} will be about 15% larger than Δt_{m1} when the application is cooled by the 70K-circuit from 300K to 90K.
The pressure differences in the 20K-circuit with the fan behind the stage are presented in Table 6.3. In other cases (70K-circuit, fan in front of the stage) the pressure differences have other absolute values, but their percentages of the pressure difference Δp_f over the fan remain the same.

$\dot{Q}_a$(W)	$\Delta p_f = \Delta p_{19}$ (mbar)	Δp_{12} (mbar)	Δp_{56} (mbar)	$\frac{\Delta p_{12}+\Delta p_{56}}{\Delta p_f}$	Δp_{34} (mbar)	Δp_{78} (mbar)	$\frac{\Delta p_{34}+\Delta p_{78}}{\Delta p_f}$
0	276.4	97.27	98.29	71	40.41	40.43	29
100	153.4	51.18	55.32	69	24.42	22.49	31
200	84.14	27.49	32.62	71	13.02	11.01	29
300	45.74	14.80	19.86	76	6.28	4.81	24
400	24.72	7.71	12.43	81	2.73	1.85	19

Table 6.3 Static pressure differences $p_{ij} := |p_i - p_j|$ (see Fig.4.23) in the 20K-circuit with the fan behind the stage as functions of the cooling power at the application $\dot{Q}_a$.

6.1.2 The influence of the inner diameter of the heat exchangers on the application temperature

Task 2 has been carried out in order to investigate how the average transfer system pressure p, the static pressure head ΔH_f of the fan, the inner diameter D_{he} and the coil diameter D_c of the two heat exchangers in a circuit influence the efficiency of the transfer system (see the beginning of paragraph 4.2.4). The input data are presented in Table 6.4.

circuit	20K	70K	circuit	20K	70K
F	1	1	N_{23}	1	1
$\dot{Q}_a$(W)	20, 60	40, 120	N_{45}	1	1
$\dot{Q}_{t1}=\dot{Q}_{t2}$ (W)	5	10	N_{67}	1	1
$\dot{Q}_{f,con}$ (W)	5	5	N_{89}	1	2
p (bar)	20, 40	20, 40	L_{23}(m)	0.16	0.38
c_p(kJ/kgK)	6.0	5.2	L_{45}(m)	0.50	0.50
ΔH_f(m)	20, 45, 70	20, 45, 70	L_{67}(m)	0.50	0.50
η_f	0.5	0.5	L_{89}(m)	0.50	0.50
D_{he}(mm)	6, 8, 10, 12	6, 8, 10, 12	S_{23} to S_{89}	0.8	0.8
D_c(m)	0.10, 0.14	0.12, 0.14	λ'_t	0.07	0.07
L_t(m)	7	7			
D_t(mm)	12.7	12.7			

Table 6.4 Input data that were used in the calculations of task 2. The symbols are clarified in paragraph 4.2.3.

The length L_{he} of a heat exchanger was calculated by

$$L_{he}(D_{he}) = \pi D_c H \,/\, (D_{he}+2S_{he}+S_c) \qquad (6\text{-}5)$$

where H=7 cm is the height of both stages, S_{he}=1 mm the tube wall thickness ($D_{he}+2S_{he}$ is the outer diameter of the heat exchanger tube) and S_c=1 mm the space between subsequent coils (S_c is presently 3.5 mm on the 20K-stage and 5.5 mm on the 70K-stage).
The calculated values of the stage temperature T_s, the application temperature T_a and the volume flow through the fan $\dot{V}_f$ have been brought together in Table 6.5.

Table 6.5 Variation of the stage temperature T_s(K), the application temperature T_a(K) and the volume flow through the fan $\dot{V}_f$(cm^3/s) with the cooling power at the application $\dot{Q}_a$, the average transfer system pressure p, the static pressure head ΔH_f of the fan and the inner diameter D_{he} and the coil diameter D_c of the two heat exchangers in a circuit. In each block of three columns T_s, T_a and $\dot{V}_f$ are read from left to right and the minimum value of T_a at fixed values of $\dot{Q}_a$, p, ΔH_f and D_c has been underlined.

circuit			20K										
	$\dot{Q}_a$(W)		20						60				
	D_c(m)		0.10			0.14			0.10			0.14		
p (bar)	ΔH_f (m)	D_{he} (mm)											
20	20	6	17.68	18.65	109	17.66	18.66	99	22.62	25.41	107	22.60	25.55	96
		8	17.86	18.58	189	17.84	18.49	180	22.81	24.76	188	22.79	24.58	178
		10	17.97	18.72	240	17.96	18.58	234	22.92	24.91	239	22.91	24.55	233
		12	18.02	18.89	263	18.02	18.70	260	22.96	25.29	262	22.96	24.77	259
	45	6	18.30	19.07	170	18.23	19.00	156	23.24	25.20	168 [1]	23.16	25.19	152
		8	18.89	19.53	291	18.83	19.40	277	23.85	25.34	290	23.78	25.13	275
		10	19.24	19.93	363	19.21	19.78	356	24.19	25.78	363	24.17	25.47	355
		12	19.38	20.20	397	19.38	20.02	393	24.34	26.21	395	24.34	25.79	392
	70	6	19.12	19.87	218	18.99	19.73	199	24.07	25.79	215	23.92	25.68	195
		8	20.21	20.89	368	20.10	20.70	351	25.19	26.59	367	25.07	26.32	349
		10	20.82	21.58	457	20.78	21.40	447	25.82	27.33	456	25.77	27.01	447
		12	21.08	21.97	497	21.07	21.78	492	26.07	27.87	496	26.07	27.48	491
40	20	6	17.91	18.47	106	17.88	18.43	98	22.87	24.35	107 [2]	22.83	24.34	99
		8	18.26	18.70	182	18.22	18.62	174	23.22	24.34	185	23.19	24.18	176
		10	18.48	18.96	234	18.47	18.85	229	23.44	24.62	235	23.43	24.37	230
		12	18.59	19.15	260	18.59	19.02	257	23.55	24.92	260	23.54	24.60	258

circuit			70K									
	$\dot{Q}_a$(W)		40				120					
	D_c(m)		0.12			0.14			0.12			0.14		
p (bar)	ΔH_f (m)	D_{he} (mm)												
20	20	6	59.00	66.48	88	59.00	66.87	84	67.14	89.44	82	67.13	90.75	77
		8	59.05	63.10	170	59.04	63.16	164	67.19	78.74	164	67.19	78.96	158
		10	59.08	62.43	228	59.07	62.31	225	67.23	76.56	223	67.23	76.27	220
		12	59.09	62.53	257	59.09	62.29	255	67.25	76.77	253	67.25	76.11	251
	45	6	59.12	63.95	141	59.11	64.17	134	67.28	81.13	134 [2]	67.27	81.87	126
		8	59.27	62.04	264	59.26	62.05	256	67.47	75.06	257	67.46	75.13	249
		10	59.37	61.77	349	59.36	61.67	344	67.60	74.01	344	67.59	73.75	338
		12	59.42	61.95	390	59.41	61.76	387	67.65	74.36	385	67.65	73.85	383
	70	6	59.29	63.19	181	59.27	63.35	172	67.49	78.35	173	67.47	78.89	164
		8	59.58	61.93	335	59.56	61.91	325	67.85	74.02	328	67.82	74.04	317
		10	59.77	61.87	439	59.76	61.76	433	68.09	73.44	433	68.08	73.19	427
		12	59.86	62.10	488	59.86	61.93	485	68.20	73.87	483	68.20	73.42	481
40	20	6	59.06	62.56	95	59.05	62.71	91	67.20	77.21	92 [4]	67.20	77.70	87
		8	59.14	61.18	176	59.14	61.18	171	67.31	72.95	173	67.31	72.96	168
		10	59.20	60.99	232	59.20	60.90	229	67.39	72.22	230	67.38	71.99	226
		12	59.23	61.12	259	59.23	60.97	258	67.42	72.53	257	67.42	72.11	256
	45	6	59.31	61.67	150	59.30	61.75	144	67.52	73.98	146	67.50	74.25	139
		8	59.60	61.09	272	59.59	61.06	265	67.89	71.74	268	67.87	71.70	261
		10	59.80	61.17	353	59.79	61.08	349	68.13	71.58	351	68.12	71.39	346
		12	59.89	61.38	392	59.89	61.25	390	68.24	71.97	390	68.24	71.65	388
	70	6	59.67	61.66	192	59.64	61.70	184	67.96	73.17	188	67.92	73.34	179
		8	60.25	61.58	344	60.21	61.53	336	68.67	71.91	340	68.63	71.84	331
		10	60.63	61.90	444	60.61	61.81	439	69.13	72.12	441	69.11	71.93	436
		12	60.80	62.20	491	60.80	62.08	488	69.34	72.60	488	69.34	72.31	486

The computer output, belonging to the blocks 1, 2, 3 and 4 in Table 6.5, is presented in appendix 10.4.

The pressures in a tube system vary with D_{he} as shown in Fig.6.1. The figure presents values in the 20K-circuit, but the form of the variations is the same in the 70K-circuit.

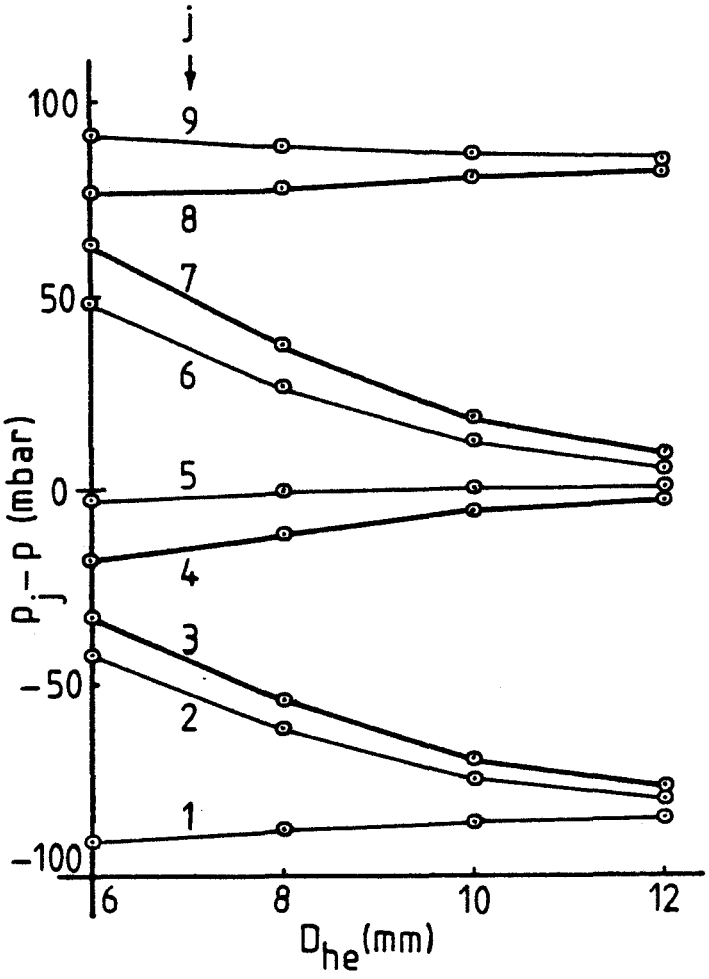

Fig.6.1 Variations of the pressures p_j ($1 \leq j \leq 9$, see Fig.4.23) with the inner diameter D_{he} of the two heat exchangers in the 20K-circuit. The following data were used: $\dot{Q}_a$=60 W, p=20 bar, ΔH_f=45 m and D_c=0.10 m (see block 1 in Table 6.5).

The temperature variations in the 20K-circuit and the 70K-circuit are shown in Fig.6.2(a) and (b) respectively.

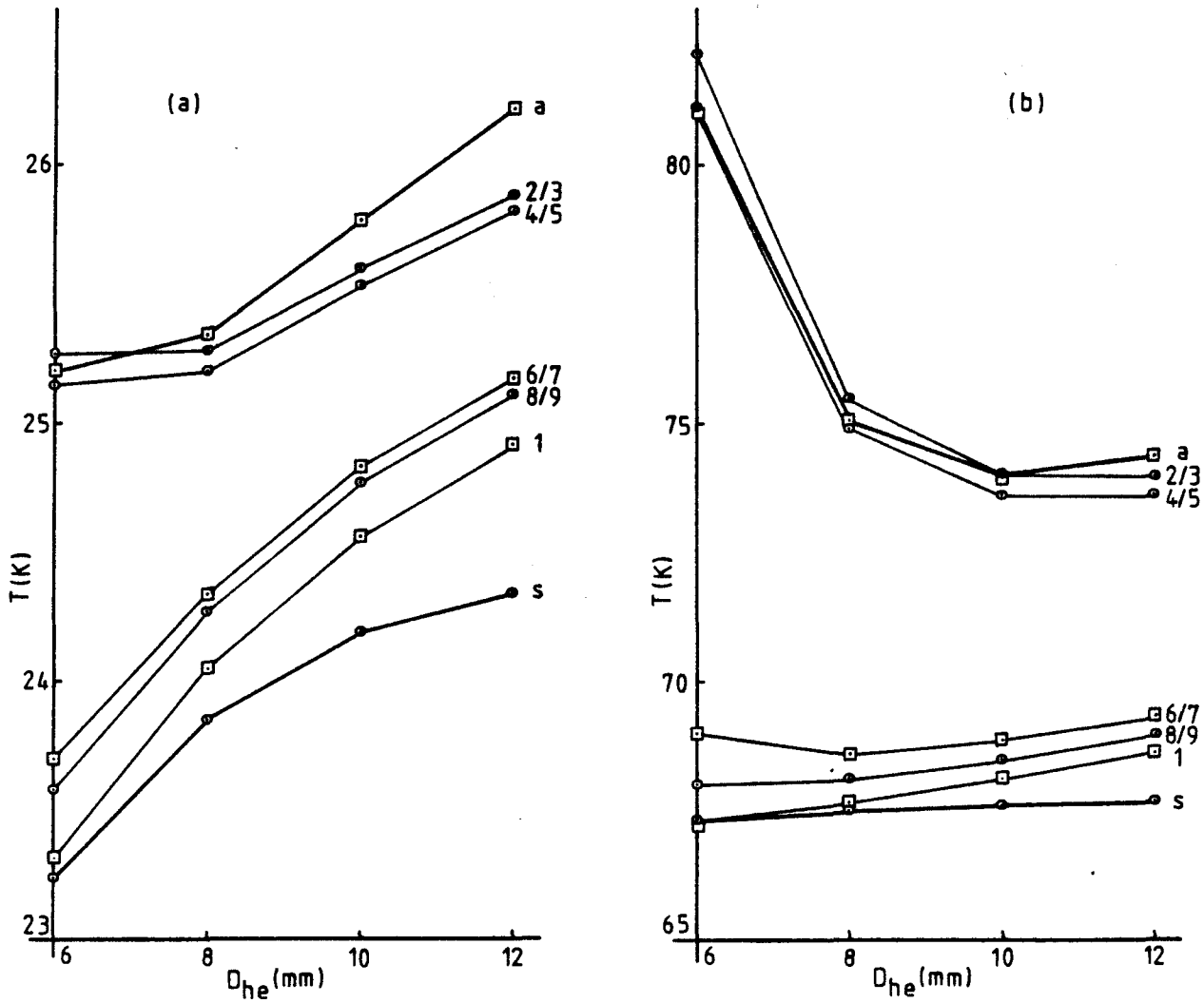

Fig.6.2 The temperature at the application (index a) and at the stage (index s) and the gas temperatures T_j ($1 \leq j \leq 9$, see Fig.4.23) as functions of the inner diameter D_{he} of the two heat exchangers in a tube system.
(a) 20K-circuit with $\dot{Q}_a$= 60 W, p=20 bar, ΔH_f=45 m and D_c=0.10 m
(b) 70K-circuit with $\dot{Q}_a$=120 W, p=20 bar, ΔH_f=45 m and D_c=0.12 m
(see the blocks 1 and 2 in Table 6.5).
Note the differently scaled T-axes.

6.2 Results of the measurements

Unfortunately it was not possible to test the calculations, presented in this report, by an intensive experimental investigation. Therefore we have to confine ourselves in this paragraph to the results of some introductory measurements concerning the fan rotation frequencies and the thermometer calibration.
The rotation frequencies ν of the 20K-fan and the 70K-fan have been measured as functions of the variable resistance inside the frequency converter. At each resistance value the impeller rotation frequencies of both fans were equal to each other. The mass flows, which increased during the cool-down period because of the increasing gas density, had no detectable influence on the rotation frequencies. The measurements were reproducible within 2 Hz (see Fig.6.3).

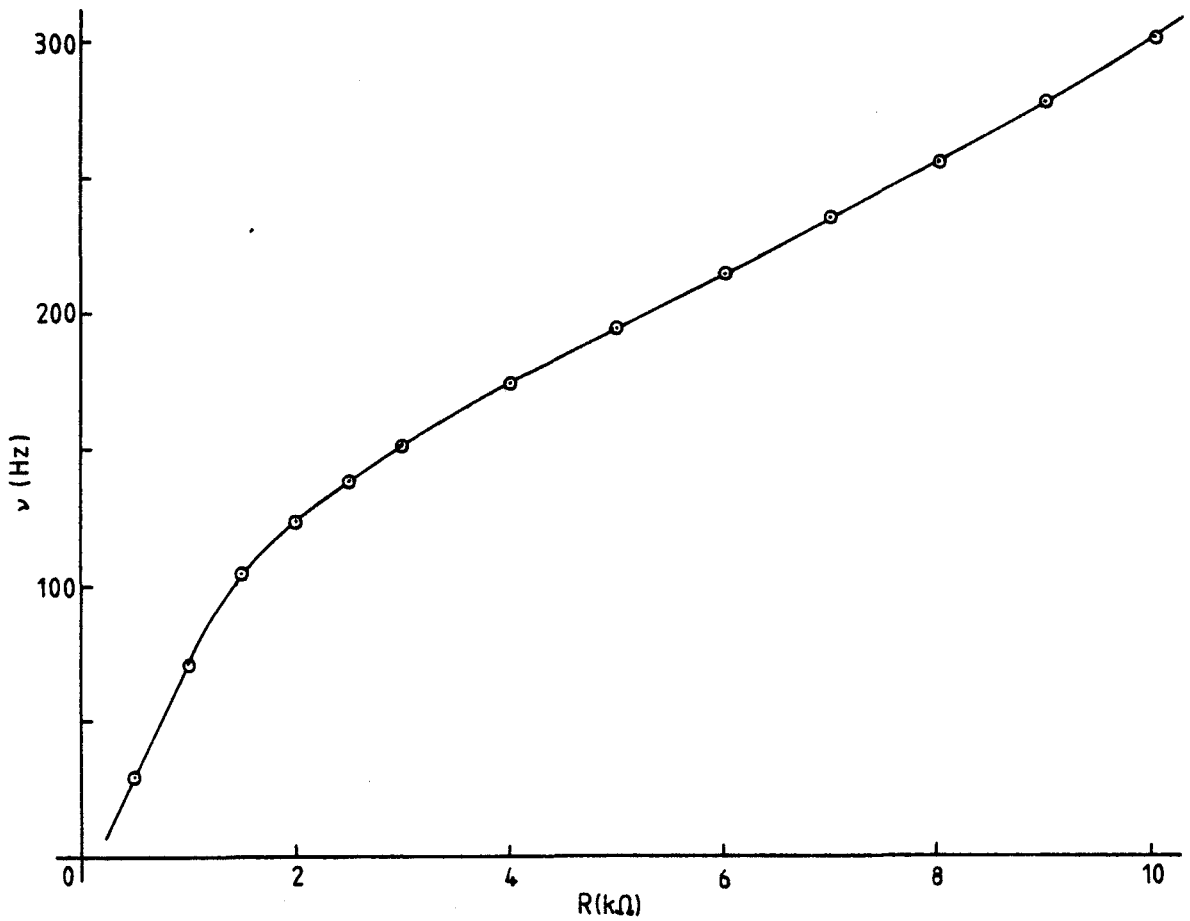

Fig.6.3 The rotation frequency ν of the fans as a function of the resistance R inside the frequency converter.

The results of the calibration of the Allen-Bradley carbon resistances inside the measuring unit have been presented in Fig.6.4 and Fig.6.5.

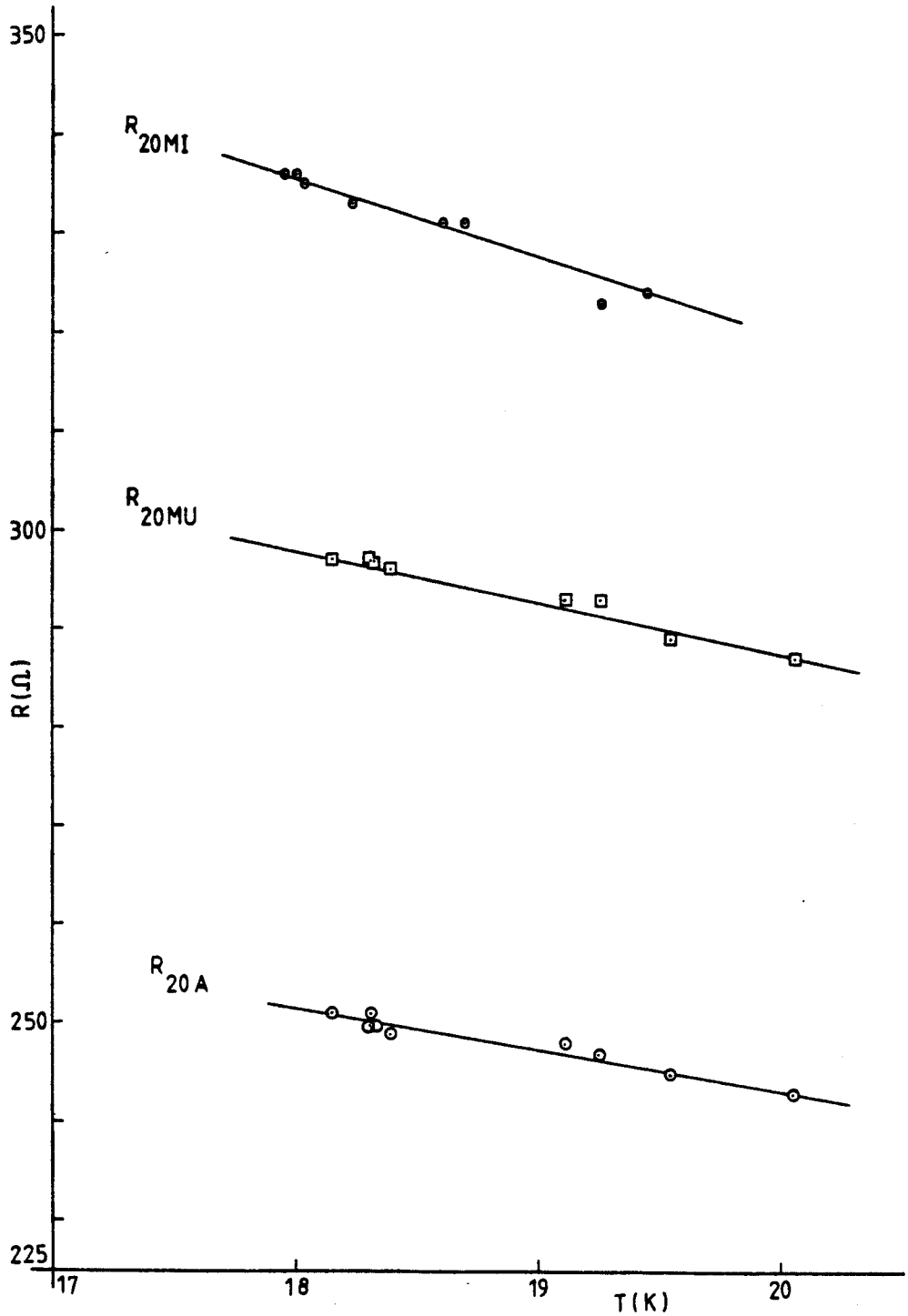

Fig.6.4 The resistance values R of the 100 Ω Allen-Bradley thermometers inside the measuring unit as functions of the temperature T. See Table 4.4 for the place of the thermometers.

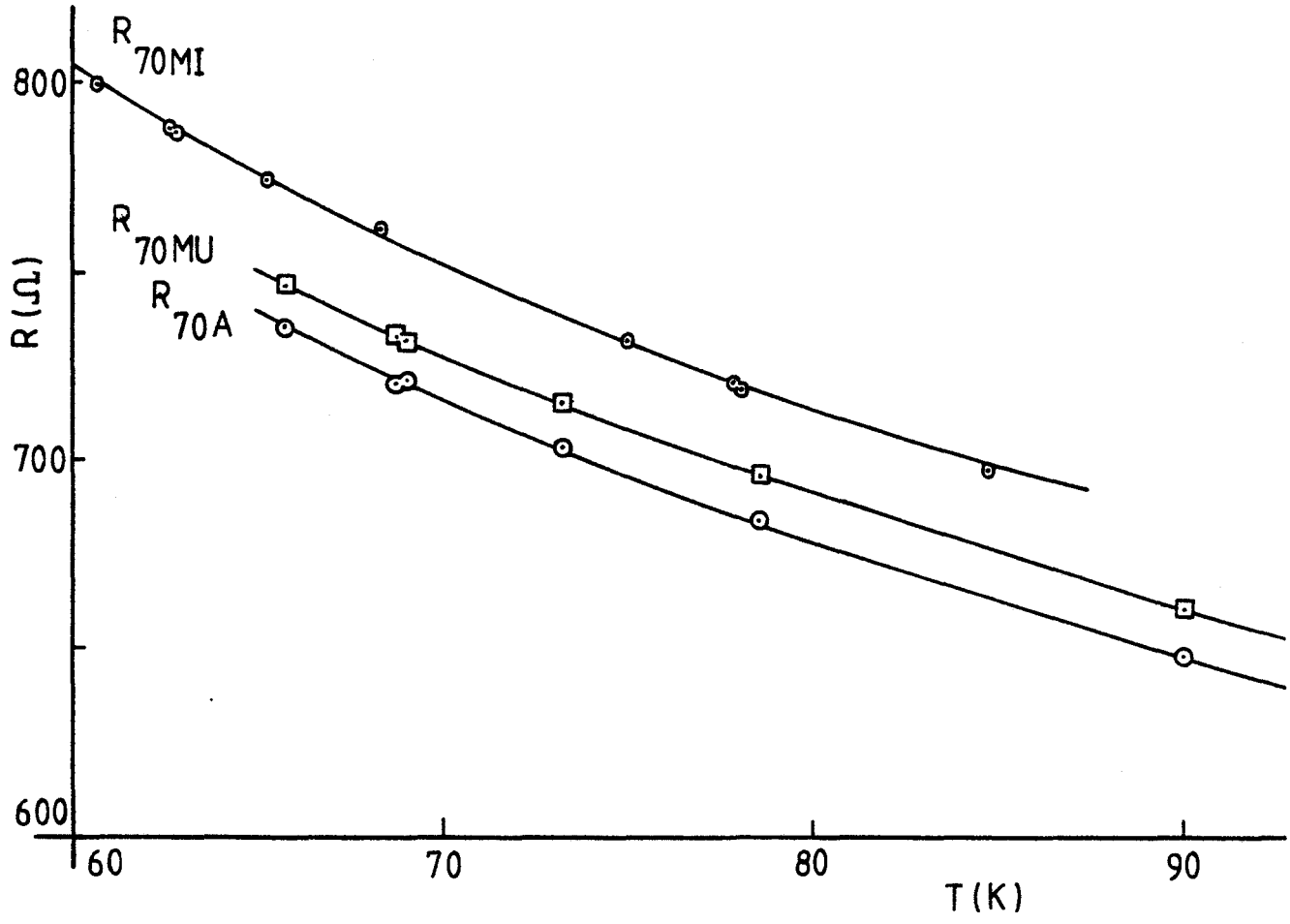

Fig.6.5 The resistance values R of the 470Ω Allen-Bradley thermometers inside the measuring unit as functions of the temperature T. See Table 4.4 for the place of the thermometers.

The 15 kΩ Allen-Bradley thermometers inside the cryogenerator have a sensitivity $dR/dT \approx 0.26$ kΩ/K between 63 K and 78 K. The results of further calibrations and measurements on the transfer system will be reported by M. Hogendoorn.

The contents of Table 6.1 are in close agreement with Table 4.3 and Fig.4.19. This means that the argumentation, developed in paragraph 4.2.1, is valid. $\dot{V}_{f1}$ corresponds with $\dot{V}_{s1}$ in Table 4.3 and $\dot{V}_{f2}$ to $\dot{V}_{a2}$ (see also Fig.4.18). According to (4-47) and (4-53) their difference should be about $0.5\Delta\dot{V}$, which is indeed the case. Note that $\dot{V}_{f1}<\dot{V}_{f2}$ while $\dot{m}_1>\dot{m}_2$.

Table 6.2 shows that the fan should be placed behind the stage (situation 1) in order to minimize the cool-down time. The profit with respect to placing the fan in front of the stage (situation 2) is larger in the 70K-circuit (15%) than in the 20K-circuit (3%), because the cooling power $\dot{Q}_a$ of the 70K-circuit is at room temperature considerably larger than that of the 20K-circuit (700 W and 400 W respectively), while the volume flow difference $\Delta\dot{V}$ between the "warm" gas leaving the application and the "cold" gas leaving the stage is approximately given by $(2/5)(\dot{Q}_a/p)$ (4-47). With an average transfer system pressure p of 20 bar, $\Delta\dot{V}$ will be small in comparison with the mean volume flow of 200 cm^3/s when $\dot{Q}_a<200$ W. In this area there will be virtually no reduction of the cool-down time when replacing situation 2 by situation 1. When $\dot{Q}_a>200$ W, $\Delta\dot{V}$ becomes significant, especially so in the 70K-circuit when $\dot{Q}_a=700$ W (compare Fig.4.19).

The pressure differences in Table 6.3 show some important features. They decrease with increasing cooling power and temperature because the pressure difference Δp_f across the fan is related to the constant pressure head ΔH_f according to $\Delta p_f=\varrho g\Delta H_f\sim\varrho\sim 1/T$. Another feature is the increase of the difference between Δp_{12} and Δp_{56} across the heat exchangers and of that between Δp_{34} and Δp_{78} across the transfer lines with increasing cooling power. It is caused by the fact that Δp is proportional to the gas temperature T: $\Delta p\sim(1/2)\varrho\dot{V}^2\sim\dot{m}^2/\varrho\sim T$. As the mean gas temperatures $\bar{T}_{12}<\bar{T}_{56}$ and $\bar{T}_{78}<\bar{T}_{34}$ (see Fig.4.20(a) and Fig.4.23), differences between the Δp's occur, although the heat exchangers as well as the transfer lines have the same geometry. A third thing to note is, that a large percentage (about 75%) of Δp_f is taken away by the two heat exchangers (inner diameter: 6 mm). This percentage becomes larger with increasing $\dot{Q}_a$ because Reynolds' number $Re\sim\dot{m}/\eta\sim$ $\sim\varrho/\eta\sim T^{-1.55}$ (see (4-38), (4-23) and (4-7)) decreases when the gas temperature T is rising. According to Fig.4.11 the friction factors of the heat exchangers will therefore increase, while those of the transfer lines remain constant (see Fig.4.12).

Table 6.5 shows the influence of several variables on T_s, T_a and $\dot{V}_f$. When only ΔH_f is changed, we see the same variations of T_s and T_a as in Fig.4.22 (ΔH_f is proportional to the square of the impeller tip speed u, see Fig.4.21). These variations are the result of two competing effects, which we will call the "mass flow effect" and the "shaft power effect". The first is positive, that is, an increasing mass flow $\dot{m}$ reduces the difference between T_a and T_s according to (4-46). The second effect is negative as an increasing shaft power $P_{sh}=\dot{m}g\Delta H_f/\eta_f$ (4-75) enlarges the cooling power at the stage $\dot{Q}_s$, and therefore T_s (see Fig.4.23 and (4-55)). The larger $\dot{Q}_a$, the larger is also the value of ΔH_f at which the two effects cancel each other and where the minimum value of T_a is reached.

In addition to the effects mentioned above, a third and negative process comes into play when only D_{he} is changed. It will be called the "heat exchanger effect" and its working can be seen, together with the other effects, in Fig.6.2. When D_{he} is increased from 6 mm to 8 mm the mass flow effect is very strong, as it reduces the temperature differences $(T_{2/3}-T_1)$ and $(T_{4/5}-T_{6/7})$ over the heat exchangers with about 100% (see Fig.6.2(a) and (b)). This is also apparent in Table 6.5 as a sharp increase of $\dot{V}_f$ and can be explained by the fact that the heat exchangers no longer dominate the flow resistance of the tube circuit when D_{he}=8 mm (see Fig.6.1). The shaft power effect shows itself most clearly in the 20K-circuit: when D_{he} is changed from 6 mm to 8 mm, the stage temperature increases so much that the mass flow effect is cancelled completely (see Fig.6.2(a)). The heat exchanger effect becomes most conspicuous when D_{he} is changed from 8 mm to 12 mm. It shows itself via the growing temperature differences (T_1-T_s) and $(T_a-T_{4/5})$ and can shortly be described as a degeneration of the heat exchangers. This process can be understood by referring to (4-34) and (4-36): the heat transfer number A characterises the quality of a heat exchanger and is proportional to $D_{he}^{-0.8}$.

During the change from D_{he}=8 mm to D_{he}=12 mm the mass flow effect and the shaft power effect become very weak as the flow resistance of the tube circuit is more and more dominated by the transfer lines (see Fig.6.2 and Fig.6.1). The negative heat exchanger effect is therefore the dominant process in this D_{he}-interval. The T_a-values of Table 6.5 suggest that D_{he}=10 mm would be a good choice, especially in the 70K-circuit. However, when the lengths of the transfer lines would be increased from 7 m to 14 m, the volume flow would only depend on the flow resistance of the transfer lines. This situation is in principle the same as that shown in Fig.6.1 at D_{he}=12 mm where, as we have just seen, the negative heat exchanger effect is dominant. Therefore it is proposed to use heat exchangers with an inner diameter D_{he} of 8 mm.

At the beginning of paragraph 4.2.2 the temperature difference ΔT_f across the fan was mentioned as a negative aspect. However, as it is given by

$$\Delta T_f = (P_{sh}+\dot{Q}_{f,con})/(\dot{m}c_p) \approx$$

$$\approx P_{sh}/(\dot{m}c_p) = g\,\Delta H_f / (c_p\,\eta_f) \qquad (7\text{-}1)$$

and approximately constant (ΔH_f=45 m: $\Delta T_f \approx$0.2 K), it does not play a role in the optimization process (see $\Delta T_f=T_{8/9}-T_1$ in Fig.6.2).

Table 6.5 shows that the influence of D_c on T_a is small: it is therefore proposed to maintain the present values: 0.10 m in the 20K-circuit and 0.12 m in the 70K-circuit.

There are two reasons why T_a-T_s is usually larger in the 70K-circuit than in the 20K-circuit. The first is that the cooling power $\dot{Q}_a$ in the stationary state tends to be the largest in the 70K-circuit, but the second and most important reason is the fact that the mass flows in the circuits differ. When the volume flow and the average transfer system pressure are the same in both circuits, it follows that

$$\dot{m}_{70}/\dot{m}_{20} = \rho_{70}/\rho_{20} = T_{20}/T_{70} \approx 2/7. \qquad (7\text{-}2)$$

As it is clear that the 70K-circuit needs optimizing mostly, we will focus our attention on this circuit, taking $\dot{Q}_a$=120 W (see Table 6.5). Once D_{he} has been chosen, there are still two ways by which $\dot{m}_{70}$ can be increased. The first is to increase ΔH_f, which is not very efficient as the tube system characteristic $\Delta H_t(\dot{V})$ becomes steeper with increasing $\dot{V}$ (see Fig.4.21 and Fig.4.22(b)). The second possibility is to increase p from 20 bar to e.g. 40 bar. The advantage gained by this step is so great that, even when ΔH_f is reduced to 20 m, T_a is smaller than in the case of p=20 bar, ΔH_f=75 m (72.95 K and 74.02 K respectively).

ΔH_f=20 m, $\dot{V}_f$=170 cm^3/s, D_{he}=8 mm and β_2=90° (see Fig.4.25) will be used as a basis for the new fan design. With ψ=1 (see Fig.4.24(a)) we find from (4-88) that u_2=u=19.8 m/s. The inner impeller diameter may not be much larger than D_{he}: therefore D_1=12 mm is chosen. With D_2/D_1=3 (a larger value is usually not allowed because of increasing friction) it is found that the outer impeller diameter D_2=D_f=36 mm. The volume flow coefficient follows from (4-89): φ=8.4 10^{-3}. Substitution in (4-96) yields $D_2/D_1 \leq 4$, which demand has been fulfilled. The rotation frequency $\nu=u_2/(\pi D_2)$=175 Hz. When the blade height B_1 at the impeller inlet is given by $B_1=D_1/2$= 6 mm, the inner blade angle follows from (4-98): β_1=6.5°. As this value is rather small in comparison with practical values ($15° \leq \beta_1 \leq 35°$, see also (4-96)), it is proposed to take B_1=5 mm and β_1=25°. B_2 is chosen equal to 3 mm (compare (4-100)). The number of blades z should be about 15 according to (4-99). As this is too large with respect to the small dimensions of the impeller, it is proposed to take z=8. The blades are drawn as circular arcs. Their construction is shown in Fig.7.1.

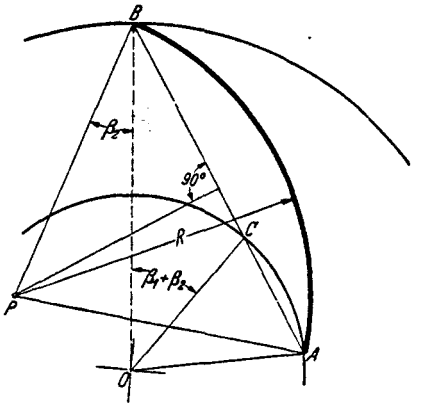

Fig.7.1 Construction of a blade, shaped as a circular arc. Its radius R is equal to $(r_2^2-r_1^2)/(2r_1\cos\beta_1-2r_2\cos\beta_2)$. The angle $\beta_1+\beta_2$ is constructed from the origin O. The intersections C and B with the inner and the outer circle are then connected to A with a straight line. When line AB is bisected at right angles and when β_2 is constructed from point B, the bisector meets the leg of β_2 at the centre P of the circular arc. This can now be drawn from A to B.

The impeller with $\beta_1=25^\circ$ and $\beta_2=90^\circ$ is shown in Fig.7.2.

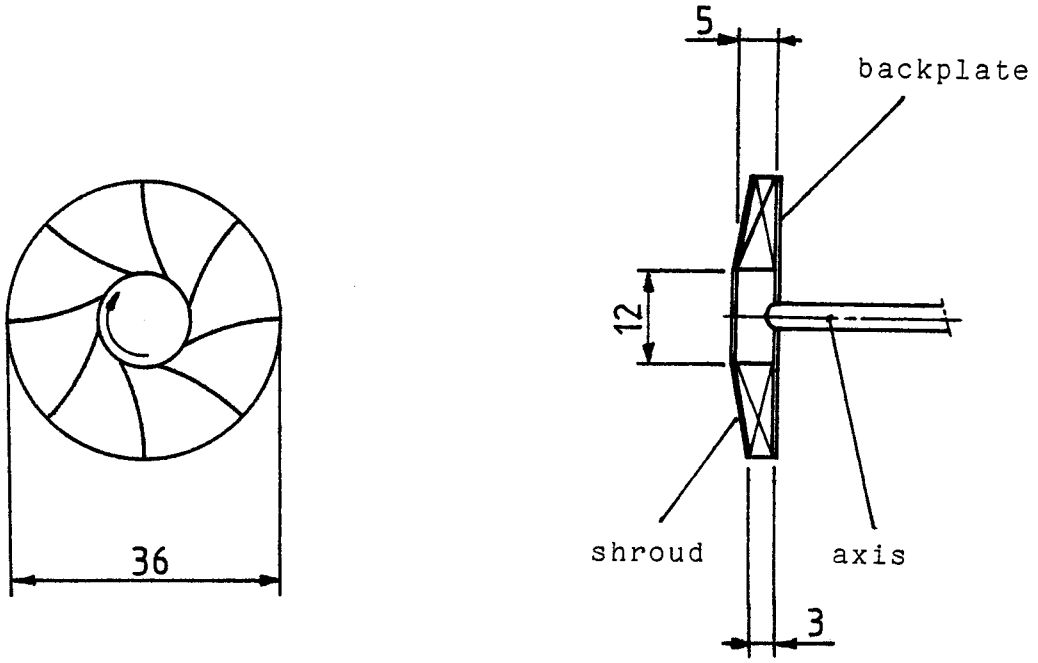

Fig.7.2 Dimensions (mm) and form of the new impeller

The impeller blades should have a sharp end at the impeller inlet, where they they could cause constriction of the gas flow.

The logarithmic spiral $r(\vartheta)$ describing the casing profile (4-104) should increase from $r_2=D_2/2=D_f/2$ to r_2+D_{he} when ϑ increases from 0 to 2π. This means that

$$r(\vartheta) = r_2\, e^{5.8\ 10^{-2}} \qquad \text{with } \vartheta \text{ in radians} \qquad (7\text{-}3)$$

$$= r_2\, e^{1.0\ 10^{-3}} \qquad \text{with } \vartheta \text{ in degrees.} \qquad (7\text{-}4)$$

The spiral is larger than is required by the flow pattern because, according to (4-105), $v_m/v_u=9.5\ 10^{-3} < 5.8\ 10^{-2}$. Because the radial clearance at the cut-off (see Fig.4.26) should not be less than 10% of r_2 (noise at blade passage frequency is thereby prevented) the spiral has been drawn in Fig.7.3 with $120^\circ<\vartheta<460^\circ$.

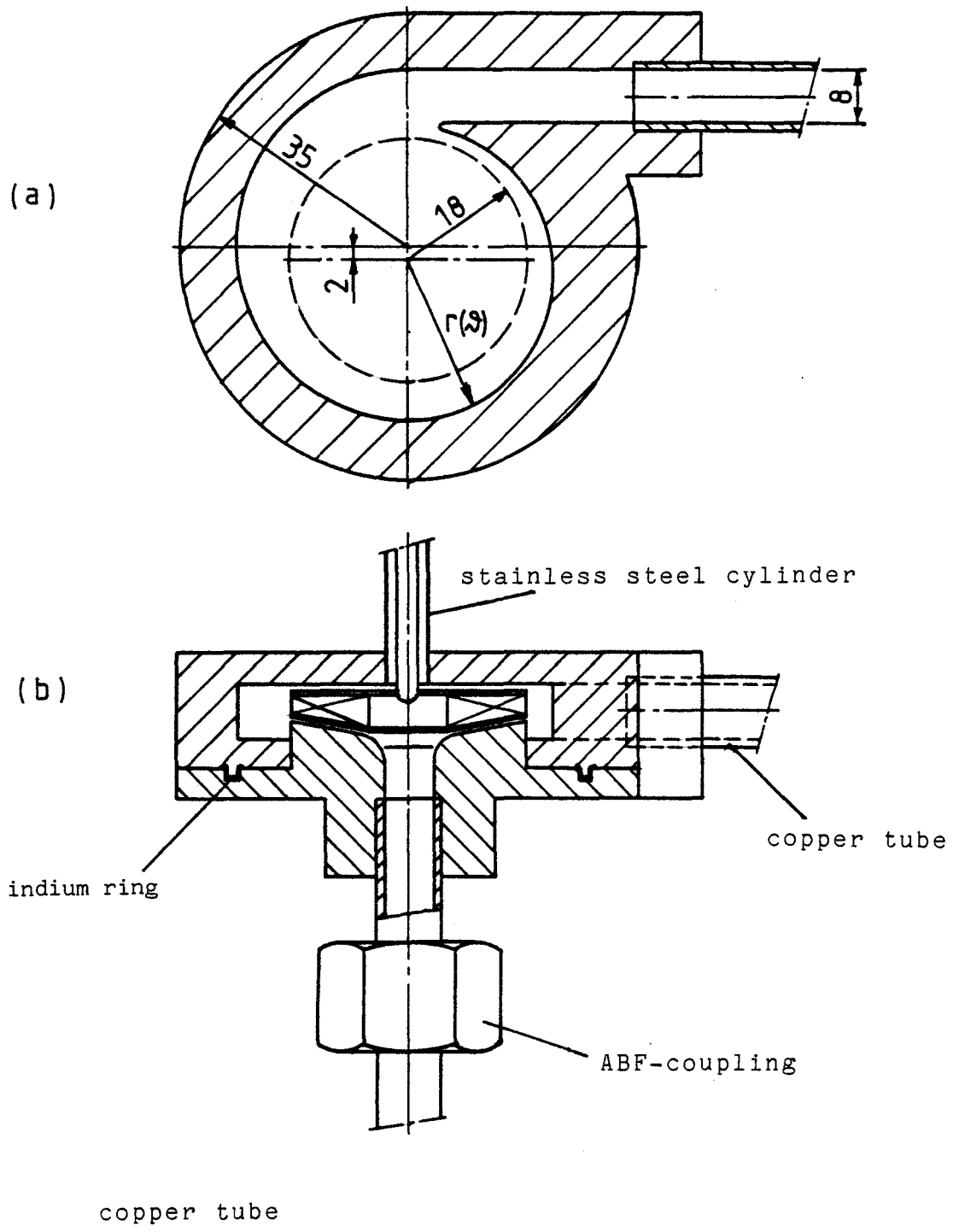

Fig.7.3 Dimensions (mm) and form of the new fan casing. In (a) the place of the impeller has been indicated by dashed lines. The fan casing as well as the vertical copper tube have been divided into two halves.

In order to withstand pressures higher than 30 bar, the walls of the stainless steel cylinder used in the present fan system would have to be made thicker, which would result in a larger cold loss by conduction $\dot{Q}_{f,con}$ (see Fig.4.7). In order to get around this problem and to get rid of the fenolhardpaper inside the cylinder, it is proposed to fix the impeller to the shaft after the fan motor has been placed on the head of the A20 cryogenerator. This can be done by dividing the fan casing and the copper tube leading towards the centre of the impeller into two halves. The two parts of the copper tube can most easily be clamped together by an ABF-coupling, which is also used in connecting the transfer lines to the heat exchangers. A high vacuum sealing between the two halves of the fan casing can be achieved by pressing a ring of indium wire into a circular groove (see Fig.7.3). When the lower part of the fan casing (connected to the upper part of the copper tube) is taken away, the impeller can be removed from or fixed to the shaft (see Fig.7.3(b)).

The tube wall thickness S of the stainless steel cylinder should be such, that it can withstand the internal pressure p. It is given by

$$S \geq f\ p\ D/\ (2\sigma) \qquad (7\text{-}5)$$

where f is a security factor (usually 5), D the inner tube diameter and σ the maximum stress (about 500 N/mm^2 for stainless steel). See Fig.7.4.

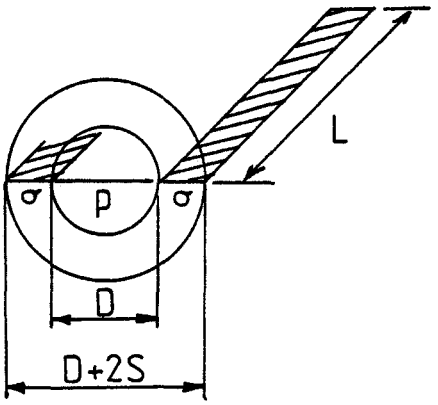

Fig.7.4 The cross-sectional dimensions of a hollow cylinder, submitted to an internal pressure p. In order to avoid breakage, (p DL) should be smaller than (σ 2SL), see (7-5).

According to (7-5) a cylinder with D=5 mm and S=0.5 mm can easily withstand a pressure of 40 bar. When compared with the present situation (D=30 mm, S=0.3 mm) the conductive heat flow through the cylinder $\dot{Q}_c$ can be reduced with a factor $(DS)_{present}/(DS)_{new}=3.6$, while $\dot{Q}_h$ disappears altogether because the fenolhardpaper is not needed anymore (see (4-17) and (4-18)).

The shaft power P_{sh} of the fan follows from (4-90). With $\eta_f=50\%$, $\lambda_p=0.017$ and $P_{sh}/\varrho=6.6\ 10^{-2}\ W\ m^3/kg$. With $\varrho(p=40\ bar, T=70K)\approx 30\ kg/m^3$ it follows that $P_{sh70}\approx 2$ W. The shaft power of the 20K-fan may be expected to be 5W as the density tends to be larger than in the 70K-circuit. An electrical power of 10 W for the fan motors should therefore be sufficient to drive the impellers.

Changing the rotation frequency ν has no influence on the fan efficiency η_f and on the dimensionless fan coefficients. When $\Delta H_f=45$ m is used in combination with p=20 bar, the impeller tip speed $u=u_2$ should be increased from 20 m/s to 30 m/s (4-88) and the rotation frequency from 175 to 265 Hz, which is about the same as the present value of 300 Hz.

The last part of this discussion is dedicated to the helium transfer lines, which are bellows because of their required flexibility. Their flow resistance can not simply be decreased by increasing their inner diameter D_t (presently 12.7 mm) because of two effects. In the first place their outer area becomes larger so that cold losses increase. The second and most important effect is, that the increase ΔL of the length L of the transfer lines, due to the pressure p, becomes larger as D_t is increased, according to

$$C\ \Delta L/L \approx p\ (\pi/4)D_t^2 \qquad (C \text{ is a constant}). \qquad (7\text{-}6)$$

Unless more spacers are used, this means that the positions of the lines inside the transfer hose become undulated, which may result in considerable cold losses towards the surroundings. Therefore, whenever flexibility is not really necessary, it should be propounded to use rigid, smooth tubes. Their friction factors are considerably smaller than those of bellows with the same dimensions and they retain their length when the pressure is increased.

8. CONCLUSIONS

In order to optimize the cold-transfer system, its behaviour has been described by a set of 23 equations, which was solved numerically.
In cooperation with Philips I&E Development Cryogenics a measuring unit has been designed and built, with which the behaviour of the transfer system can be analysed experimentally.
Temperature measurements have been facilitated by the realisation of a switching unit. If it would be connected, after some minor alterations, to a central processing unit, automatic temperature measurements could be carried out.
The static pressures at several points in the transfer system have been conducted to two differential pressure transducers via a number of three-way valves. Using the valves, the static pressure differences across the fans, the heat exchangers and the transfer lines can be measured.

The cold-transfer system can be optimized in several respects.

1. The shield inside the transfer hose is a bellows with a corrugated surface and the transfer lines have a braded cover of stainless steel. As the thermal contact between the radiation shield and the 70K transfer line returning to the cryogenerator may therefore be expected to be poor (see paragraph 4.1.4), it should be considered whether the transfer lines can be centered inside the transfer hose without the shield. This would result in a construction that would be simpler and less costly than the present one. (An experimental indication of the weakness of the thermal contact was already found via a Pt100 thermometer, mounted on the inside of the radiation shield. It registered a temperature of 190 K: see Fig.4.16).

2. The inner diameters of the heat exchangers around the stages of the cryogenerator should be increased from 6 mm to 8 mm, while the distance between their subsequent coils should be decreased to about 1 mm. This will enlarge the mass flow with 50% to 100% without impairing the quality of the heat exchangers.

3. The heat exchangers at the application side of the transfer system should be chosen with great care. To be more specific, their heat transfer numbers should not be small and their flow resistances not large in comparison with the corresponding values for the heat exchangers at the cryogenerator side of the transfer system.

4. Of the way in which the centrifugal fans can be improved the most important points are
   a. a decrease of the blade angles at the impeller inlet from 90° to 25° and a circular blade form instead of a straight one,
   b. a spirally shaped fan casing profile instead of a circular one,
   c. a division of the fan casing into two parts and an ABF-coupling on the tube at the fan inlet, in order to connect or disconnect the impeller after the fan motor has been placed on the head of the cryogenerator,
   d. a reduction of the diameter of the stainless steel cylinder, which connects the fan casing to the head of the cryogenerator, from 30 mm to 4 a 5 mm (approximately the shaft diameter) and omission of the fenolhardpaper inside the cylinder.

The points a. and b. will probably improve the fan efficiency from 50% to about 80%. By c. and d. the cold loss by conduction will be reduced with about a factor 3.

5. The average transfer system pressure should be increased from 20 bar to e.g. 40 bar (after 4.d. has been realised, the fans can withstand such a pressure). By this step the mass flow is doubled, while the volume flow can remain the same. This is especially useful in the 70K-circuit, where the temperature difference between the stage and the application is usually larger than in the 20K-circuit.

6. As the 20K-circuit does not need as high a pressure as 40 bar in order to function optimally, it should be considered to use separate circuit pressures: e.g. 20 bar in the 20K-circuit and 40 bar in the 70K-circuit. When this is done, an eventual helium leak in the transfer system can more easily be located than is presently the case. In addition, the 20K-circuit will no longer contain about 70/20 = 3.5 times as much helium as the 70K-circuit.

7. In combination with 5. the rotation frequencies of the fans can be reduced from 300 Hz to 175 Hz. Otherwise they should remain the same.

8. Whenever flexibility of the transfer lines is not really necessary, it should be propounded to use rigid, smooth tubes. Their friction factors are considerably smaller than those of bellows with the same dimensions, and they retain their length when the pressure is increased. Another advantage is, that only a few spacers are needed for centering them inside the transfer hose. The oscillations of the cooling machine usually cause vibrations that propagate through the walls of the transfer lines and the transfer hose towards the application. In order to absorb these vibrations, the rigid tubes could be alternated with short bellows.

9. In order to minimize the cool-down time the fans should be placed behind the stages. The profit with respect to placing the fan in front of the stage is larger in the 70K-circuit than in the 20K-circuit: 15% and 3% respectively. It is therefore not urgent to alter the present fan situation (70K-fan behind the stage, 20K-fan in front of the stage).

9. LITERATURE

BEU70 Beuger J.J.B. and Rauwerdink H.J.,
A cold-transfer system,
Philips Research Laboratories, Report nr.4847 (1970)

BOH71 Bohl W.,
Technische Stromungslehre,
Vogel-Verlag, Würzburg (1971)

CHE83 Cheremisinoff N.P. and Gupta R. (ed.),
Handbook of fluids in motion,
Ann Arbor Science Publishers, Michigan (1983)

DOO80 Doornbos R.,
Statistische theorie van proefopzetten,
Eindhoven University of Technology, syllabus nr. 2.222 (1980)

ECK72 Eck B.,
Ventilatoren,
Springer-Verlag, Berlin (1972)

EDE81 Eder F.X.,
Arbeitsmethoden der Thermodynamik I (Temperaturmessung),
Springer-Verlag, Berlin (1981)

FAN74 Fan technology and practice,
(Conference Report 18th-19th April 1972)
The Institution of Mechanical Engineers, London (1974)

FAS70 Fastowski W.G., Petrowski J.W. and Rowinski A.E.,
Kryotechnik,
Akademie-Verlag, Berlin (1970)

FLU56 Flügge S. (ed.),
Low Temperature Physics I,
Springer-Verlag, Berlin (1956)

FRE81 Frey H. and Haefer R.A.,
Tieftemperaturtechnologie,
VDI-Verlag GmbH, Düsseldorf (1981)

GIJ80 Gijsman H.M.,
Kryogene Technieken,
Eindhoven University of Technology, syllabus nr. 3.315 (1980)

HAA69a Haarhuis G.,
Vakuümtechniek (DK1),
Philips I&E (Industrial & Electro-acoustical Systems Division),
Cryogenic Department (1969)

HAA69b Haarhuis G.,
Kryogene Technieken (DK2),
Philips I&E Cryogenic Department (1969)

HAA69c Haarhuis G.,
Isolatietechnieken (DK4),
Philips I&E Cryogenic Department (1969)

HOL69 Holland J.,
Transport van koude (DK3),
Philips I&E Cryogenic Department (1969)

KEL82 Keltjens J.,
De beweging van ^{3}He-^{4}He-mengsels beneden 100 mK,
Eindhoven University of Technology, Graduate Report (1982)

MUL67 Mulder J.,
A cold-transfer system,
Philips Research Laboratories, Report nr. 4237 (1967)

NAG81 NAG Algol60 Library Manual,
Mark 8, Volume 1,
Numerical Algorithms Group Ltd, Oxford (1981)

NBS72 National Bureau of Standards, Technical Note 631,
Thermophysical properties of helium-4 from 2 to 1500 K
with pressures to 1000 atmospheres,
US Department of Commerce, Boulder Colorado (1972)

OSB77 Osborne W.C.,
Fans,
Pergamon Press, Oxford (1977)

OSB79 Osborne W.C.,
The selection and use of fans,
Oxford University Press, Oxford (1979)

OXF79 Oxford Instruments,
Choosing a temperature sensor,
Product and Application Note nr. TS11 (1979)

PET83 Peters A.J.M.,
Cryogene NMR-magneetkoeling met de A20-koelmachine,
Philips CFT (Centre for manufacturing Technology),
Report nr. 096/83 (1983)

Appendix 10.1 Thermophysical properties of He

T-s-diagram of ^4He

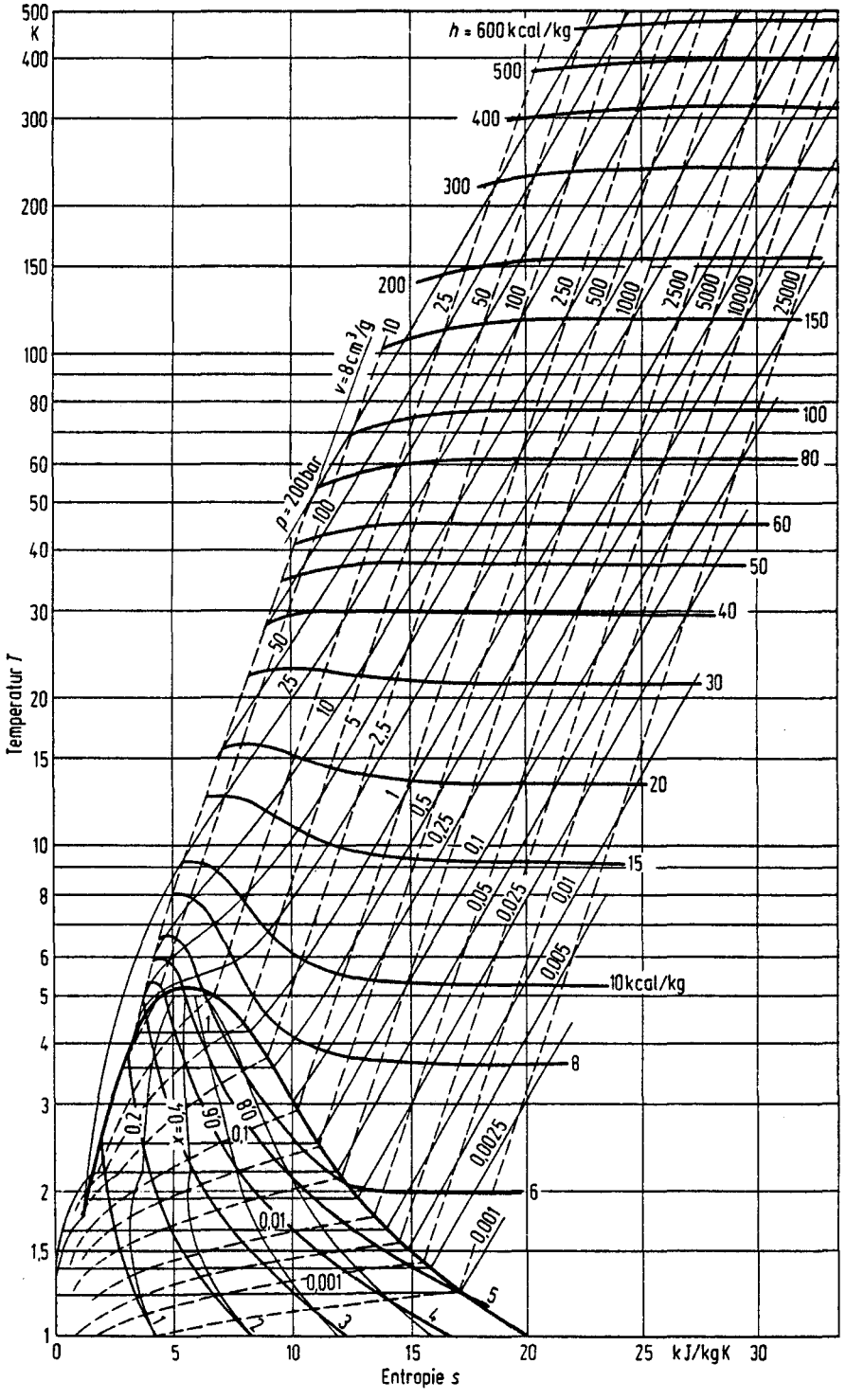

Source: EDE81

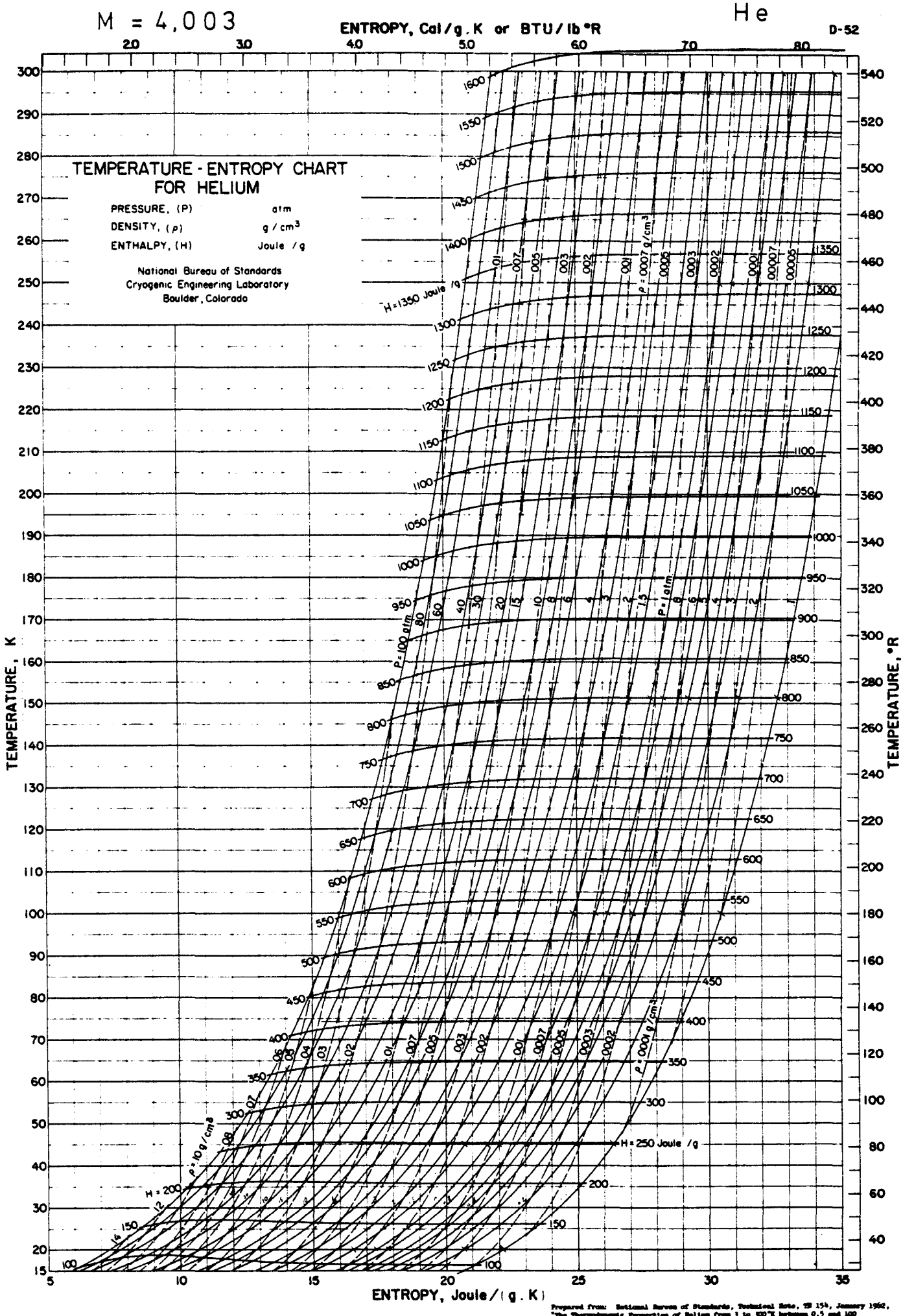

Prepared from: National Bureau of Standards, Technical Note, TN 154, January 1962, "The Thermodynamic Properties of Helium from 3 to 300°K between 0.5 and 100 Atmospheres", Douglas B. Mann; by the Cryogenic Data Center, National Bureau of Standards, Boulder, Colorado.

Source: NBS72

THERMODYNAMIC PROPERTIES OF HELIUM 4

20.0 ATMOSPHERE ISOBAR

TEMPERATURE DEG. K	VOLUME CC/G ** X .01	ISOTHERM DERIVATIVE CC-ATM/G	ISOCHORE DERIVATIVE ATM/K	INTERNAL ENERGY J/G	ENTHALPY J/G	ENTROPY J/G-K	CV J/G-K	CP J/G-K	VELOCITY OF SOUND M/S
2.0	0.05334	1160.0	1.45	3.269	15.09	1.302	1.953	1.966	344.1
2.5	0.05858	1190.0	2.15	3.857	15.73	1.605	1.297	1.331	351.3
3.0	0.05898	1150.0	3.47	4.436	16.39	1.868	1.596	1.707	352.5
3.5	0.05960	1080.0	4.57	5.153	17.23	2.142	1.768	2.012	353.0
4.0	0.06046	1000.0	5.33	6.006	18.26	2.422	1.917	2.336	352.2
4.5	0.06155	924.0	5.74	7.026	19.50	2.714	2.092	2.708	348.2
5.0	0.06288	845.0	5.88	8.254	21.00	3.020	2.291	3.111	340.8
5.1	0.06318	830.0	5.88	8.529	21.33	3.083	2.330	3.190	339.4
5.2	0.06348	819.0	5.89	8.816	21.68	3.147	2.367	3.246	338.7
5.3	0.06378	804.0	5.88	9.082	22.01	3.209	2.327	3.265	338.2
5.4	0.06408	790.0	5.87	9.349	22.33	3.270	2.332	3.311	337.8
5.5	0.06439	775.0	5.85	9.620	22.67	3.331	2.339	3.359	335.8
5.6	0.06470	761.0	5.83	9.893	23.01	3.392	2.347	3.409	334.5
5.7	0.06503	746.0	5.81	10.17	23.35	3.453	2.357	3.461	333.2
5.8	0.06536	732.0	5.78	10.45	23.70	3.514	2.367	3.514	331.8
5.9	0.06571	718.0	5.76	10.73	24.05	3.574	2.378	3.569	330.4
6.0	0.06606	704.0	5.73	11.02	24.41	3.635	2.390	3.626	328.9
6.5	0.06795	636.0	5.54	12.51	26.28	3.938	2.457	3.925	321.0
7.0	0.07010	574.0	5.32	14.11	28.32	4.242	2.528	4.250	312.6
7.5	0.07254	516.0	5.07	15.82	30.52	4.549	2.599	4.594	304.0
8.0	0.07531	464.0	4.80	17.64	32.90	4.859	2.667	4.954	295.5
8.5	0.07847	418.0	4.52	19.58	35.48	5.174	2.730	5.321	287.5
9.0	0.08205	380.0	4.23	21.62	38.25	5.494	2.789	5.685	280.1
9.5	0.08608	349.0	3.95	23.78	41.21	5.816	2.843	6.028	273.7
10.0	0.09057	325.0	3.67	25.99	44.34	6.141	2.891	6.330	268.4
11.0	0.1039	298.0	3.12	30.72	51.17	6.798	2.971	6.687	260.8
12.0	0.1123	296.0	2.68	35.37	58.12	7.409	3.018	6.734	258.5
13.0	0.1239	305.0	2.33	39.80	64.91	7.956	3.048	6.632	259.4
14.0	0.1355	320.0	2.05	43.98	71.45	8.443	3.068	6.510	262.1
15.0	0.1471	335.0	1.84	47.95	77.76	8.880	3.083	6.420	265.7
16.0	0.1591	354.0	1.67	51.91	84.14	9.292	3.101	6.342	270.7
17.0	0.1710	374.0	1.53	55.79	90.44	9.674	3.115	6.263	276.1
18.0	0.1829	396.0	1.41	59.59	96.67	10.03	3.126	6.185	281.8
19.0	0.1948	419.0	1.31	63.34	102.8	10.36	3.134	6.112	287.6
20.0	0.2066	442.0	1.22	67.02	108.9	10.67	3.140	6.044	293.4
21.0	0.2184	465.0	1.14	70.65	114.9	10.97	3.144	5.981	299.3
22.0	0.2300	488.0	1.07	74.24	120.9	11.24	3.148	5.924	305.1
23.0	0.2416	512.0	1.01	77.79	126.8	11.51	3.150	5.871	310.9
24.0	0.2531	536.0	0.958	81.31	132.6	11.75	3.152	5.823	316.6
25.0	0.2645	559.0	0.910	84.80	138.4	11.99	3.153	5.780	322.3
26.0	0.2759	583.0	0.867	88.26	144.2	12.22	3.154	5.740	327.8
28.0	0.2984	630.0	0.792	95.10	155.6	12.64	3.155	5.672	338.7
30.0	0.3207	676.0	0.729	101.9	166.9	13.03	3.155	5.614	349.2
32.0	0.3428	722.0	0.676	108.6	178.0	13.39	3.154	5.566	359.4
34.0	0.3647	768.0	0.631	115.2	189.1	13.73	3.153	5.525	369.2
36.0	0.3865	813.0	0.591	121.8	200.1	14.04	3.152	5.490	378.8
38.0	0.4081	858.0	0.556	128.4	211.1	14.34	3.151	5.461	388.2
40.0	0.4296	903.0	0.525	134.9	222.0	14.62	3.150	5.435	397.3
45.0	0.4830	1010.0	0.462	151.1	249.0	15.25	3.147	5.384	419.0
50.0	0.5359	1120.0	0.412	167.2	275.8	15.82	3.145	5.347	439.6
55.0	0.5885	1230.0	0.372	183.2	302.5	16.33	3.143	5.319	459.1
60.0	0.6408	1340.0	0.340	199.2	329.0	16.79	3.140	5.298	477.8
65.0	0.6930	1440.0	0.312	215.1	355.5	17.21	3.139	5.281	495.7
70.0	0.7449	1550.0	0.289	230.9	381.9	17.60	3.137	5.268	513.0
75.0	0.7968	1650.0	0.269	246.7	408.2	17.97	3.136	5.257	529.6
80.0	0.8485	1760.0	0.252	262.5	434.4	18.31	3.134	5.248	545.8
90.0	0.9518	1960.0	0.224	294.0	486.8	18.92	3.132	5.235	576.6
100.0	1.055	2170.0	0.201	325.4	539.1	19.47	3.130	5.225	605.9
125.0	1.312	2690.0	0.160	403.7	669.6	20.64	3.127	5.211	673.4
150.0	1.568	3200.0	0.133	481.9	799.8	21.59	3.125	5.204	734.6
175.0	1.825	3710.0	0.114	560.1	929.8	22.39	3.124	5.200	791.1
200.0	2.081	4220.0	0.100	638.1	1060.0	23.08	3.123	5.198	843.9
225.0	2.337	4740.0	0.0888	716.1	1190.0	23.70	3.122	5.196	893.5
250.0	2.593	5250.0	0.0799	794.1	1320.0	24.24	3.122	5.195	940.5
275.0	2.849	5760.0	0.0727	872.1	1449.0	24.74	3.121	5.194	985.3
300.0	3.105	6270.0	0.0666	950.1	1579.0	25.19	3.121	5.194	1028.0
350.0	3.617	7290.0	0.0571	1106.0	1839.0	25.99	3.120	5.193	1109.0
400.0	4.129	8320.0	0.0499	1262.0	2099.0	26.68	3.120	5.193	1184.0
450.0	4.641	9340.0	0.0444	1418.0	2358.0	27.30	3.119	5.192	1255.0
500.0	5.153	10400.0	0.0400	1574.0	2618.0	27.84	3.119	5.192	1322.0
600.0	6.177	12400.0	0.0333	1885.0	3137.0	28.79	3.119	5.192	1447.0
700.0	7.201	14500.0	0.0285	2197.0	3656.0	29.59	3.118	5.192	1561.0
800.0	8.225	16500.0	0.0250	2509.0	4175.0	30.28	3.118	5.192	1668.0
900.0	9.249	18500.0	0.0222	2820.0	4695.0	30.89	3.118	5.192	1769.0
1000.0	10.27	20600.0	0.0200	3132.0	5214.0	31.44	3.118	5.192	1864.0
1100.0	11.30	22600.0	0.0182	3444.0	5733.0	31.94	3.118	5.192	1954.0
1200.0	12.32	24700.0	0.0167	3755.0	6252.0	32.39	3.118	5.192	2041.0
1300.0	13.35	26700.0	0.0154	4067.0	6772.0	32.80	3.118	5.192	2124.0
1400.0	14.37	28800.0	0.0143	4379.0	7291.0	33.19	3.118	5.192	2204.0
1500.0	15.40	30800.0	0.0133	4690.0	7810.0	33.55	3.118	5.193	2281.0

* TWO-PHASE BOUNDARY
** NUMBERS IN THIS COLUMN HAVE BEEN MULTIPLIED BY THE INDICATED FACTOR

THERMOPHYSICAL PROPERTIES OF HELIUM 4

20.0 ATMOSPHERE ISOBAR

TEMPERATURE DEG.K	DENSITY G/CC ** X 100	$V(\partial H/\partial V)_p$ J/G	$V(\partial P/\partial U)_v$ ATM-CC/J	$-V(\partial P/\partial V)_T$ ATM	$(\partial V/\partial T)/V_p$ 1/DEG.K	THERMAL CONDUCTIVITY MW/CM-K	VISCOSITY G/CM-S ** X 1000000	THERMAL DIFFUSIVITY SQ-CM/S	DIELECTRIC CONSTANT	PRANDTL NUMBER
2.0	17.14	269.0	4.34	199.0	0.00730	0.145	78.3	0.000429	1.06469	1.06
2.5	17.07	125.6	9.71	203.0	0.0106	0.206	79.6	0.000907	1.06443	0.514
3.0	16.96	35.8	12.8	194.0	0.0178	0.229	75.9	0.000791	1.06398	0.566
3.5	16.79	79.8	15.4	181.0	0.0252	0.246	71.0	0.000730	1.06330	0.580
4.0	16.54	72.8	16.8	166.0	0.0321	0.263	66.1	0.000682	1.06239	0.586
4.5	16.25	70.8	16.9	150.0	0.0382	0.279	61.5	0.000635	1.06126	0.596
5.0	15.90	71.1	16.1	134.0	0.0438	0.294	57.5	0.000594	1.05994	0.609
5.1	15.83	71.2	16.0	131.0	0.0448	0.296	56.7	0.000587	1.05965	0.611
5.2	15.75	71.1	15.9	128.0	0.0456	0.299	56.0	0.000584	1.05936	0.609
5.3	15.68	70.1	16.1	126.0	0.0466	0.301	55.4	0.000588	1.05908	0.600
5.4	15.61	69.5	16.1	123.0	0.0476	0.304	54.7	0.000587	1.05880	0.597
5.5	15.53	69.1	16.1	120.0	0.0486	0.306	54.1	0.000586	1.05851	0.594
5.6	15.45	68.7	16.1	118.0	0.0496	0.308	53.5	0.000585	1.05822	0.593
5.7	15.38	68.4	16.0	115.0	0.0506	0.310	53.0	0.000583	1.05792	0.591
5.8	15.30	68.0	16.0	112.0	0.0516	0.312	52.4	0.000581	1.05762	0.590
5.9	15.22	67.8	15.9	109.0	0.0527	0.314	51.9	0.000578	1.05732	0.590
6.0	15.14	67.5	15.8	107.0	0.0537	0.316	51.4	0.000576	1.05701	0.590
6.5	14.72	66.3	15.3	93.7	0.0592	0.324	49.1	0.000561	1.05539	0.595
7.0	14.27	65.3	14.8	81.8	0.0651	0.329	47.1	0.000543	1.05367	0.608
7.5	13.79	64.4	14.2	71.1	0.0713	0.333	45.4	0.000525	1.05183	0.627
8.0	13.28	63.5	13.6	61.6	0.0780	0.334	44.0	0.000508	1.04989	0.652
8.5	12.74	62.8	13.0	53.3	0.0848	0.334	42.7	0.000493	1.04786	0.681
9.0	12.19	62.2	12.5	46.3	0.0914	0.333	41.7	0.000480	1.04574	0.713
9.5	11.62	61.9	11.9	40.5	0.0974	0.333	40.8	0.000472	1.04357	0.745
10.0	11.04	61.9	11.5	35.9	0.102	0.328	40.1	0.000469	1.04138	0.776
11.0	9.907	63.3	10.6	29.6	0.106	0.321	39.2	0.000485	1.03709	0.816
12.0	8.937	66.2	10.0	25.3	0.102	0.316	38.8	0.000527	1.03331	0.827
13.0	8.071	70.2	9.46	24.6	0.0944	0.314	38.9	0.000587	1.03015	0.821
14.0	7.379	74.7	9.08	23.6	0.0871	0.315	39.3	0.000655	1.02754	0.812
15.0	6.737	79.3	8.79	22.7	0.0810	0.317	39.8	0.000725	1.02536	0.807
16.0	6.237	84.4	8.57	22.2	0.0752	0.319	40.4	0.000800	1.02344	0.803
17.0	5.847	89.5	8.40	21.9	0.0699	0.322	41.0	0.000880	1.02179	0.798
18.0	5.466	95.0	8.25	21.6	0.0651	0.326	41.8	0.000964	1.02036	0.792
19.0	5.133	101.0	8.12	21.5	0.0608	0.330	42.5	0.00105	1.01911	0.787
20.0	4.840	106.0	8.01	21.4	0.0570	0.335	43.3	0.00115	1.01801	0.781
21.0	4.579	112.0	7.92	21.3	0.0536	0.340	44.1	0.00124	1.01704	0.776
22.0	4.347	117.0	7.83	21.2	0.0505	0.345	44.9	0.00134	1.01617	0.771
23.0	4.139	123.0	7.76	21.2	0.0479	0.350	45.7	0.00144	1.01539	0.767
24.0	3.951	129.0	7.70	21.2	0.0453	0.355	46.6	0.00154	1.01469	0.763
25.0	3.780	134.0	7.64	21.1	0.0431	0.361	47.4	0.00165	1.01405	0.759
26.0	3.625	140.0	7.58	21.1	0.0410	0.366	48.2	0.00176	1.01347	0.756
28.0	3.351	151.0	7.49	21.1	0.0375	0.378	49.9	0.00199	1.01245	0.750
30.0	3.118	162.0	7.41	21.1	0.0346	0.389	51.6	0.00222	1.01158	0.744
32.0	2.917	173.0	7.35	21.1	0.0321	0.400	53.2	0.00246	1.01084	0.740
34.0	2.742	185.0	7.29	21.1	0.0299	0.411	54.8	0.00272	1.01018	0.736
36.0	2.588	196.0	7.24	21.0	0.0281	0.423	56.4	0.00298	1.00961	0.733
38.0	2.450	207.0	7.20	21.0	0.0264	0.434	58.0	0.00324	1.00910	0.730
40.0	2.328	218.0	7.16	21.0	0.0250	0.445	59.6	0.00352	1.00864	0.727
45.0	2.070	245.0	7.08	21.0	0.0220	0.473	63.5	0.00425	1.00768	0.722
50.0	1.856	272.0	7.02	20.9	0.0197	0.501	67.2	0.00502	1.00692	0.717
55.0	1.679	298.0	6.97	20.9	0.0178	0.524	70.9	0.00584	1.00630	0.714
60.0	1.530	325.0	6.93	20.8	0.0163	0.545	74.4	0.00671	1.00579	0.710
65.0	1.403	352.0	6.90	20.8	0.0150	0.561	77.9	0.00763	1.00535	0.707
70.0	1.292	378.0	6.87	20.8	0.0139	0.603	81.2	0.00859	1.00498	0.704
75.0	1.195	404.0	6.85	20.7	0.0130	0.633	84.5	0.00960	1.00465	0.702
80.0	1.179	431.0	6.83	20.7	0.0122	0.659	87.8	0.0107	1.00437	0.699
90.0	1.051	483.0	6.79	20.6	0.0108	0.709	94.1	0.0129	1.00389	0.695
100.0	0.9460	535.0	6.77	20.6	0.00976	0.758	100.6	0.0153	1.00351	0.691
125.0	0.7523	666.0	6.72	20.5	0.00783	0.875	113.0	0.0220	1.00282	0.673
150.0	0.6376	796.0	6.69	20.4	0.00654	0.986	127.0	0.0297	1.00236	0.669
175.0	0.5481	926.0	6.67	20.3	0.00562	1.09	140.0	0.0383	1.00203	0.667
200.0	0.4806	1060.0	6.66	20.3	0.00492	1.19	153.0	0.0478	1.00178	0.665
225.0	0.4279	1190.0	6.65	20.3	0.00438	1.29	165.0	0.0580	1.00158	0.665
250.0	0.3857	1320.0	6.64	20.2	0.00395	1.38	177.0	0.0690	1.00143	0.665
275.0	0.3510	1450.0	6.63	20.2	0.00359	1.47	189.0	0.0807	1.00130	0.666
300.0	0.3221	1570.0	6.63	20.2	0.00330	1.56	200.0	0.0931	1.00119	0.667
350.0	0.2765	1830.0	6.62	20.2	0.00283	1.73	222.0	0.120	1.00102	0.667
400.0	0.2422	2090.0	6.61	20.1	0.00248	1.90	243.0	0.151	1.00090	0.667
450.0	0.2155	2350.0	6.61	20.1	0.00221	2.06	264.0	0.184	1.00080	0.667
500.0	0.1941	2610.0	6.60	20.1	0.00199	2.21	284.0	0.220	1.00072	0.667
600.0	0.1619	3130.0	6.60	20.1	0.00166	2.51	322.0	0.299	1.00060	0.666
700.0	0.1389	3650.0	6.59	20.1	0.00142	2.80	359.0	0.388	1.00051	0.666
800.0	0.1216	4170.0	6.59	20.1	0.00125	3.08	395.0	0.487	1.00045	0.666
900.0	0.1081	4690.0	6.59	20.1	0.00111	3.34	429.0	0.595	1.00040	0.666
1000.0	0.09734	5210.0	6.59	20.0	0.00100	3.60	462.0	0.712	1.00036	0.666
1100.0	0.08851	5730.0	6.58	20.0	0.000917	3.85	494.0	0.838	1.00033	0.666
1200.0	0.08115	6250.0	6.58	20.0	0.000831	4.10	525.0	0.972	1.00030	0.666
1300.0	0.07492	6770.0	6.58	20.0	0.000768	4.34	556.0	1.11	1.00028	0.666
1400.0	0.06958	7280.0	6.58	20.0	0.000713	4.57	586.0	1.27	1.00026	0.666
1500.0	0.06495	7800.0	6.58	20.0	0.000665	4.80	616.0	1.42	1.00024	0.666

* TWO-PHASE BOUNDARY
** NUMBERS IN THIS COLUMN HAVE BEEN MULTIPLIED BY THE INDICATED FACTOR

THERMODYNAMIC PROPERTIES OF HELIUM 4

25.0 ATMOSPHERE ISOBAR

TEMPERATURE DEG. K	VOLUME CC/G ** X .01	ISOTHERM DERIVATIVE CC-ATM/G	ISOCHORE DERIVATIVE ATM/K	INTERNAL ENERGY J/G	ENTHALPY J/G	ENTROPY J/G-K	CV J/G-K	CP J/G-K	VELOCITY OF SOUND M/S
2.0	0.05696	1260.0	2.50	3.559	17.99	1.289	1.587	1.619	360.2
2.5	0.05721	1310.0	2.25	4.051	18.54	1.559	1.226	1.258	369.7
3.0	0.05756	1290.0	3.50	4.575	19.16	1.807	1.521	1.617	372.8
3.5	0.05809	1230.0	4.68	5.227	19.94	2.065	1.690	1.902	375.1
4.0	0.05882	1160.0	5.51	6.007	20.91	2.330	1.847	2.212	375.9
4.5	0.05973	1090.0	5.98	6.949	22.08	2.605	2.034	2.568	373.1
5.0	0.06083	1010.0	6.16	8.093	23.50	2.895	2.243	2.948	366.9
5.1	0.06107	1000.0	6.18	8.350	23.82	2.955	2.283	3.021	365.6
5.2	0.06132	986.0	6.19	8.619	24.15	3.015	2.302	3.073	365.2
5.3	0.06156	972.0	6.19	8.866	24.46	3.073	2.283	3.087	364.9
5.4	0.06181	958.0	6.19	9.115	24.77	3.131	2.290	3.127	364.0
5.5	0.06206	943.0	6.18	9.365	25.09	3.189	2.299	3.169	363.0
5.6	0.06231	929.0	6.17	9.619	25.40	3.246	2.308	3.212	361.9
5.7	0.06257	915.0	6.16	9.875	25.73	3.304	2.319	3.257	360.8
5.8	0.06284	901.0	6.15	10.13	26.05	3.361	2.330	3.303	359.6
5.9	0.06311	887.0	6.13	10.40	26.38	3.418	2.342	3.351	358.4
6.0	0.06339	873.0	6.11	10.66	26.72	3.475	2.355	3.399	357.2
6.5	0.06488	805.0	5.97	12.04	28.47	3.757	2.425	3.653	350.4
7.0	0.06652	740.0	5.79	13.50	30.35	4.039	2.498	3.921	343.1
7.5	0.06835	680.0	5.59	15.05	32.37	4.320	2.570	4.200	335.6
8.0	0.07038	625.0	5.36	16.70	34.53	4.602	2.637	4.485	328.1
8.5	0.07264	574.0	5.12	18.44	36.84	4.885	2.700	4.775	320.8
9.0	0.07513	529.0	4.87	20.26	39.30	5.170	2.757	5.065	313.8
9.5	0.07789	490.0	4.62	22.18	41.91	5.455	2.809	5.350	307.4
10.0	0.08092	456.0	4.36	24.17	44.66	5.741	2.856	5.623	301.6
11.0	0.08795	405.0	3.84	28.52	50.80	6.332	2.939	6.074	291.1
12.0	0.09591	379.0	3.36	32.97	57.27	6.901	2.992	6.329	284.9
13.0	0.1045	372.0	2.96	37.37	63.83	7.431	3.027	6.405	282.3
14.0	0.1132	376.0	2.62	41.62	70.33	7.915	3.052	6.379	282.3
15.0	0.1221	386.0	2.35	45.69	76.62	8.353	3.070	6.323	283.8
16.0	0.1312	400.0	2.14	49.68	82.93	8.760	3.091	6.291	287.1
17.0	0.1405	416.0	1.96	53.60	89.20	9.140	3.107	6.247	291.1
18.0	0.1498	434.0	1.81	57.46	95.42	9.496	3.120	6.197	295.5
19.0	0.1592	454.0	1.67	61.27	101.6	9.829	3.130	6.143	300.3
20.0	0.1685	474.0	1.56	65.02	107.7	10.14	3.138	6.090	305.3
21.0	0.1779	496.0	1.46	68.72	113.8	10.44	3.144	6.037	310.5
22.0	0.1872	518.0	1.37	72.37	119.8	10.72	3.149	5.987	315.7
23.0	0.1964	540.0	1.29	75.99	125.7	10.98	3.153	5.939	321.0
24.0	0.2056	562.0	1.22	79.57	131.7	11.24	3.155	5.894	326.3
25.0	0.2148	585.0	1.16	83.12	137.5	11.48	3.157	5.852	331.5
26.0	0.2240	608.0	1.11	86.63	143.4	11.70	3.159	5.812	336.7
28.0	0.2421	654.0	1.01	93.59	154.9	12.13	3.161	5.742	347.0
30.0	0.2601	700.0	0.927	100.5	166.3	12.53	3.161	5.681	357.1
32.0	0.2779	746.0	0.858	107.3	177.6	12.89	3.161	5.629	367.0
34.0	0.2956	792.0	0.799	114.0	188.9	13.23	3.160	5.584	376.6
36.0	0.3131	838.0	0.747	120.7	200.0	13.55	3.159	5.545	385.9
38.0	0.3306	883.0	0.703	127.3	211.0	13.85	3.158	5.512	395.0
40.0	0.3479	928.0	0.663	133.9	222.0	14.13	3.157	5.482	403.9
45.0	0.3909	1040.0	0.581	150.3	249.3	14.77	3.154	5.423	425.3
50.0	0.4335	1150.0	0.518	166.5	276.3	15.34	3.151	5.380	445.6
55.0	0.4758	1260.0	0.468	182.6	303.1	15.85	3.149	5.347	464.9
60.0	0.5179	1360.0	0.426	198.6	329.8	16.32	3.146	5.321	483.3
65.0	0.5597	1470.0	0.392	214.5	356.3	16.74	3.144	5.301	501.1
70.0	0.6014	1580.0	0.363	230.4	382.8	17.13	3.142	5.285	518.1
75.0	0.6430	1680.0	0.338	246.3	409.2	17.50	3.140	5.272	534.6
80.0	0.6845	1790.0	0.316	262.1	435.5	17.84	3.139	5.261	550.6
90.0	0.7673	1990.0	0.280	293.7	488.0	18.46	3.136	5.245	581.2
100.0	0.8498	2200.0	0.251	325.2	540.4	19.01	3.134	5.233	610.2
125.0	1.056	2720.0	0.200	403.6	671.0	20.17	3.130	5.216	677.2
150.0	1.261	3230.0	0.167	481.9	801.3	21.12	3.128	5.207	738.1
175.0	1.466	3740.0	0.143	560.1	931.4	21.93	3.126	5.202	794.3
200.0	1.671	4250.0	0.125	638.2	1061.0	22.62	3.125	5.199	846.8
225.0	1.876	4770.0	0.111	716.2	1191.0	23.23	3.124	5.197	896.2
250.0	2.080	5280.0	0.100	794.3	1321.0	23.78	3.123	5.195	943.1
275.0	2.285	5790.0	0.0908	872.3	1451.0	24.28	3.122	5.194	987.7
300.0	2.490	6300.0	0.0832	950.3	1581.0	24.73	3.122	5.194	1030.0
350.0	2.899	7320.0	0.0713	1106.0	1841.0	25.53	3.121	5.193	1111.0
400.0	3.309	8340.0	0.0624	1262.0	2100.0	26.22	3.121	5.193	1186.0
450.0	3.718	9370.0	0.0555	1418.0	2360.0	26.83	3.120	5.192	1257.0
500.0	4.128	10400.0	0.0499	1574.0	2619.0	27.38	3.120	5.192	1323.0
600.0	4.947	12400.0	0.0416	1886.0	3139.0	28.33	3.119	5.192	1448.0
700.0	5.766	14500.0	0.0357	2197.0	3658.0	29.13	3.119	5.192	1563.0
800.0	6.585	16500.0	0.0312	2509.0	4177.0	29.82	3.119	5.192	1669.0
900.0	7.404	18600.0	0.0278	2821.0	4696.0	30.43	3.119	5.192	1770.0
1000.0	8.224	20600.0	0.0250	3132.0	5215.0	30.98	3.119	5.192	1865.0
1100.0	9.043	22700.0	0.0227	3444.0	5735.0	31.47	3.118	5.192	1955.0
1200.0	9.862	24700.0	0.0208	3756.0	6254.0	31.93	3.118	5.192	2042.0
1300.0	10.68	26800.0	0.0192	4067.0	6773.0	32.34	3.118	5.192	2125.0
1400.0	11.50	28800.0	0.0178	4379.0	7292.0	32.73	3.118	5.192	2204.0
1500.0	12.32	30900.0	0.0167	4691.0	7812.0	33.08	3.118	5.192	2281.0

* TWO-PHASE BOUNDARY
** NUMBERS IN THIS COLUMN HAVE BEEN MULTIPLIED BY THE INDICATED FACTOR

25.0 ATMOSPHERE ISOBAR

TEMPERATURE	DENSITY	$V(\partial H/\partial V)_P$	$V(\partial P/\partial U)_V$	$-V(\partial P/\partial V)_T$	$(\partial V/\partial T)/V_P$	THERMAL CONDUCTIVITY	VISCOSITY	THERMAL DIFFUSIVITY	DIELECTRIC CONSTANT	PRANDTL NUMBER
DEG.K	G/CC ** X 100	J/G	ATM-CC/J	ATM	1/DEG.K	MW/CM-K	G/CM-S ** X 1000000	SQ-CM/S		
2.0	17.56	143.0	8.97	220.0	0.0113	0.147	91.2	0.000518	1.06630	1.00
2.5	17.48	128.0	10.5	230.0	0.00981	0.214	91.2	0.000971	1.06599	0.537
3.0	17.37	103.0	13.3	224.0	0.0156	0.238	86.1	0.000846	1.06559	0.586
3.5	17.21	86.4	16.1	212.0	0.0220	0.256	79.9	0.000782	1.06498	0.594
4.0	17.00	79.5	17.5	198.0	0.0278	0.274	73.9	0.000729	1.06416	0.597
4.5	16.74	78.3	17.5	182.0	0.0328	0.292	68.6	0.000678	1.06316	0.604
5.0	16.44	79.5	16.7	166.0	0.0371	0.307	63.9	0.000634	1.06200	0.613
5.1	16.37	79.8	16.5	163.0	0.0378	0.310	63.0	0.000627	1.06175	0.614
5.2	16.31	79.8	16.5	161.0	0.0385	0.313	62.2	0.000625	1.06149	0.610
5.3	16.24	78.7	16.7	158.0	0.0392	0.316	61.4	0.000630	1.06125	0.600
5.4	16.18	78.3	16.7	155.0	0.0400	0.319	60.7	0.000630	1.06100	0.596
5.5	16.11	77.9	16.7	152.0	0.0407	0.321	60.0	0.000629	1.06075	0.592
5.6	16.05	77.6	16.7	149.0	0.0414	0.324	59.3	0.000628	1.06050	0.589
5.7	15.98	77.3	16.6	146.0	0.0421	0.326	58.7	0.000627	1.06024	0.586
5.8	15.91	77.0	16.6	143.0	0.0429	0.329	58.1	0.000625	1.05998	0.583
5.9	15.84	76.8	16.5	140.0	0.0436	0.331	57.5	0.000624	1.05972	0.582
6.0	15.78	76.5	16.4	138.0	0.0444	0.333	56.9	0.000622	1.05945	0.580
6.5	15.41	75.9	16.0	124.0	0.0481	0.343	54.2	0.000609	1.05806	0.578
7.0	15.03	75.3	15.4	111.0	0.0520	0.351	52.0	0.000595	1.05660	0.582
7.5	14.63	74.8	14.9	100.0	0.0561	0.356	50.1	0.000579	1.05506	0.591
8.0	14.21	74.3	14.3	88.8	0.0604	0.360	48.5	0.000564	1.05345	0.605
8.5	13.77	73.7	13.8	79.1	0.0648	0.362	47.1	0.000550	1.05176	0.622
9.0	13.31	73.2	13.3	70.4	0.0692	0.362	46.0	0.000537	1.05002	0.643
9.5	12.84	72.9	12.8	62.9	0.0734	0.362	45.0	0.000527	1.04822	0.665
10.0	12.36	72.7	12.4	56.3	0.0774	0.360	44.2	0.000518	1.04639	0.689
11.0	11.37	72.9	11.5	46.0	0.0834	0.355	42.9	0.000515	1.04264	0.733
12.0	10.43	74.4	10.8	39.5	0.0851	0.350	42.2	0.000531	1.03905	0.762
13.0	9.574	77.1	10.2	35.6	0.0830	0.347	41.9	0.000565	1.03582	0.774
14.0	8.831	80.8	9.74	33.2	0.0799	0.345	42.0	0.000612	1.03332	0.777
15.0	8.191	84.9	9.36	31.6	0.0764	0.345	42.3	0.000665	1.03160	0.776
16.0	7.619	89.5	9.09	30.5	0.0743	0.345	42.7	0.000720	1.02845	0.778
17.0	7.117	94.4	8.86	29.6	0.0662	0.347	43.2	0.000780	1.02556	0.779
18.0	6.674	99.4	8.67	29.0	0.0623	0.349	43.8	0.000844	1.02489	0.778
19.0	6.282	105.0	8.51	28.5	0.0587	0.352	44.5	0.000912	1.02342	0.776
20.0	5.934	110.0	8.37	28.1	0.0554	0.355	45.2	0.000983	1.02211	0.774
21.0	5.623	115.0	8.26	27.9	0.0524	0.359	45.9	0.00106	1.02095	0.771
22.0	5.343	121.0	8.15	27.7	0.0496	0.363	46.6	0.00114	1.01990	0.768
23.0	5.091	126.0	8.06	27.5	0.0471	0.368	47.4	0.00122	1.01895	0.765
24.0	4.863	132.0	7.98	27.4	0.0447	0.372	48.1	0.00130	1.01810	0.762
25.0	4.655	137.0	7.90	27.2	0.0426	0.377	48.9	0.00138	1.01732	0.759
26.0	4.465	143.0	7.84	27.2	0.0407	0.382	49.7	0.00147	1.01661	0.757
28.0	4.131	154.0	7.72	27.0	0.0373	0.392	51.3	0.00165	1.01536	0.751
30.0	3.845	165.0	7.62	26.9	0.0344	0.402	52.9	0.00184	1.01430	0.747
32.0	3.599	176.0	7.54	26.9	0.0319	0.413	54.5	0.00204	1.01338	0.743
34.0	3.383	187.0	7.47	26.8	0.0298	0.424	56.0	0.00224	1.01257	0.739
36.0	3.194	198.0	7.41	26.7	0.0279	0.434	57.6	0.00245	1.01186	0.735
38.0	3.025	209.0	7.35	26.7	0.0263	0.445	59.1	0.00267	1.01124	0.732
40.0	2.874	220.0	7.31	26.7	0.0249	0.456	60.7	0.00289	1.01067	0.730
45.0	2.558	248.0	7.21	26.6	0.0219	0.483	64.5	0.00348	1.00950	0.724
50.0	2.307	275.0	7.13	26.5	0.0196	0.510	68.1	0.00411	1.00856	0.719
55.0	2.102	302.0	7.07	26.4	0.0177	0.536	71.7	0.00477	1.00780	0.715
60.0	1.931	328.0	7.02	26.3	0.0162	0.563	75.2	0.00548	1.00716	0.711
65.0	1.787	355.0	6.98	26.3	0.0149	0.589	78.6	0.00622	1.00663	0.708
70.0	1.663	382.0	6.94	26.2	0.0138	0.615	82.0	0.00700	1.00617	0.705
75.0	1.555	408.0	6.91	26.1	0.0129	0.640	85.3	0.00781	1.00577	0.702
80.0	1.461	434.0	6.89	26.1	0.0121	0.665	88.5	0.00866	1.00542	0.700
90.0	1.303	487.0	6.85	26.0	0.0108	0.715	94.7	0.0105	1.00483	0.695
100.0	1.177	539.0	6.81	25.9	0.00971	0.763	101.0	0.0124	1.00436	0.691
125.0	0.9474	670.0	6.76	25.7	0.00779	0.880	116.0	0.0178	1.00351	0.673
150.0	0.7932	800.0	6.72	25.6	0.00651	0.991	127.0	0.0240	1.00294	0.669
175.0	0.6822	930.0	6.70	25.5	0.00559	1.10	141.0	0.0309	1.00253	0.667
200.0	0.5986	1060.0	6.68	25.5	0.00490	1.20	153.0	0.0385	1.00222	0.665
225.0	0.5332	1190.0	6.66	25.4	0.00437	1.29	165.0	0.0467	1.00197	0.664
250.0	0.4807	1320.0	6.65	25.4	0.00394	1.39	177.0	0.0555	1.00178	0.664
275.0	0.4376	1450.0	6.64	25.3	0.00358	1.47	189.0	0.0649	1.00162	0.665
300.0	0.4016	1580.0	6.64	25.3	0.00329	1.56	200.0	0.0748	1.00149	0.667
350.0	0.3449	1840.0	6.63	25.3	0.00282	1.73	222.0	0.0967	1.00128	0.667
400.0	0.3022	2100.0	6.62	25.2	0.00248	1.90	244.0	0.121	1.00112	0.666
450.0	0.2689	2360.0	6.61	25.2	0.00220	2.06	264.0	0.147	1.00100	0.666
500.0	0.2423	2620.0	6.61	25.2	0.00198	2.21	284.0	0.176	1.00090	0.666
600.0	0.2022	3140.0	6.60	25.1	0.00166	2.51	323.0	0.240	1.00075	0.666
700.0	0.1734	3650.0	6.59	25.1	0.00142	2.80	359.0	0.311	1.00064	0.666
800.0	0.1519	4170.0	6.59	25.1	0.00124	3.08	395.0	0.390	1.00056	0.666
900.0	0.1351	4690.0	6.59	25.1	0.00111	3.34	429.0	0.477	1.00050	0.666
1000.0	0.1216	5210.0	6.59	25.1	0.00100	3.60	462.0	0.570	1.00045	0.666
1100.0	0.1106	5730.0	6.59	25.1	0.000906	3.85	494.0	0.671	1.00041	0.666
1200.0	0.1014	6250.0	6.58	25.1	0.000831	4.10	525.0	0.778	1.00038	0.666
1300.0	0.09362	6770.0	6.58	25.1	0.000767	4.34	556.0	0.892	1.00035	0.666
1400.0	0.08695	7290.0	6.58	25.0	0.000712	4.57	586.0	1.01	1.00032	0.666
1500.0	0.08116	7810.0	6.58	25.0	0.000665	4.80	616.0	1.14	1.00030	0.666

* TWO-PHASE BOUNDARY
** NUMBERS IN THIS COLUMN HAVE BEEN MULTIPLIED BY THE INDICATED FACTOR

THERMODYNAMIC PROPERTIES OF HELIUM 4

30.0 ATMOSPHERE ISOBAR

TEMPERATURE DEG. K	VOLUME CC/G ** X .01	ISOTHERM DERIVATIVE CC-ATM/G	ISOCHORE DERIVATIVE ATM/K	INTERNAL ENERGY J/G	ENTHALPY J/G	ENTROPY J/G-K	CV J/G-K	CP	VELOCITY OF SOUND M/S
2.0	0.05572	1320.0	4.01	3.849	20.79	1.262	1.373	1.450	376.3
2.5	0.05603	1430.0	2.52	4.276	21.31	1.516	1.181	1.216	385.8
3.0	0.05635	1420.0	3.61	4.753	21.88	1.754	1.454	1.542	390.9
3.5	0.05682	1380.0	4.80	5.348	22.62	1.999	1.618	1.810	394.9
4.0	0.05745	1310.0	5.67	6.067	23.53	2.250	1.784	2.112	396.8
4.5	0.05825	1240.0	6.18	6.947	24.65	2.513	1.982	2.458	394.9
5.0	0.05919	1170.0	6.40	8.026	26.02	2.791	2.201	2.825	389.5
5.1	0.05939	1150.0	6.43	8.269	26.32	2.847	2.243	2.896	388.5
5.2	0.05961	1140.0	6.45	8.524	26.64	2.905	2.264	2.945	388.1
5.3	0.05981	1130.0	6.46	8.757	26.94	2.961	2.246	2.955	388.0
5.4	0.06002	1120.0	6.46	8.991	27.23	3.016	2.255	2.992	387.2
5.5	0.06023	1100.0	6.46	9.228	27.54	3.071	2.264	3.030	386.4
5.6	0.06044	1090.0	6.46	9.466	27.84	3.126	2.275	3.070	385.5
5.7	0.06066	1070.0	6.45	9.708	28.15	3.181	2.287	3.111	384.5
5.8	0.06088	1060.0	6.44	9.95	28.46	3.236	2.299	3.153	383.5
5.9	0.06111	1040.0	6.43	10.20	28.77	3.290	2.313	3.196	382.4
6.0	0.06134	1030.0	6.41	10.45	29.09	3.344	2.327	3.239	381.3
6.5	0.06257	963.0	6.31	11.74	30.76	3.613	2.400	3.467	375.4
7.0	0.06392	898.0	6.17	13.11	32.54	3.879	2.476	3.704	368.9
7.5	0.06539	836.0	6.00	14.56	34.43	4.144	2.549	3.946	362.1
8.0	0.06700	779.0	5.80	16.09	36.45	4.408	2.618	4.191	355.4
8.5	0.06875	725.0	5.59	17.70	38.60	4.672	2.680	4.438	348.7
9.0	0.07067	676.0	5.37	19.38	40.87	4.934	2.738	4.683	342.2
9.5	0.07275	631.0	5.14	21.15	43.26	5.197	2.789	4.925	336.1
10.0	0.07502	592.0	4.91	22.98	45.78	5.459	2.836	5.161	330.4
11.0	0.08021	525.0	4.42	27.04	51.42	6.003	2.920	5.592	319.1
12.0	0.08612	480.0	3.95	31.27	57.45	6.534	2.977	5.913	310.8
13.0	0.09261	456.0	3.53	35.54	63.69	7.038	3.015	6.100	305.7
14.0	0.09945	448.0	3.16	39.76	69.99	7.510	3.042	6.172	303.3
15.0	0.1065	449.0	2.85	43.88	76.24	7.944	3.062	6.173	302.9
16.0	0.1137	456.0	2.60	47.85	82.42	8.342	3.083	6.186	304.5
17.0	0.1212	467.0	2.38	51.77	88.61	8.717	3.101	6.177	307.1
18.0	0.1287	481.0	2.20	55.65	94.77	9.070	3.115	6.155	310.3
19.0	0.1363	497.0	2.04	59.48	100.9	9.402	3.127	6.123	314.1
20.0	0.1440	515.0	1.90	63.26	107.0	9.715	3.136	6.088	318.2
21.0	0.1516	534.0	1.78	67.00	113.1	10.01	3.144	6.049	322.6
22.0	0.1593	554.0	1.67	70.70	119.1	10.29	3.149	6.009	327.2
23.0	0.1670	574.0	1.58	74.36	125.1	10.56	3.154	5.970	331.9
24.0	0.1746	596.0	1.49	77.98	131.1	10.81	3.158	5.931	336.6
25.0	0.1822	617.0	1.42	81.57	137.0	11.05	3.160	5.894	341.5
26.0	0.1898	639.0	1.35	85.14	142.8	11.28	3.162	5.858	346.3
28.0	0.2050	684.0	1.23	92.18	154.5	11.71	3.165	5.791	355.9
30.0	0.2200	729.0	1.13	99.13	166.0	12.11	3.166	5.731	365.5
32.0	0.2349	774.0	1.04	106.0	177.4	12.48	3.167	5.678	374.9
34.0	0.2497	819.0	0.969	112.8	188.7	12.82	3.166	5.632	384.2
36.0	0.2645	864.0	0.906	119.6	199.9	13.14	3.166	5.591	393.3
38.0	0.2791	909.0	0.851	126.3	211.1	13.44	3.165	5.555	402.1
40.0	0.2936	954.0	0.803	132.9	222.2	13.73	3.164	5.523	410.8
45.0	0.3297	1070.0	0.703	149.4	249.6	14.38	3.160	5.458	431.8
50.0	0.3654	1180.0	0.626	165.7	276.8	14.95	3.157	5.410	451.7
55.0	0.4008	1280.0	0.564	181.9	303.7	15.46	3.154	5.372	470.7
60.0	0.4359	1390.0	0.514	198.0	330.5	15.93	3.152	5.343	488.9
65.0	0.4709	1500.0	0.472	214.0	357.2	16.35	3.149	5.320	506.4
70.0	0.5058	1600.0	0.437	230.0	383.7	16.75	3.147	5.301	523.3
75.0	0.5405	1710.0	0.406	245.9	410.2	17.11	3.145	5.286	539.7
80.0	0.5752	1820.0	0.380	261.8	436.6	17.45	3.143	5.274	555.5
90.0	0.6442	2020.0	0.336	293.4	489.2	18.07	3.140	5.255	585.8
100.0	0.7131	2230.0	0.302	324.9	541.7	18.63	3.138	5.241	614.6
125.0	0.8847	2750.0	0.241	403.5	672.4	19.79	3.133	5.221	681.1
150.0	1.056	3260.0	0.200	481.9	802.8	20.74	3.130	5.210	741.6
175.0	1.227	3770.0	0.171	560.1	933.0	21.55	3.128	5.204	797.5
200.0	1.397	4290.0	0.150	638.3	1063.0	22.24	3.127	5.200	849.7
225.0	1.568	4800.0	0.133	716.3	1193.0	22.85	3.125	5.197	898.9
250.0	1.739	5310.0	0.120	794.4	1323.0	23.40	3.125	5.196	945.6
275.0	1.909	5820.0	0.109	872.4	1453.0	23.90	3.124	5.195	990.1
300.0	2.080	6330.0	0.100	950.4	1583.0	24.35	3.123	5.194	1033.0
350.0	2.421	7350.0	0.0856	1106.0	1842.0	25.15	3.122	5.193	1113.0
400.0	2.762	8370.0	0.0749	1262.0	2102.0	25.84	3.122	5.192	1188.0
450.0	3.103	9390.0	0.0666	1418.0	2362.0	26.45	3.121	5.192	1258.0
500.0	3.444	10400.0	0.0599	1574.0	2621.0	27.00	3.121	5.192	1325.0
600.0	4.127	12500.0	0.0499	1886.0	3140.0	27.95	3.120	5.192	1449.0
700.0	4.809	14500.0	0.0428	2198.0	3659.0	28.75	3.120	5.192	1564.0
800.0	5.492	16500.0	0.0375	2509.0	4179.0	29.44	3.120	5.192	1670.0
900.0	6.174	18600.0	0.0333	2821.0	4698.0	30.05	3.119	5.192	1771.0
1000.0	6.857	20600.0	0.0300	3133.0	5217.0	30.60	3.119	5.192	1866.0
1100.0	7.540	22700.0	0.0272	3444.0	5736.0	31.09	3.119	5.192	1956.0
1200.0	8.222	24700.0	0.0250	3756.0	6255.0	31.55	3.119	5.192	2042.0
1300.0	8.905	26800.0	0.0231	4068.0	6775.0	31.96	3.119	5.192	2125.0
1400.0	9.588	28800.0	0.0214	4379.0	7294.0	32.35	3.119	5.192	2205.0
1500.0	10.27	30900.0	0.0200	4691.0	7813.0	32.71	3.118	5.192	2282.0

* TWO-PHASE BOUNDARY
** NUMBERS IN THIS COLUMN HAVE BEEN MULTIPLIED BY THE INDICATED FACTOR

THERMOPHYSICAL PROPERTIES OF HELIUM 4

30.0 ATMOSPHERE ISOBAR

TEMPERATURE	DENSITY	V(DH/DV)$_P$	V(DP/DU)$_V$	-V(DP/DV)$_T$	(DV/DT)/V$_P$	THERMAL CONDUCTIVITY	VISCOSITY	THERMAL DIFFUSIVITY	DIELECTRIC CONSTANT	PRANDTL NUMBER
DEG.K	G/CC ** X 100	J/G	ATM-CC/J	ATM	1/DEG.K	MW/CM-K	G/CM-S ** X 1000000	SQ-CM/S		
2.0	17.95	85.9	16.3	238.0	0.0169	0.150	105.0	0.000576	1.06780	1.02
2.5	17.85	123.0	11.9	255.0	0.00988	0.221	104.0	0.00102	1.06742	0.571
3.0	17.75	108.0	14.0	252.0	0.0143	0.246	96.8	0.000898	1.06713	0.667
3.5	17.60	91.3	16.9	242.0	0.0198	0.265	89.2	0.000832	1.06646	0.669
4.0	17.40	85.1	18.3	228.0	0.0240	0.284	82.3	0.000773	1.06571	0.610
4.5	17.17	84.7	18.2	213.0	0.0290	0.303	75.7	0.000717	1.06480	0.615
5.0	16.90	87.0	17.2	197.0	0.0325	0.320	70.3	0.000670	1.06375	0.621
5.1	16.84	87.5	17.0	194.0	0.0331	0.323	69.3	0.000662	1.06353	0.621
5.2	16.78	87.6	17.0	192.0	0.0336	0.326	68.3	0.000660	1.06330	0.617
5.3	16.72	86.4	17.2	189.0	0.0342	0.329	67.5	0.000666	1.06308	0.606
5.4	16.66	86.1	17.2	186.0	0.0348	0.332	66.6	0.000666	1.06286	0.600
5.5	16.60	85.8	17.2	183.0	0.0353	0.335	65.8	0.000666	1.06263	0.596
5.6	16.54	85.5	17.2	180.0	0.0359	0.338	65.1	0.000665	1.06240	0.591
5.7	16.49	85.3	17.1	177.0	0.0365	0.341	64.3	0.000664	1.06217	0.587
5.8	16.42	85.1	17.1	174.0	0.0370	0.343	63.6	0.000663	1.06194	0.584
5.9	16.36	85.0	17.0	171.0	0.0376	0.346	62.9	0.000662	1.06171	0.581
6.0	16.30	84.9	16.9	168.0	0.0382	0.348	62.3	0.000660	1.06147	0.579
6.5	15.98	84.5	16.5	154.0	0.0410	0.360	59.3	0.000649	1.06024	0.571
7.0	15.65	84.4	15.9	140.0	0.0439	0.369	56.7	0.000637	1.05895	0.570
7.5	15.29	84.2	15.4	128.0	0.0469	0.376	54.6	0.000623	1.05760	0.573
8.0	14.93	83.9	14.9	116.0	0.0499	0.381	52.8	0.000609	1.05620	0.580
8.5	14.55	83.7	14.3	105.0	0.0530	0.385	51.2	0.000596	1.05474	0.591
9.0	14.15	83.4	13.9	95.6	0.0562	0.387	49.9	0.000584	1.05323	0.604
9.5	13.74	83.1	13.4	86.8	0.0593	0.388	48.8	0.000573	1.05168	0.620
10.0	13.33	82.9	13.0	78.9	0.0623	0.388	47.8	0.000564	1.05009	0.637
11.0	12.47	82.7	12.1	65.4	0.0676	0.385	46.3	0.000552	1.04681	0.673
12.0	11.61	83.4	11.4	55.7	0.0709	0.381	45.3	0.000554	1.04355	0.704
13.0	10.80	85.1	10.8	49.2	0.0717	0.377	44.8	0.000572	1.04046	0.726
14.0	10.05	87.9	10.3	45.6	0.0702	0.373	44.6	0.000602	1.03765	0.737
15.0	9.393	91.4	9.90	42.2	0.0675	0.372	44.7	0.000641	1.03514	0.742
16.0	8.792	95.5	9.58	43.1	0.0648	0.371	45.0	0.000682	1.03287	0.750
17.0	8.252	100.0	9.32	38.6	0.0618	0.371	45.3	0.000728	1.03083	0.755
18.0	7.769	105.0	9.09	37.4	0.0588	0.372	45.8	0.000778	1.02901	0.758
19.0	7.336	109.0	8.90	36.5	0.0559	0.374	46.4	0.000832	1.02738	0.760
20.0	6.946	114.0	8.73	35.8	0.0532	0.376	47.0	0.000889	1.02592	0.760
21.0	6.595	120.0	8.59	35.2	0.0506	0.379	47.6	0.000950	1.02460	0.760
22.0	6.278	125.0	8.46	34.8	0.0481	0.382	48.3	0.00101	1.02340	0.760
23.0	5.990	130.0	8.35	34.4	0.0459	0.386	49.0	0.00108	1.02232	0.758
24.0	5.727	136.0	8.25	34.1	0.0438	0.389	49.7	0.00115	1.02134	0.757
25.0	5.488	141.0	8.17	33.9	0.0418	0.393	50.4	0.00122	1.02044	0.755
26.0	5.268	146.0	8.09	33.7	0.0400	0.398	51.2	0.00129	1.01962	0.754
28.0	4.879	157.0	7.95	33.3	0.0368	0.407	52.7	0.00144	1.01816	0.750
30.0	4.545	168.0	7.83	33.1	0.0340	0.416	54.2	0.00160	1.01691	0.746
32.0	4.257	179.0	7.73	32.9	0.0316	0.426	55.7	0.00176	1.01583	0.743
34.0	4.004	191.0	7.65	32.8	0.0296	0.436	57.2	0.00193	1.01489	0.739
36.0	3.781	202.0	7.57	32.7	0.0277	0.446	58.7	0.00211	1.01406	0.736
38.0	3.583	213.0	7.51	32.6	0.0261	0.456	60.2	0.00229	1.01332	0.734
40.0	3.406	224.0	7.45	32.5	0.0247	0.467	61.7	0.00248	1.01266	0.731
45.0	3.033	251.0	7.33	32.3	0.0217	0.493	65.4	0.00298	1.01127	0.725
50.0	2.737	278.0	7.24	32.2	0.0194	0.519	69.1	0.00350	1.01016	0.720
55.0	2.495	305.0	7.17	32.0	0.0176	0.545	72.6	0.00406	1.00926	0.716
60.0	2.294	332.0	7.11	31.9	0.0161	0.571	76.0	0.00466	1.00851	0.712
65.0	2.124	359.0	7.06	31.8	0.0148	0.596	79.4	0.00528	1.00788	0.708
70.0	1.977	385.0	7.02	31.7	0.0138	0.622	82.7	0.00593	1.00734	0.705
75.0	1.850	412.0	6.98	31.6	0.0128	0.647	86.0	0.00662	1.00686	0.702
80.0	1.739	438.0	6.95	31.6	0.0120	0.672	89.2	0.00733	1.00645	0.700
90.0	1.552	491.0	6.90	31.4	0.0107	0.721	95.4	0.00884	1.00576	0.695
100.0	1.402	543.0	6.86	31.3	0.00964	0.769	101.0	0.0109	1.00520	0.691
125.0	1.130	674.0	6.79	31.1	0.00774	0.885	114.0	0.0150	1.00419	0.673
150.0	0.9472	804.0	6.75	30.9	0.00648	1.00	128.0	0.0202	1.00351	0.669
175.0	0.8153	934.0	6.72	30.8	0.00557	1.13	141.0	0.0259	1.00302	0.666
200.0	0.7157	1060.0	6.70	30.7	0.00489	1.26	154.0	0.0323	1.00265	0.665
225.0	0.6378	1190.0	6.68	30.6	0.00435	1.38	166.0	0.0391	1.00236	0.664
250.0	0.5752	1320.0	6.67	30.5	0.00392	1.49	178.0	0.0465	1.00213	0.664
275.0	0.5238	1450.0	6.66	30.5	0.00357	1.60	189.0	0.0543	1.00194	0.665
300.0	0.4808	1580.0	6.65	30.4	0.00328	1.70	200.0	0.0625	1.00178	0.666
350.0	0.4131	1840.0	6.63	30.4	0.00282	1.90	222.0	0.0808	1.00153	0.666
400.0	0.3621	2100.0	6.63	30.3	0.00247	1.90	244.0	0.101	1.00134	0.666
450.0	0.3222	2360.0	6.62	30.3	0.00220	2.06	264.0	0.123	1.00119	0.666
500.0	0.2903	2620.0	6.61	30.2	0.00198	2.22	284.0	0.147	1.00108	0.666
600.0	0.2423	3140.0	6.60	30.2	0.00165	2.52	323.0	0.200	1.00090	0.666
700.0	0.2079	3660.0	6.60	30.2	0.00142	2.80	359.0	0.260	1.00077	0.666
800.0	0.1821	4180.0	6.59	30.1	0.00124	3.08	395.0	0.325	1.00067	0.666
900.0	0.1620	4700.0	6.59	30.1	0.00111	3.34	429.0	0.398	1.00060	0.666
1000.0	0.1458	5220.0	6.59	30.1	0.00100	3.60	462.0	0.476	1.00054	0.666
1100.0	0.1326	5730.0	6.59	30.1	0.000905	3.85	494.0	0.560	1.00049	0.666
1200.0	0.1216	6250.0	6.58	30.1	0.000830	4.10	525.0	0.649	1.00045	0.666
1300.0	0.1123	6770.0	6.58	30.1	0.000767	4.34	556.0	0.744	1.00042	0.666
1400.0	0.1043	7290.0	6.58	30.1	0.000712	4.57	586.0	0.845	1.00039	0.666
1500.0	0.09737	7810.0	6.58	30.1	0.000665	4.80	616.0	0.950	1.00036	0.665

* TWO-PHASE BOUNDARY
** NUMBERS IN THIS COLUMN HAVE BEEN MULTIPLIED BY THE INDICATED FACTOR

Appendix 10.2 Thermal conductivity integrals and specific heats of several solids

Source: CON70

T. (°K)	*Intégrales de la conductibilité thermique* $\int_{T_1}^{T_2} K_{(T)} dT$ $(T_1 = 4\ °K)$										*T.* (°K)
	Watts/cm							Milliwatts/cm			
	Monel (recuit)	Monel (écroui)	Inconel (recuit)	Inconel (écroui)	Cuivre OFHC	Laiton	Z_3CN 18.10	Verre	Teflon	Nylon	
6	0,0235	0,0123	0,0133	0,00712	6,1	0,053	0,0063	2,11	1,13	0,321	6
8	0,0605	0,0329	0,0348	0,0185	14,5	0,129	0,0159	4,43	2,62	0,807	8
10	0,112	0,0629	0,0653	0,0345	25,2	0,229	0,0293	6,81	4,4	1,48	10
15	0,315	0,181	0,182	0,0975	61,4	0,594	0,0816	13,1	9,85	4,10	15
20	0,618	0,364	0,356	0,195	110	1,12	0,163	20,0	16,4	8,23	20
25	1,01	0,614	0,592	0,325	168	1,81	0,277	27,9	23,9	13,9	25
30	1,48	0,929	0,882	0,488	228	2,65	0,424	36,8	32,2	20,8	30
35	2,01	1,30	1,22	0,685	285	3,63	0,607	47,1	41,3	29,0	35
40	2,58	1,73	1,60	0,918	338	4,76	0,824	58,6	50,8	38,5	40
50	3,85	2,73	2,47	1,48	426	7,36	1,35	84,6	71,6	60,4	50
60	5,23	3,88	3,45	2,15	496	10,4	1,98	115	93,6	85,9	60
70	6,69	5,13	4,52	2,94	554	13,9	2,70	151	116	113	70
76	7,61	5,92	5,19	3,47	586	16,2	3,17	175	130	131	76
80	8,24	6,47	5,66	3,84	606	17,7	3,49	194	139	142	80
90	9,86	7,91	6,85	4,84	654	22,0	4,36	240	163	173	90
100	11,5	9,40	8,06	5,93	700	26,5	5,28	292	187	204	100
120	15,0	12,6	10,6	8,33	788	36,5	7,26	408	237	269	120
140	18,7	15,9	13,1	11,0	874	47,8	9,39	542	287	336	140
160	22,5	19,5	15,7	13,8	956	60,3	11,7	694	338	405	160
180	26,4	23,2	18,3	16,8	1040	73,8	14,1	858	390	475	180
200	30,5	27,1	21,0	19,9	1120	88,3	16,6	1 030	442	545	200
250	41,2	37,3	28,0	28,1	1320	128	23,4	1 500	572	720	250
300	52,5	48,0	35,4	36,9	1520	172	30,6	1 990	702	895	300

Temp. (°K)	Al *Aluminium*		Be *Béryllium*		Ti *Titane*	
	C_p (j/g °K)	H (j/g)	C_p (j/g-°K)	H (j/g)	C_p (j/g-°K)	H (j/g)
	0,000 10*					
1	0,000 051	0,000 025	0,000 025	0,000 013	0,000 071	0,000 035
2	0,000 108	0,000 105	0,000 051	0,000 051	0,000 146	0,000 143
3	0,000 176	0,000 246	0,000 079	0,000 116	0,000 226	0,000 329
4	0,000 261	0,000 463	0,000 109	0,000 209	0,000 317	0,000 599
6	0,000 50	0,001 21	0,000 180	0,000 496	0,000 54	0,001 45
8	0,000 88	0,002 6	0,000 271	0,000 944	0,000 84	0,002 81
10	0,001 4	0,004 9	0,000 389	0,001 60	0,001 26	0,004 89
15	0,004 0	0,018	0,000 842	0,004 57	0,003 3	0,015 6
20	0,008 9	0,048	0,001 61	0,010 5	0,007 0	0,040
25	0,017 5	0,112	0,002 79	0,021 2	0,013 4	0,090
30	0,031 5	0,232	0,004 50	0,039 2	0,024 5	0,182
35	0,051 5	0,436				
40	0,077 5	0,755	0,009 96	0,109	0,057 1	0,581
50	0,142	1,85	0,019 2	0,253	0,099 2	1,358
60	0,214	3,64	0,034 1	0,523	0,146 7	2,592
70	0,287	6,15	0,056 2	0,971	0,189	4,27
80	0,357	9,37	0,090 6	1,69	0,230	6,37
90	0,422	13,25	0,139	2,82	0,267	8,86
100	0,481	17,76	0,199	4,51	0,300	11,69
120	0,580	28,4	0,345	9,87	0,352	18,24
140	0,654	40,7	0,525	18,5	0,391	25,69
160	0,713	54,4	0,723	31,0	0,422	33,84
180	0,760	69,2	0,921	47,4	0,446	42,54
200	0,797	84,8	1,11	67,8	0,465	51,66
220	0,826	101,0	1,29	91,8	0,480	61,11
240	0,849	117,8	1,47	120	0,493	70,84
260	0,869	135,0	1,64	151	0,504	80,82
280	0,886	152,5	1,81	185	0,514	91,01
300	0,902	170,4	1,97	223	0,522	101,39

*Supraconducteur.

Temp. °K)	Cu *Cuivre*		Au *Or*		Ag *Argent*	
	C_p (j/g °K)	H (j/g)	C_p (j/g-°K)	H (j/g)	C_p (j/g-°K)	H (j/g)
1	0,000 012	0,000 006	0,000 006	0,000 002	0,000 0072	0,000 0032
2	0,000 028	0,000 025	0,000 025	0,000 016	0,000 0239	0,000 0176
3	0,000 053	0,000 064	0,000 070	0,000 061	0,000 0595	0,000 0574
4	0,000 091	0,000 13	0,000 16	0,000 17	0,000 124	0,000 146
6	0,000 23	0,000 44	0,000 50	0,000 78	0,000 39	0,000 62
8	0,000 47	0,001 12	0,001 2	0,002 4	0,000 91	0,001 87
10	0,000 86	0,002 4	0,002 2	0,005 6	0,001 8	0,004 52
15	0,002 7	0,010 7	0,007 4	0,028	0,006 4	0,023 3
20	0,007 7	0,034	0,015 9	0,086	0,015 5	0,076
25	0,016	0,090	0,026 3	0,191	0,028 7	0,185
30	0,027	0,195	0,037 1	0,349	0,044 2	0,368
40	0,060	0,61	0,057 2	0,821	0,078	0,979
50	0,099	1,40	0,072 6	1,47	0,108	1,91
60	0,137	2,58	0,084 2	2,25	0,133	3,12
70	0,173	4,13	0,092 8	3,14	0,151	4,54
80	0,205	6,02	0,099 2	4,10	0,166	6,13
90	0,232	8,22	0.104 3	5,12	0,177	7.85
100	0,254	10,6	0,108 3	6,18	0,187	9,67
120	0,288	16,1	0,113 7	8,41	0,200	13,55
140	0,313	22,1	0,117 5	10,72	0,209	17,65
160	0,332	28,5	0,120 2	13,10	0,216	21,91
180	0,346	35,3	0,122 1	15,52	0,221	26,29
200	0,356	42,4	0,123 5	17,98	0,225	30,75
220	0,364	49,6	0,124 7	20,46	0,228	35,28
240	0,371	56,9	0,125 7	22,96	0,231	39,86
260	0,376	64,4	0,126 7	25,49	0,234	44,50
280	0,381	72,0	0,127 6	28,03	0,235	49,20
300	0,386	79,6	0,128 5	30,59	0,236	53,91

Appendix 10.3 The derivation of (4-33) and (4-34)

Eliminating $d\dot{Q}$ from (4-31) and (4-32) gives

$$\frac{dT}{T-T_{he}} = -\alpha \frac{\pi D}{\dot{m} c_p} dx \qquad \text{(A3-1)}.$$

Using Nusselt's number

$$Nu := \frac{\alpha D}{\lambda} \qquad \text{(A3-2)}$$

where the thermal conductivity λ of the gas is given by (4-8), and using the empirical relationship for turbulent tube flow

$$Nu = 0.02\ Re^{0.8} \qquad \text{(A3-3)}$$

where Reynold's number is given by

$$Re := \frac{\rho v D}{\eta} = \frac{4}{\pi} \frac{\dot{m}}{\eta D} = \frac{4}{\pi} \frac{\dot{m}}{8.3\ 10^{-7}\ T^{0.55}\ D} \qquad \text{(A3-4)},$$

we find

$$\alpha = 11.4 \frac{T^{0.11}\ \dot{m}^{0.8}}{D^{1.8}} \qquad \text{(A3-5)}.$$

Substitution in (A3-1) yields

$$\int_{T_i}^{T(x)} \frac{dT}{(T-T_{he})\ T^{0.11}} = -\frac{11.4\ \pi}{c_p} \frac{x}{\dot{m}^{0.2}\ D^{0.8}} \qquad \text{(A3-6)}.$$

In order to evaluate the integral, $T^{0.11}$ is approximated by

$$1.80\ 10^{-3}\ T + 1.42 \qquad \text{(A3-7)}$$

between 20K and 300K, the maximum error being 5%.

Splitting up the denominator of the integrand into

$$\frac{C_1}{T-T_{he}} \quad \text{and} \quad \frac{C_2}{1.80\ 10^{-3}\ T\ +\ 1.42} \qquad \text{(A3-8)}$$

with $C_1 := (1.80\ 10^{-3}\ T_{he} + 1.42)^{-1}$ and $C_2 := -1.80\ 10^{-3}\ C_1$, (A3-6) yields

$$T(x) = \frac{FR\ T_{he} + 1.42\ e^{-\Lambda x/L}}{FR - 1.80\ 10^{-3}\ e^{-\Lambda x/L}} \quad \text{where } FR := \frac{1.80\ 10^{-3} T_i + 1.42}{T_i - T_{he}}$$

$$\text{and } \Lambda = \frac{11.4\ \pi}{c_p} \frac{(1.80\ 10^{-3}\ T_{he} + 1.42)\ L}{\dot{m}^{0.2}\ D^{0.8}} \qquad \text{(A3-9)}$$

When $T^{0.11}$ is approximated by a constant, (A3-9) is reduced to

$$T(x) = T_{he} + (T_i - T_{he})\ e^{-\Lambda x/L} \qquad \text{(A3-10)} \quad \text{(4-33)}$$

which is also obvious from (A3-6). Together with

$$\Lambda = \frac{11.4\ \pi}{c_p} \frac{T_{he}^{0.11}\ L}{\dot{m}^{0.2}\ D^{0.8}} \qquad \text{(4-34)}$$

(A3-10) shows maximum deviations of 3% with respect to (A3-9). Because of its simple form (A3-10) will be used for further calculations instead of (A3-9).

Appendix 10.4 The Algol computer program with input and output data

The numerical calculations described in this report, were performed on the Burroughs 7900 computer at the Eindhoven University of Technology. In the programs use was made of library facilities, offered by the calculation centre of the university.
The Algol computer program, which was designed to analyse the influence of the place of the fans on the application temperature and the cool-down time, has been reproduced below. It belongs to task 1 mentioned at the beginning of paragraph 4.2.4.

TS
DATE & TIME PRINTED: THURSDAY, NOVEMBER 7, 1985 @ 16:37:34.

```
  100    BEGIN
  200      $ INCLUDE 'NAGALIB/ALGOL/DECLARATION ON APPL'
  300      $ INCLUDE 'NAGALIB/ALGOL/C05NAA ON APPL'
  400      FILE INTS(KIND=DISK,FILETYPE=7),
  450           OUTTS(KIND=DISK,NEWFILE=TRUE,PROTECTION=SAVE);
  500      BOOLEAN CIRCUIT20K;
  600      INTEGER F,N23,N45,N67,N89,N,IPRINT,MAXCAL,IFAIL,I,J;
  700      REAL QA,QT1,QT2,QFC,P,CP,DHF,EF,M,R,G,SM,SP,
  800           LS,DS,DSC,LA,DA,DAC,LT,DT1,DT2,L23,L45,L67,L89,
  900           ZE23,ZE45,ZE67,ZE89,LACT,
 1000           LSCH,LACH,T,FF,PI,FTOL,DELTA,STEPMX;
 1100      REAL ARRAY K[0:26],A[1:23];
 1200    %
 1300      PROCEDURE RESID(N,XC,RC);
 1400      VALUE N;
 1500      INTEGER N;
 1600      REAL ARRAY XC,RC[*];
 1700      BEGIN
 1800        RC[1]:=F*SM*XC[10]*CP*(XC[12]-XC[11])-XC[23];
 1900        RC[2]:=F*SM*XC[10]*CP*(XC[15]-XC[16])-QA;
 2000        RC[3]:=F*SM*XC[10]*CP*(XC[13]-XC[14])-QT1;
 2100        RC[4]:=F*SM*XC[10]*CP*(XC[17]-XC[18])-QT2;
 2200        RC[5]:=F*SM*XC[10]*CP*(XC[19]-XC[11])-XC[22]-QFC;
 2300        RC[6]:=XC[12]-XC[13];
 2400        RC[7]:=XC[14]-XC[15];
 2500        RC[8]:=XC[16]-XC[17];
 2600        RC[9]:=XC[18]-XC[19];
 2700        RC[10]:=IF CIRCUIT20K THEN K[1]*LN(XC[20]/K[2])-XC[23]
 2800                ELSE K[1]*(XC[20]**2-K[2])**0.5-K[0]-XC[23];
 2900        RC[11]:=SM*XC[10]*G*DHF/EF-XC[22];
 3000        LSCH:=(K[12]*PI/CP)**(-1)*(SM*XC[10])**(1-K[9])
 3100              *DS**K[9]/XC[20]**K[13];
 3200        LACH:=(K[12]*PI/CP)**(-1)*(SM*XC[10])**(1-K[9])
 3300              *DA**K[9]/XC[21]**K[13];
 3400        RC[12]:=(XC[12]-XC[20])*EXP(-F*LS/LSCH)-(XC[11]-XC[20]);
 3500        RC[13]:=(XC[16]-XC[21])*EXP(-F*LA/LACH)-(XC[15]-XC[21]);
 3600        RC[14]:=M*P*2*G*DHF/(R*(XC[11]+XC[19]))-F*SP*(XC[9]-XC[1]);
 3700        RC[15]:=A[1]*(LACT/DT1**5)*(SM*XC[10])**2*LT*(XC[13]+XC[14])/2
 3800              -F*SP*(XC[4]-XC[3]);
 3900        RC[16]:=A[1]*(LACT/DT2**5)*(SM*XC[10])**2*LT*(XC[17]+XC[18])/2
 4000              -F*SP*(XC[8]-XC[7]);
 4100        RC[17]:=A[2]*DS**(K[24]-5)*(1+3.74*DS/DSC)
 4200                *(SM*XC[10])**(2-K[24])
 4300                *(LS*XC[20]*(K[25]*XC[20]+K[26])
 4400                  +LSCH*(XC[1.5+F/2]-XC[20])*(1-EXP(-LS/LSCH))
 4500                  *(K[25]*(2*XC[20]+(1+EXP(-LS/LSCH))
 4600                           *(XC[1.5+F/2]+XC[20])/2)
 4700                    +K[26]))-F*SP*(XC[2]-XC[1]);
 4800        RC[18]:=A[2]*DA**(K[24]-5)*(1+3.74*DA/DAC)
 4900                *(SM*XC[10])**(2-K[24])
 5000                *(LA*XC[21]*(K[25]*XC[21]+K[26])
 5100                  +LACH*(XC[5.5+F/2]-XC[21])*(1-EXP(-LA/LACH))
 5200                  *(K[25]*(2*XC[21]+(1+EXP(-LA/LACH))
 5300                           *(XC[5.5+F/2]+XC[21])/2)
 5400                    +K[26]))-F*SP*(XC[6]-XC[5]);
 5500        RC[19]:=A[2]*DS**(K[24]-5)*(SM*XC[10])**(2-K[24])
 5600                *XC[12]**(1+K[11]*K[24])*L23
 5700                +A[1]*DS**(-4)*(SM*XC[10])**2*XC[12]*N23*ZE23
 5800                -F*SP*(XC[3]-XC[2]);
 5900        RC[20]:=A[2]*DA**(K[24]-5)*(SM*XC[10])**(2-K[24])
 6000                *XC[15]**(1+K[11]*K[24])*L45
 6100                +A[1]*DA**(-4)*(SM*XC[10])**2*XC[15]*N45*ZE45
 6200                -F*SP*(XC[5]-XC[4]);
 6300        RC[21]:=A[2]*DA**(K[24]-5)*(SM*XC[10])**(2-K[24])
 6400                *XC[16]**(1+K[11]*K[24])*L67
 6500                +A[1]*DA**(-4)*(SM*XC[10])**2*XC[16]*N67*ZE67
 6600                -F*SP*(XC[7]-XC[6]);
 6700        RC[22]:=A[2]*DS**(K[24]-5)*(SM*XC[10])**(2-K[24])
 6800                *XC[19]**(1+K[11]*K[24])*L89
 6900                +A[1]*DS**(-4)*(SM*XC[10])**2*XC[19]*N89*ZE89
 7000                -F*SP*(XC[9]-XC[8]);
 7100        RC[23]:=2*P-SP*(XC[1]+XC[9])
 7200      END;
 7300    %
 7400      PROCEDURE MONIT(N,XC,RC,FC,NCALL);
 7500      VALUE N,FC,NCALL;
 7600      INTEGER N,NCALL;
 7700      REAL FC;
 7800      REAL ARRAY XC,RC[*];
 7900      BEGIN WRITE(OUTTS,<X1,I3,X11,E15.8>,NCALL,FC)
 8000      END;
 8100    %
```

```
 8100    %
 8200      READ(INTS,/,CIRCUIT20K,F,QA,QT1,QT2,QFC,P,CP,DHF,EF,M,R,G,SM,SP,
 8300                  LS,DS,DSC,LA,DA,DAC,LT,DT1,DT2,N23,N45,N67,N89,
 8400                  L23,L45,L67,L89,ZE23,ZE45,ZE67,ZE89,LACT);
 8500      PI:=3.141592654; K[0]:=55;
 8600      IF CIRCUIT20K THEN BEGIN K[1]:=160; K[2]:=14 END
 8700                    ELSE BEGIN K[1]:=5.0; K[2]:=2.9@3 END;
 8800      K[6]:=6.4@-3; K[7]:=0.55; K[8]:=0.02; K[9]:=0.8;
 8900      K[10]:=8.3@-7; K[11]:=0.55;
 9000      K[12]:=K[6]*K[8]*(PI*K[10]/4)**(-K[9]); K[13]:=K[7]-K[9]*K[11];
 9100      K[23]:=0.32; K[24]:=0.25; K[25]:=2.60@-3; K[26]:=1.54;
 9200      A[1]:=8*R/(PI**2*M*P); A[2]:=A[1]*K[23]*(PI*K[10]/4)**K[24];
 9300      N:=23; IPRINT:=0; MAXCAL:=5*N; IFAIL:=0;
 9400      FTOL:=@-5; DELTA:=@-5; STEPMX:=100;
 9500    %
 9600      BEGIN
 9700        REAL ARRAY X,RR[1:N],AJINV[1:N,1:N],
 9800                   Q,FT,IL,LAMS,LAMA,REMIN,REMAX[0:4],XX[0:4,1:N];
 9900        FOR I:=0 STEP 1 UNTIL 4 DO
10000        BEGIN IF CIRCUIT20K THEN Q[I]:=100*I ELSE Q[I]:=200*I; QA:=Q[I];
10100          FOR J:=1 STEP 1 UNTIL 9 DO X[J]:=P/SP;
10200          IF CIRCUIT20K
10300          THEN BEGIN T:=K[2]*EXP(QA/K[1]);
10400               X[10]:=(10@-3/SM)*K[2]/T; X[22]:=10*K[2]/T END
10500          ELSE BEGIN T:=((QA+K[0])/K[1])**2+K[2])**0.5;
10600               X[10]:=(3@-3/SM)*55/T; X[22]:=3*55/T END;
10700          FOR J:=11 STEP 1 UNTIL 21 DO X[J]:=T;
10800          X[23]:=QA+QT1+QT2+QFC+X[22];
10900    %
11000          COSNAA(N,X,RR,FF,AJINV,FTOL,DELTA,STEPMX,
11100                 RESID,MONIT,IPRINT,MAXCAL,IFAIL);
11200          FOR J:=1 STEP 1 UNTIL 9 DO XX[I,J]:=SP*X[J]-P;
11300          XX[I,10]:=SM*X[10];
11400          FOR J:=11 STEP 1 UNTIL 23 DO XX[I,J]:=X[J];
11500          FT[I]:=FF; IL[I]:=IFAIL; LAMS[I]:=LS/LSCH; LAMA[I]:=LA/LACH;
11600          REMIN[I]:=IF F=1
11700                    THEN (4/PI)*SM*X[10]/(K[10]*X[13]**K[11]*DT1)
11800                    ELSE (4/PI)*SM*X[10]/(K[10]*X[18]**K[11]*DT2);
11900          REMAX[I]:=(4/PI)*SM*X[10]/(K[10]*X[1.5-F/2]**K[11]*DS);
```

```
12000        END;
12100    %
12200        WRITE(OUTTS,<"CIRCUIT: ",A3,X20,"FAN: ",A21,////,
12300        "CIRCUIT20K",A6,X10,"P (PA)",X5,E10.3,X10,"LS (M) ",F10.2,X10,
12400        "N23",X4,I5,X10,"ZE23",F5.1,/,
12500        "F",X9,I6,X10,"CP (J/KG K)",E10.1,X10,"DS (M) ",E10.1,X10,
12600        "N45",X4,I5,X10,"ZE45",F5.1,/,
12700        "QA (W)",X4,A6,X10,"DHF (M)",X4,I10,X10,"DSC (M)",F10.2,X10,
12800        "N67",X4,I5,X10,"ZE67",F5.1,/,
12900        "QT1 (W)",X3,I6,X10,"EF",X9,F10.2,X10,"LA (M) ",F10.2,X10,
13000        "N89",X4,I5,X10,"ZE89",F5.1,/,
13100        "QT2 (W)",X3,I6,X10,"M (KG/MOL) ",E10.3,X10,
13200        "DA (M) ",E10.1,X10,"L23 (M)",F5.2,X10,"LACT",F5.2,/,
13300        "QFC (W)",X3,I6,X10,"R (J/MOL K)",F10.3,X10,
13400        "DAC (M)",F10.2,X10,"L45 (M)",F5.2,/,
13500        X26,"G (M/S**2) ",F10.2,X10,"LT (M) ",F10.1,X10,
13600        "L67 (M)",F5.2,/,
13700        X26,"SM",X9,E10.3,X10,"DT1 (M)",E10.3,X10,"L89 (M)",F5.2,/,
13800        X26,"SP",X9,E10.3,X10,"DT2 (M)",E10.3,////////,
13900        "QA (W)",X5,"DP1 (PA)",X3,"DP2 (PA)",X3,"DP3 (PA)",X3,
14000        "DP4 (PA)",X3,"DP5 (PA)",X3,"DP6 (PA)",X3,"DP7 (PA)",X3,
14100        "DP8 (PA)",X3,"DP9 (PA)",/,
14200        5(/,E10.3,9(X1,E10.3)),/////,
14300        "MD (KG/S)",X2,"T1 (K)",X5,"T2 (K)",X5,"T3 (K)",X5,"T4 (K)",X5,
14400        "T5 (K)",X5,"T6 (K)",X5,"T7 (K)",X5,"T8 (K)",X5,"T9 (K)",/,
14500        5(/,E10.3,9(X1,E10.3)),/////,
14600        "TS (K)",X5,"TA (K)",X5,"PSH (W)",X5,"QS (W)",X5,"FF",X9,
14700        "IFAIL",X6,"LAMS",X7,"LAMA",X7,"REMIN",X6,"REMAX",/,
14800        5(/,E10.3,9(X1,E10.3))>,
14900        IF CIRCUIT20K THEN "20K" ELSE "70K",IF F=1 THEN
15000        "BEHIND THE STAGE" ELSE "IN FRONT OF THE STAGE",
15100        IF CIRCUIT20K THEN "TRUE" ELSE "FALSE",P,LS,N23,ZE23,
15200        F,CP,DS,N45,ZE45,"QA",DHF,DSC,N67,ZE67,
15300        QT1,EF,LA,N89,ZE89,QT2,M,DA,L23,LACT,QFC,R,DAC,L45,
15400        G,LT,L67,SM,DT1,L89,SP,DT2,
15500        FOR I:=0 STEP 1 UNTIL 4 DO [Q[I],
15600         FOR J:=1 STEP 1 UNTIL 9 DO XX[I,J]],
15700        FOR I:=0 STEP 1 UNTIL 4 DO
15800         FOR J:=10 STEP 1 UNTIL 19 DO XX[I,J],
15900        FOR I:=0 STEP 1 UNTIL 4 DO
16000        [FOR J:=20 STEP 1 UNTIL N DO XX[I,J],
16100        FT[I],IL[I],LAMS[I],LAMA[I],REMIN[I],REMAX[I]])
16200      END
16300    END.
```

In the following discussion the lines of the program will be referred to by their numbers: "2400" means "line 2400".
The heart of the program is formed by the procedure C05NAA from the NAG-library (see 200, 300, 11000 and 11100) as it is this procedure which solves the set of 23 equations, presented in paragraph 4.2.3. (The NAG-library contains routines and procedures for solving numeric and statistic problems and is maintained by the Numerical Algorithms Group Ltd in England. It can be called in Fortran as well as in Algol programs.)
C05NAA (see (NAG81)) makes use of the two auxiliary procedures RESID (1300 to 1700) and MONIT (7400 to 8000). After the 23 equations (4-65) to (4-87) have been rewritten in their residual form

$$\begin{aligned} RR_1\ (X_1,X_2,\ldots,X_{23}) &= 0 \\ RR_2\ (X_1,X_2,\ldots,X_{23}) &= 0 \\ &\text{----------} \\ RR_{23}(X_1,X_2,\ldots,X_{23}) &= 0 \end{aligned} \qquad \text{(A4-1)}$$

the expressions RR_1 to RR_{23} are brought together in RESID. The variables X_1 to X_9 correspond with p_1 to p_9, X_{10} with $\dot{m}$, X_{11} to X_{19} with T_1 to T_9, X_{20} with T_s, X_{21} with T_a, X_{22} with P_{sh} and X_{23} with $\dot{Q}_s$ respectively (see Fig.4.23). When X_1 to X_{23} are supplied with their initial values, the expressions RR_1 to RR_{23} in (A4-1) will usually not be equal to zero. Therefore they are called residuals. It is the task of C05NAA to minimize the sum of the squared residuals until it falls below a specified value FTOL (usually 10^{-5}):

$$FF = \sum_{i=1}^{23} RR_i^{\,2} \leq FTOL. \qquad \text{(A4-2)}$$

This is achieved by a number of iterations, after each one of which C05NAA alters the current values XC_i of X_i and thereby the current values RC_i of RR_i in the procedure RESID ($i=1,2,\ldots,23$). In order to facilitate the iteration process, it is important that X_1 to X_{23} have the same order of magnitude. The orders of magnitude of the quantities are 10 bar = 10^6 Pa (pressures), 10^{-3} to 10^{-2} kg/s (mass flow), 10 K to 100 K (temperatures) and 10 W to 100 W (shaft power and cooling power). Therefore X_1 to X_9 have been defined as $X_i = p_i/SP$ and X_{10} as $\dot{m}/SM$, the scaling factors being $SP = 10^5$ and $SM = 10^{-4}$ or 10^{-3}.
With the procedure MONIT, mentioned above, it is possible to print the current values of the variables and the residuals after every IPRINT iterations (see 11100): IPRINT=0,1,2,3,etc. With IPRINT=0 MONIT is not used. For more information on C05NAA and its auxiliary procedures, the reader is referred to the description presented below (source: (NAG81)).

C05NAA

1. Purpose

C05NAA finds a solution to the N nonlinear equations in the form $\underline{R}(\underline{X})=\underline{0}$ where $\underline{X}=(X_1,X_2,\ldots,X_N)^T$ by a hybrid method due to Powell. Formulae to calculate the values of the functions R_i for any value of $\underline{X}$ need to be supplied.

IMPORTANT: before using this routine, read the appropriate machine implementation document to check the interpretation of italicised terms and other implementation-dependent details.

2. Specification (Algol 60)

```
procedure C05NAA(N,X,R,F,AJINV,FTOL,DELTA,STEPMX,RESID,MONIT,IPRINT,
                 MAXCAL,IFAIL);
  value N,FTOL,DELTA,STEPMX,IPRINT,MAXCAL;
  integer N,IPRINT,MAXCAL,IFAIL;
  real F,FTOL,DELTA,STEPMX;
  real array X,R,AJINV;
  procedure RESID,MONIT;
```

3. Description

C05NAA is based on the FORTRAN subroutine given by Powell (1968). The user must specify his system of equations by providing a procedure which will calculate the values of the residuals $R_1,R_2,\ldots,R_N$ corresponding to any given set of the variables $\underline{X}$. The method is iterative and so requires an initial estimate of the position of a solution.

A typical iteration starts with the best point found so far, $\underline{X}$, a steplength bound, B, and approximations to the Jacobian matrix J and its inverse J^{-1}. (Thus J is the matrix whose (i,j)th element is $\partial R_i/\partial X_j$.) These approximations are used to estimate the Newton step and the step to the minimum along the direction of steepest descent. The actual step taken, $\underline{\delta}$, is a linear combination of these estimates, chosen so that the length of $\underline{\delta}$ is less than B. The residuals are evaluated at $\underline{X}+\underline{\delta}$ and the size of B is then adjusted according to how successful $\underline{\delta}$ was in reducing the sum of squares of the residuals. Finally the approximations to J and J^{-1} are updated so as to be consistent with the changes produced in $\underline{R}$ by the step $\underline{\delta}$.

The overall aim of the algorithm is to combine the Newton and steepest descent methods in such a way as to give steady progress and a fast rate of ultimate convergence. To start with it may take small steps which are biased towards the direction of steepest descent, but B will usually increase to allow the full Newton steps to be taken later on.

C05NAA

4. References

[1] POWELL, M.J.D.
A FORTRAN subroutine for solving systems of non-linear algebraic equations.
Harwell Report AERE - R5947, H.M.S.O., 1968.
Reprinted in [3].

[2] POWELL, M.J.D.
A hybrid method for non-linear equations.
In [3], 1970.

[3] RABINOWITZ, P.
Numerical Methods for Non-linear Algebraic Equations.
Gordon and Breach, 1970.

5. Parameters

N - integer, called by value.
On entry, N must specify the number of equations and variables.

X - real array, bounds [1:N].
Before entry, the first N elements of X must be set to a guess at the solution, that is the estimated position of the minimum of the sum of squares of the residuals.
On exit, X contains the point which yielded the final value in F.

R - real array, bounds [1:N].
On exit, R contains the values of the residuals at the point which yielded the final value in F.

F - real.
On exit, F contains the smallest sum of squares of the residuals found by the routine.

AJINV - real array, bounds [1:N,1:N].
On exit, AJINV[I,J],I,J = 1,...,N contain an approximation to the inverse Jacobian matrix at the final point.
This matrix may be useful for estimating the accuracy of the solution (see Further Comments).

FTOL - real, called by value.
On entry, FTOL must specify the accuracy to which the sum of squares of the residuals is required.
An exit will be made from C05NAA and IFAIL set to 0 when:

$$F = \sum_{i=1}^{N} (R_i)^2 \leq FTOL$$

FTOL should not be set less than the value supplied by X02AAA, that is the machine accuracy.

C05NAA

5. Parameters (contd)

DELTA - real, called by value.
On entry, DELTA must specify a suitable steplength for making difference estimates of the partial derivatives of R. The approximation used is:

$$\frac{\partial R_i}{\partial X_j} \simeq \frac{R_i(\underline{X} + \text{DELTA}*\underline{e}_j) - R_i(\underline{X})}{\text{DELTA}}$$

where $\underline{e}_j$ is the jth co-ordinate direction. This estimate must be fairly accurate for each R_i so the variables, X, must be of similar magnitudes (see Chapter Introduction). DELTA has to be small enough for the difference estimates to be close to the true derivatives, but not so small that the calculated differences are dominated by rounding errors.

STEPMX - real, called by value.
On entry, STEPMX must specify an estimate of the Euclidean distance between the expected minimum and the starting point supplied by the user in X. If C05NAA predicts steps much larger than STEPMX a failure will occur. Note: STEPMX must be greater than DELTA.

RESID - procedure, supplied by the user.
RESID must calculate the values of the N residuals at XC and assign these values to RC. It should be tested separately before being used in conjunction with C05NAA (see the Chapter Introduction). Its specification is:

```
procedure RESID(N,XC,RC);
   value N,XC;
   integer N;
   real array XC,RC;
```

N - integer, called by value.
On entry, N specifies the number of variables.

XC - real array, bounds [1:N], called by value.
On entry, XC contains the current point.

RC - real array, bounds [1:N].
On exit, RC must contain the values of the residuals at the current point XC.

C05NAA

5. Parameters (contd)

MONIT - procedure, supplied by the user.
The frequency with which MONIT is called in C05NAA is controlled by IPRINT (see below). It can be used to print out the current values of any selection of its parameters, but must not be used to change the values of the parameters. Its specification is:

```
procedure MONIT(N,XC,RC,FC,NCALL);
   value N,XC,RC,FC,NCALL;
   integer N,NCALL;
   real FC;
   real array XC,RC;
```

N - integer, called by value.
On entry, N specifies the number of variables.

XC - real array, bounds [1:N], called by value.
On entry, XC contains the current estimate of the solution.

RC - real array, bounds [1:N], called by value.
On entry, RC contains the values of the residuals at the current point XC.

FC - real, called by value.
On entry, FC contains the value of the sum of squares of the residuals calculated at XC.

NCALL - integer, called by value.
On entry, NCALL contains the number of calls of RESID that have been carried out.

IPRINT - integer, called by value.
On entry, IPRINT specifies the frequency of the call of MONIT. If IPRINT $\leq$ 0 there are no calls of MONIT. When IPRINT $\geq$ 1, MONIT is called once every IPRINT calls of RESID.

MAXCAL - integer, called by value.
On entry, MAXCAL specifies the maximum number of iterations that are allowed. A suggested value for C05NAA is 10*N.

IFAIL - integer.
Before entry, IFAIL must be assigned a value. For users not familiar with this parameter (described in Chapter P01) the recommended value is 0. Unless the routine detects an error (see Section 6), IFAIL contains 0 on exit.

6. Error Indicators

Errors detected by the routine:-

IFAIL = 1 One of the input parameters to C05NAA lies outside its permitted range.

IFAIL = 2 MAXCAL iterations have been completed, C05NAA has been terminated prematurely. If progress, as indicated by the size of FC in MONIT, was satisfactory prior to termination then MAXCAL may be increased. Otherwise, the coding of the routine RESID should be checked before increasing MAXCAL.

IFAIL = 3 A nearby stationary point of the function F is predicted. This condition may occur because there is no solution of the equations close to the user's initial estimate. Try a different starting point.

IFAIL = 4 N+4 calls of RESID have failed to improve the residuals.

IFAIL = 5 F failed to decrease when a new Jacobian was used.

IFAIL = 6 An attempt has been made to invert an estimate of the Jacobian which is singular, or nearly so. Try restarting from a different point. If the failure persists, it may indicate that one or more X_j are redundant.

If IFAIL is 4 or 5, some more thought should be given to the choice of parameters for C05NAA. In particular, DELTA may be too large. Alternatively, if F is small on exit, these failures may indicate that rounding errors are so large that the required accuracy, FTOL, cannot be attained; the final point may be the best that can be found. Otherwise, these failures may be due to programming errors in the calling program or in RESID.

7. Auxiliary Routines

This routine calls the NAG Library routines F01AAA,P01AAA and X03AAA.

8. Timing

This depends on the number of variables, the behaviour of the equations, the distance of the solution from the starting point and the accuracy demanded.

The number of operations performed in most iterations of C05NAA is roughly proportional to N^2. In addition, each iteration makes at least one call of RESID. So, if RESID is lengthy, the run-time will be dominated by the time spent evaluating R.

9. Storage

The storage required by internally declared arrays, including those of auxiliary routines is 3*N*(N+2) real elements.

10. Accuracy

After a normal exit from C05NAA:

$$F = \sum_{i=1}^{N} [R_i(\underline{X})]^2 \leq FTOL .$$

Some idea of the accuracies of X_j may be obtained by monitoring the progress of C05NAA to see how many figures remain unchanged during the last few iterations. Alternatively, the accuracy of the solution can be estimated using AJINV and R (see Chapter Introduction).

Greater accuracy can be requested by choosing a smaller value of FTOL although, if unreasonable accuracy is demanded, rounding errors may become important and cause a failure.

AJINV can be used to estimate the sensitivity of X to any uncertainty in the specification of $R_k(\underline{X})$,k=1,...,N (see Chapter Introduction).

11. Further Comments

C05NAA uses STEPMX to control the lengths of steps taken and DELTA to calculate differences. In both these processes it is important that the user should scale the variables (perhaps by multiplying them by appropriate constants) so that their magnitudes are similar (see Chapter Introduction).

12. Keywords

Hybrid Minimization Method.
Nonlinear Equations.
Powell's Nonlinear Equations Method.

The variables mentioned in paragraph 4.2.3 have been represented in the program (see 600 to 1000) by the following identifiers (see Table A4.1):

par. 4.2.3	program	par.4.2.3	program
F	F	L_{he} at stage	LS
$\dot{Q}_a$	QA	L_{ch} ,, ,,	LSCH
$\dot{Q}_{t1}$	QT1	D_{he} ,, ,,	DS
$\dot{Q}_{t2}$	QT2	D_c ,, ,,	DSC
$\dot{Q}_{f,con}$	QFC	L_{he} at application	LA
p	P	L_{ch} ,, ,,	LACH
c_p	CP	D_{he} ,, ,,	DA
ΔH_f	DHF	D_c ,, ,,	DAC
η_f	EF	L_t	LT
M	M	D_{t1}	DT1
R	R	D_{t2}	DT2
g	G	N_{23} to N_{89}	N23 to N89
		L_{23} to L_{89}	L23 to L89
		ζ_{23} to ζ_{89}	ZE23 to ZE89
		λ'_t	LACT

Table A4.1 Clarification of the identifiers

The boolean variable CIRCUIT20K is used to distinguish between the 20K-circuit (value TRUE) and the 70K-circuit (value FALSE). The array elements A[1] and A[2] are given in 9200 and have been introduced to simplify the expressions in 3700 to 7000. The constant elements of the array K[0:26] have been defined as follows.

K[0] to K[2]: see (4-55),

$\lambda = K[6]\ T^{K[7]}$ (4-8),

$Nu = K[8]\ Re^{K[9]}$ (A3-3),

$\eta = K[10]\ T^{K[11]}$ (4-7),

$K[12] := K[6]\ K[8]\ (\pi\ K[10]/4)^{-K[9]}$,

$K[13] := K[7] - K[9]\ K[11]$,

$\lambda'(Re) = K[23]\ Re^{K[24]}$ (4-40)

and $T^{0.14} \approx K[25]\ T + K[26]$. below (4-80)

The remaining elements of K[0:26] have not been used.
The residuals RC[1] to RC[23] (see 1800 to 7100) correspond with the equations (4-65) to (4-87) respectively. In 8200 to 9400 and in 10000 values are assigned to the constants. An example of the input file INTS is listed below.

```
(TNNVKT5)INTS ON USER4
DATE & TIME PRINTED: THURSDAY, NOVEMBER 14, 1985 @ 10:00:48.

100     TRUE,1,20,10,10,5,2@6,6.0@3,20,0.50,4.003@-3,8.314,9.81,@-3,85,
200     0,0,0.10,0,0,0.10,7,1.27@-2,1.27@-2,1,1,1,1,
300     0.38,0.50,0.50,0.50,0.8,0.8,0.8,0.8,0.07,
```

In 10100 to 10800 initial values are assigned to the 23 variables. After C05NAA has been called (see 11000 and 11100) the output is prepared in 11200 to 11900, after which the write statement (see 12200 to 16100) concludes the program. In 9800 the arrays LAMS, LAMA, REMIN and REMAX have been declared. LAMS and LAMA contain values of Λ_s and Λ_a respectively (see (4-76) and (4-77)). REMIN and REMAX contain the minimum and the maximum value of Re in a circuit. The minimum value occurs at the highest temperature and the largest tube diameter, while the maximum value is reached at the lowest temperature and the smallest tube diameter (see (4-38) and (4-7)).
For carrying out task 2 (see the beginning of paragraph 4.2.4) a number of changes were made from 9600 onwards. The most essential alteration was made in 10010, where the heat exchanger length is related to the tube diameter according to (6-5). The changed part is given below, where arrows indicate the altered lines.

```
 9500    Z
 9600      BEGIN
 9700        REAL ARRAY X,RR[1:N],AJINV[1:N,1:N],
 9800 ——>             D,L,FT,IL,LAMS,LAMA,REMIN,REMAX[1:4],XX[1:4,1:N];
 9900 ——>    FOR I:=1 STEP 1 UNTIL 4 DO
10000 ——>    BEGIN D[I]:=(2*I+4)*0-3; DS:=D[I]; DA:=DS;
10010 ——>      L[I]:=PI*DSC*70-2/(DS+30-3); LS:=L[I]; LA:=LS;
10100          FOR J:=1 STEP 1 UNTIL 9 DO X[J]:=P/SP;
10200          IF CIRCUIT20K
10300          THEN BEGIN T:=K[2]*EXP(QA/K[1]);
10400               X[10]:=(100-3/SM)*K[23/T; X[22]:=10*K[22/T END
10500          ELSE BEGIN T:=(((QA+K[0])/K[1])**2+K[2])**0.5;
10600               X[10]:=(30-3/SM)*55/T; X[22]:=3*55/T END;
10700          FOR J:=11 STEP 1 UNTIL 21 DO X[J]:=T;
10800          X[23]:=QA+QT1+QT2+QFC+X[22];
10900    Z
11000          COSNAA(N,X,RR,FF,AJINV,FTOL,DELTA,STEPMX,
11100                 RESID,MONIT,IPRINT,MAXCAL,IFAIL);
11200          FOR J:=1 STEP 1 UNTIL 9 DO XX[I,J]:=SP*X[J]-P;
11300          XX[I,10]:=SM*X[10];
11400          FOR J:=11 STEP 1 UNTIL 23 DO XX[I,J]:=X[J];
11500          FT[I]:=FF; IL[I]:=IFAIL; LAMS[I]:=LS/LSCH; LAMA[I]:=LA/LACH;
11600          REMIN[I]:=IF F=1
11700                    THEN (4/PI)*SM*X[10]/(K[10]*X[13]**K[11]*DT1)
11800                    ELSE (4/PI)*SM*X[10]/(K[10]*X[18]**K[11]*DT2);


11900          REMAX[I]:=(4/PI)*SM*X[10]/(K[10]*X[1.5-F/2]**K[11]*DS);
12000        END;
12100    Z
12200        WRITE(OUTTS,<"CIRCUIT: ",A3,X20,"FAN: ",A21,////,
12300 ——>    "CIRCUIT20K",A6,X10,"P (PA)",X5,E10.3,X10,"LS (M) ",X8,A2,X10,
12400        "N23",X4,I5,X10,"ZE23",F5.1,/,
12500 ——>    "F",X9,I6,X10,"CP (J/KG K)",E10.1,X10,"DS (M) ",X8,A2,X10,
12600        "N45",X4,I5,X10,"ZE45",F5.1,/,
12700 ——>    "QA (W)",X4,I6,X10,"DHF (M)",X4,I10,X10,"DSC (M)",F10.2,X10,
12800        "N67",X4,I5,X10,"ZE67",F5.1,/,
12900 ——>    "QT1 (W)",X3,I6,X10,"EF",X9,F10.2,X10,"LA (M) ",X8,A2,X10,
13000        "N89",X4,I5,X10,"ZE89",F5.1,/,
13100        "QT2 (W)",X3,I6,X10,"M (KG/MOL) ",E10.3,X10,
13200 ——>    "DA (M) ",X8,A2,X10,"L23 (M)",F5.2,X10,"LACT",F5.2,/,
13300        "QFC (W)",X3,I6,X10,"R (J/MOL K)",F10.3,X10,
13400        "DAC (M)",F10.2,X10,"L45 (M)",F5.2,/,
13500        X26,"G (M/S**2) ",F10.2,X10,"LT (M) ",F10.1,X10,
13600        "L67 (M)",F5.2,/,
13700        X26,"SM",X9,E10.3,X10,"DT1 (M)",E10.3,X10,"L89 (M)",F5.2,/,
13800        X26,"SP",X9,E10.3,X10,"DT2 (M)",E10.3,////////,
13900 ——>    "DS=DA (M)",X2,"DP1 (PA)",X3,"DP2 (PA)",X3,"DP3 (PA)",X3,
14000        "DP4 (PA)",X3,"DP5 (PA)",X3,"DP6 (PA)",X3,"DP7 (PA)",X3,
14100        "DP8 (PA)",X3,"DP9 (PA)",/,
14200 ——>    4(/,E10.3,9(X1,E10.3)),/////,
14300        "MD (KG/S)",X2,"T1 (K)",X5,"T2 (K)",X5,"T3 (K)",X5,"T4 (K)",X5,
14400        "T5 (K)",X5,"T6 (K)",X5,"T7 (K)",X5,"T8 (K)",X5,"T9 (K)",/,
14500 ——>    4(/,E10.3,9(X1,E10.3)),/////,
14600        "TS (K)",X5,"TA (K)",X5,"PSH (W)",X5,"QS (W)",X5,"FF",X9,
14700 ——>    "LS=LA (M)",X2,"LAMS",X7,"LAMA",X7,"REMIN",X6,"REMAX",/,
14800 ——>    4(/,E10.3,9(X1,E10.3))>,
14900        IF CIRCUIT20K THEN "20K" ELSE "70K",IF F=1 THEN
15000        "BEHIND THE STAGE" ELSE "IN FRONT OF THE STAGE",
15100 ——>    IF CIRCUIT20K THEN "TRUE" ELSE "FALSE",P,"LS",N23,ZE23,
15200 ——>    F,CP,"DS",N45,ZE45,QA,DHF,DSC,N67,ZE67,
15300 ——>    QT1,EF,"LA",N89,ZE89,QT2,M,"DA",L23,LACT,QFC,R,DAC,L45,
15400        G,LT,L67,SM,DT1,L89,SP,DT2,
15500 ——>    FOR I:=1 STEP 1 UNTIL 4 DO [D[I],
15600         FOR J:=1 STEP 1 UNTIL 9 DO XX[I,J],
15700 ——>    FOR I:=1 STEP 1 UNTIL 4 DO
15800         FOR J:=10 STEP 1 UNTIL 19 DO XX[I,J],
15900 ——>    FOR I:=1 STEP 1 UNTIL 4 DO
16000        [FOR J:=20 STEP 1 UNTIL N DO XX[I,J],
16100 ——>    FT[I],L[I],LAMS[I],LAMA[I],REMIN[I],REMAX[I]])
16200      END
16300    END.
```

Of task 1 (the influence of the place of the fans on T_a) all the calculated results are listed below. Of task 2 (the influence of the heat exchanger diameter and several other variables on T_a) only the essential ones are given, corresponding with the marked blocks in Table 6.5.
In reading the output data, it should be noted that the pressures DP1 to DP9 have been defined as DPj = p_j - p, so that they give the values of p_j relative to the average pressure p (see Fig.4.23 and Fig.6.1). For the interpretation of the other symbols, the reader is referred to Table A4.1. The most important quantities are the stage temperature TS, the application temperature TA, the mass flow MD and the shaft power PSH. The other quantities are used for analysing the "internal" behaviour of the cold-transfer system. The volume flows $\dot{V}_f$ in Table 6.5 have been calculated from P_{sh}, η_f=50% and Δp_f=(2 DP9) (see (4-87)) via $P_{sh} = \dot{V}_f \Delta p_f / \eta_f$.

OUTTS
DATE & TIME PRINTED: WEDNESDAY, NOVEMBER 6, 1985 @ 10:31:07.

TASK 1.1: SEE TABLE 6.1

CIRCUIT: 20K FAN: BEHIND THE STAGE

CIRCUIT20K??TRUE		P (PA)	2.0000E+06	LS (M)	1.80	N23	0	ZE23 0.0
F	1	CP (J/KG K)	5.2E+03	DS (M)	6.0E-03	N45	0	ZE45 0.8
QA (W)	????QA	DHF (M)	45	DSC (M)	0.11	N67	0	ZE67 0.0
QT1 (W)	1	EF	0.46	LA (M)	1.80	N89	0	ZE89 0.8
QT2 (W)	1	M (KG/MOL)	4.0030E-03	DA (M)	6.0E-03	L23 (M)	0.00	LACT 0.07
QFC (W)	0	R (J/MOL K)	8.314	DAC (M)	0.11	L45 (M)	0.00	
		G (M/SA*2)	9.81	LT (M)	7.0	L67 (M)	0.00	
		SM	1.0000E-03	DT1 (M)	1.270E-02	L89 (M)	0.00	
		SP	1.0000E+05	DT2 (M)	1.270E-02			

QA (W)	DP1 (PA)	DP2 (PA)	DP3 (PA)	DP4 (PA)	DP5 (PA)	DP6 (PA)	DP7 (PA)	DP8 (PA)	DP9 (PA)
0.	-1.382E+04	-4.093E+03	-4.093E+03	-5.160E+01	-5.160E+01	9.777E+03	9.777E+03	1.382E+04	1.382E+04
1.000E+02	-7.671E+03	-2.553E+03	-2.553E+03	-1.105E+02	-1.105E+02	5.422E+03	5.422E+03	7.671E+03	7.671E+03
2.000E+02	-4.207E+03	-1.458E+03	-1.458E+03	-1.559E+02	-1.559E+02	3.106E+03	3.106E+03	4.207E+03	4.207E+03
3.000E+02	-2.287E+03	-8.074E+02	-8.074E+02	-1.795E+02	-1.795E+02	1.806E+03	1.806E+03	2.287E+03	2.287E+03
4.000E+02	-1.236E+03	-4.651E+02	-4.651E+02	-1.918E+02	-1.918E+02	1.051E+03	1.051E+03	1.236E+03	1.236E+03

MD (KG/S)	T1 (K)	T2 (K)	T3 (K)	T4 (K)	T5 (K)	T6 (K)	T7 (K)	T8 (K)	T9 (K)
1.447E-02	1.529E+01	1.547E+01	1.547E+01	1.547E+01	1.547E+01	1.547E+01	1.547E+01	1.547E+01	1.547E+01
8.050E-03	2.762E+01	3.019E+01	3.019E+01	3.019E+01	3.019E+01	2.780E+01	2.780E+01	2.780E+01	2.780E+01
4.176E-03	5.043E+01	5.982E+01	5.982E+01	5.982E+01	5.962E+01	5.061E+01	5.061E+01	5.061E+01	5.061E+01
2.036E-03	9.284E+01	1.214E+02	1.214E+02	1.214E+02	1.214E+02	9.303E+01	9.303E+01	9.303E+01	9.303E+01
9.261E-04	1.719E+02	2.552E+02	2.552E+02	2.552E+02	2.552E+02	1.721E+02	1.721E+02	1.721E+02	1.721E+02

TS (K)	TA (K)	PSH (W)	QS (W)	FF	IFAIL	LAMS	LAMA	REMIN	REMAX
1.527E+01	1.547E+01	1.388E+01	1.388E+01	4.867E-07	0.	2.333E+00	2.336E+00	5.673E+05	7.146E+05
2.745E+01	3.034E+01	7.725E+00	1.077E+02	3.223E-06	0.	2.798E+00	2.829E+00	1.492E+05	3.970E+05
5.010E+01	6.011E+01	4.008E+00	2.040E+02	2.249E-09	0.	3.409E+00	3.478E+00	5.315E+04	2.058E+05
9.241E+01	1.217E+02	1.953E+00	3.020E+02	2.675E-06	0.	4.210E+00	4.359E+00	1.756E+04	1.002E+05
1.715E+02	2.555E+02	8.688E-01	4.009E+02	4.320E-09	0.	5.275E+00	5.511E+00	5.306E+03	4.560E+04

OUTTS
DATE & TIME PRINTED: WEDNESDAY, NOVEMBER 6, 1985 @ 16:36:15.

TASK 1.2: SEE TABLE 6.1

CIRCUIT: 20K FAN: IN FRONT OF THE STAGE

CIRCUIT2=K??TKU=		P (PA)	2.000E+06	LS (M)	1.80	N25	L	ZE25	0.0
F	-1	CP (J/KG K)	5.2E+03	DS (M)	6.0E-03	N45	0	ZE45	0.0
QA (W)	????QA	DHF (M)	45	DSC (M)	0.11	N67	0	ZE67	0.0
QT1 (W)	0	EF	0.46	LA (M)	1.80	N89	0	ZE89	0.0
QT2 (W)	0	M (KG/MOL)	4.003E-03	DA (M)	6.0E-03	L23 (M)	0.00	LACT	0.07
QFC (W)	0	R (J/MOL K)	8.314	DAC (M)	0.11	L45 (M)	0.00		
		G (M/S**2)	9.81	LT (M)	7.0	L67 (M)	0.00		
		SM	1.000E-03	DT1 (M)	1.27DE-02	L89 (M)	0.00		
		SP	1.000E+05	DT2 (M)	1.27DE-02				

QA (W)	DP1 (PA)	DP2 (PA)	DP3 (PA)	DP4 (PA)	DP5 (PA)	DP6 (PA)	DP7 (PA)	DP8 (PA)	DP9 (PA)
0.	1.362E+04	4.033E+03	4.033E+03	-1.269E+01	-1.269E+01	-9.80DE+03	-9.80DE+03	-1.352E+04	-1.382E+04
1.000E+02	7.949E+03	2.314E+03	2.314E+03	2.750E+02	2.750E+02	-4.826E+03	-4.826E+03	-7.049E+03	-7.049E+03
2.000E+02	3.590E+03	1.211E+03	1.211E+03	3.253E+02	3.253E+02	-2.437E+03	-2.437E+03	-3.506E+03	-3.506E+03
3.000E+02	1.672E+03	6.073E+02	6.073E+02	2.813E+02	2.813E+02	-1.225E+03	-1.225E+03	-1.672E+03	-1.672E+03
4.000E+02	7.523E+02	3.115E+02	3.115E+02	2.213E+02	2.213E+02	-5.797E+02	-5.797E+02	-7.323E+02	-7.323E+02

MD (KG/S)	T1 (K)	T2 (K)	T3 (K)	T4 (K)	T5 (K)	T6 (K)	T7 (K)	T8 (K)	T9 (K)
1.450E-02	1.548E+01	1.529E+01	1.529E+01	1.529E+01	1.529E+01	1.529E+01	1.529E+01	1.529E+01	1.529E+01
7.698E-03	3.024E+01	2.756E+01	2.756E+01	2.756E+01	2.756E+01	3.006E+01	3.006E+01	3.006E+01	3.006E+01
3.761E-03	6.072E+01	5.031E+01	5.031E+01	5.031E+01	5.031E+01	6.054E+01	6.054E+01	6.054E+01	6.054E+01
1.679E-03	1.272E+02	9.266E+01	9.266E+01	9.266E+01	9.266E+01	1.270E+02	1.270E+02	1.270E+02	1.270E+02
6.489E-04	2.904E+02	1.716E+02	1.716E+02	1.716E+02	1.716E+02	2.902E+02	2.902E+02	2.902E+02	2.902E+02

TS (K)	TA (K)	PSH (W)	QS (W)	FF	IFAIL	LAMS	LAMA	REMIN	REMAX
1.527E+01	1.529E+01	1.392E+01	1.392E+01	7.130E-06	0.	2.332E+00	2.332E+00	3.909E+05	7.130E+05
2.739E+01	3.021E+01	7.388E+00	1.074E+02	3.827E-06	0.	2.823E+00	2.853E+00	1.431E+05	3.786E+05
4.998E+01	6.084E+01	3.609E+00	2.036E+02	9.485E-06	0.	3.480E+00	3.556E+00	4.755E+04	1.850E+05
9.222E+01	1.274E+02	1.611E+00	3.016E+02	3.161E-06	0.	4.374E+00	4.532E+00	1.412E+04	6.262E+04
1.712E+02	2.905E+02	6.228E-01	4.006E+02	7.027E-06	0.	5.663E+00	6.002E+00	3.466E+03	3.194E+04

OUTTS
DATE & TIME PRINTED: WEDNESDAY, NOVEMBER 6, 1985 @ 16:37:57.

TASK 1.3: SEE TABLE 6.1

CIRCUIT: 70K FAN: BEHIND THE STAGE

CIRCUIT2-K?	FALSE	P (PA)	2.000E+06	LS (M)	1.80	N23	0	ZE23	0.8
F	1	CP (J/KG K)	5.2E+03	DS (M)	6.0E-03	N45	0	ZE45	0.8
QA (W)	????QA	DHF (M)	45	DSC (M)	0.11	N67	0	ZE67	0.8
QT1 (W)	0	EF	0.40	LA (M)	1.80	N89	0	ZE89	0.8
QT2 (W)	0	M (KG/MOL)	4.003E-03	DA (M)	6.0E-03	L23 (M)	0.00	LACT	0.07
QFC (W)	0	R (J/MOL K)	8.314	DAC (M)	0.11	L45 (M)	0.00		
		G (M/S**2)	9.81	LT (M)	7.0	L67 (M)	0.00		
		SM	1.000E-03	DT1 (M)	1.270E-02	L89 (M)	0.00		
		SP	1.000E+05	DT2 (M)	1.270E-02				

QA (W)	DP1 (PA)	DP2 (PA)	DP3 (PA)	DP4 (PA)	DP5 (PA)	DP6 (PA)	DP7 (PA)	DP8 (PA)	DP9 (PA)
0.	-3.849E+03	-1.093E+03	-1.093E+03	-4.848E+00	-4.848E+00	2.761E+03	2.761E+03	3.849E+03	3.849E+03
2.000E+02	-2.837E+03	-9.364E+02	-9.364E+02	-1.317E+02	-1.317E+02	2.161E+03	2.161E+03	2.837E+03	2.837E+03
4.000E+02	-1.993E+03	-7.617E+02	-7.617E+02	-2.262E+02	-2.262E+02	1.618E+03	1.618E+03	1.993E+03	1.993E+03
6.000E+02	-1.490E+03	-6.739E+02	-6.739E+02	-3.056E+02	-3.056E+02	1.279E+03	1.279E+03	1.490E+03	1.490E+03
8.000E+02	-1.179E+03	-6.391E+02	-6.391E+02	-3.801E+02	-3.801E+02	1.059E+03	1.059E+03	1.179E+03	1.179E+03

MD (KG/S)	T1 (K)	T2 (K)	T3 (K)	T4 (K)	T5 (K)	T6 (K)	T7 (K)	T8 (K)	T9 (K)
3.970E-03	5.513E+01	5.531E+01	5.531E+01	5.531E+01	5.531E+01	5.531E+01	5.531E+01	5.531E+01	5.531E+01
2.686E-03	7.483E+01	8.933E+01	8.933E+01	8.933E+01	8.933E+01	7.501E+01	7.501E+01	7.501E+01	7.501E+01
1.676E-03	1.066E+02	1.526E+02	1.526E+02	1.526E+02	1.526E+02	1.068E+02	1.068E+02	1.068E+02	1.068E+02
1.089E-03	1.425E+02	2.487E+02	2.487E+02	2.487E+02	2.487E+02	1.427E+02	1.427E+02	1.427E+02	1.427E+02
7.277E-04	1.802E+02	3.918E+02	3.918E+02	3.918E+02	3.918E+02	1.804E+02	1.804E+02	1.804E+02	1.804E+02

TS (K)	TA (K)	PSH (W)	QS (W)	FF	IFAIL	LAMS	LAMA	REMIN	REMAX
5.512E+01	5.531E+01	3.810E+00	3.810E+00	4.896E-06	0.	3.480E+00	3.481E+00	5.276E+04	1.956E+05
7.452E+01	8.961E+01	2.578E+00	2.026E+02	3.597E-10	0.	3.690E+00	3.969E+00	2.742E+04	1.323E+05
1.060E+02	1.531E+02	1.609E+00	4.016E+02	2.553E-07	0.	4.443E+00	4.626E+00	1.275E+04	8.255E+04
1.418E+02	2.492E+02	1.045E+00	6.010E+02	3.370E-08	0.	5.001E+00	5.321E+00	6.333E+03	5.363E+04
1.794E+02	3.923E+02	6.983E-01	8.007E+02	5.771E-10	0.	5.563E+00	6.053E+00	3.294E+03	3.582E+04

OUTTS
DATE & TIME PRINTED: THURSDAY, NOVEMBER 7, 1985 @ 17:03:15.

CIRCUIT: 70K FAN: IN FRONT OF THE STAGE

CIRCUIT2=K?	FALSE	P (PA)	2.000E+06	LS (M)	1.80	N25	0	ZE25	0.8
F	-1	CP (J/KG K)	5.2E+03	DS (M)	6.0E-03	N45	0	ZE45	0.8
QA (W)	????.0	DHF (M)	45	DSC (M)	0.11	N67	0	ZE67	0.8
QT1 (W)	0	EF	1.46	LA (M)	1.80	N89	0	ZE89	0.8
QT2 (W)	1	M (KG/MOL)	4.013E-03	DA (M)	6.0E-03	L25 (M)	0.10	LACT	0.07
QFC (W)	0	R (J/MOL K)	8.314	DAL (M)	0.11	L45 (M)	0.00		
		G (M/S**2)	9.81	LT (M)	7.0	L67 (M)	0.00		
		SN	1.000E-04	DT1 (M)	1.270E-02	L89 (M)	0.00		
		SP	1.000E+05	DT2 (M)	1.270E-02				

QA (W)	DP1 (PA)	DP2 (PA)	DP3 (PA)	DP4 (PA)	DP5 (PA)	DP6 (PA)	DP7 (PA)	DP8 (PA)	DP9 (PA)
0.	3.849E+03	1.287E+03	1.287E+03	-2.385E-01	-2.385E-01	-2.762E+03	-2.762E+03	-3.849E+03	-3.849E+03
2.000E+02	2.337E+03	7.725E+02	7.725E+02	2.385E+02	2.385E+02	-1.686E+03	-1.686E+03	-2.337E+03	-2.337E+03
4.000E+02	1.265E+03	5.156E+02	5.156E+02	3.125E+02	3.125E+02	-9.365E+02	-9.365E+02	-1.265E+03	-1.265E+03
6.000E+02	5.959E+02	3.493E+02	3.493E+02	2.977E+02	2.977E+02	-4.667E+02	-4.667E+02	-5.959E+02	-5.959E+02
0.	0.	0.	0.	0.	0.	0.	0.	0.	0.

MD (KG/S)	T1 (K)	T2 (K)	T3 (K)	T4 (K)	T5 (K)	T6 (K)	T7 (K)	T8 (K)	T9 (K)
3.975E-03	5.531E+01	5.513E+01	5.513E+01	5.513E+01	5.513E+01	5.513E+01	5.513E+01	5.513E+01	5.513E+01
2.396E-03	9.103E+01	7.480E+01	7.480E+01	7.480E+01	7.480E+01	9.085E+01	9.085E+01	9.085E+01	9.085E+01
1.246E-03	1.664E+02	1.065E+02	1.065E+02	1.065E+02	1.065E+02	1.682E+02	1.682E+02	1.682E+02	1.682E+02
5.388E-04	3.562E+02	1.424E+02	1.424E+02	1.424E+02	1.424E+02	3.566E+02	3.566E+02	3.566E+02	3.566E+02
0.	0.	0.	0.	0.	0.	0.	0.	0.	0.

TS (K)	TA (K)	PSH (W)	QS (W)	FF	IFAIL	LAMS	LAMA	REMIN	REMAX
5.512E+01	5.513E+01	3.814E+00	3.814E+00	5.946E-08	0.	3.479E+00	3.479E+00	5.291E+04	1.956E+05
7.449E+01	9.113E+01	2.299E+00	2.023E+02	1.183E-07	0.	3.979E+00	4.069E+00	2.424E+04	1.179E+05
1.059E+02	1.687E+02	1.196E+00	4.012E+02	3.279E-08	0.	4.714E+00	4.962E+00	8.963E+03	6.133E+04
1.417E+02	3.569E+02	5.170E-01	6.005E+02	5.287E-07	0.	5.756E+00	6.372E+00	2.569E+03	2.651E+04
0.	0.	0.	0.	0.	0.	0.	0.	0.	0.

CIRCUIT: 20K FAN: BEHIND THE STAGE

CIRCUIT2?K??TRUE		F (PA)	2.000E+06	LS (M)	LS	N25	1	ZE23	0.8
F	1	CP (J/KG K)	0.0E+03	DS (M)	DS	N45	1	ZE45	0.8
QA (W)	60	DHF (M)	45	DSC (M)	7.10	N67	1	ZE67	0.8
QT1 (W)	5	EF	0.50	LA (M)	LA	N89	1	ZE89	0.8
QT2 (W)	5	M (KG/MOL)	4.003E-03	DA (M)	DA	L23 (M)	0.16	LACT	0.07
QFC (W)	5	R (J/MOL K)	8.314	DAC (M)	0.10	L45 (M)	0.50		
		G (M/S**2)	9.81	LT (M)	7.0	L67 (M)	0.50		
		S4	1.000E-03	DT1 (M)	1.27LE-02	L89 (M)	0.50		
		SP	1.000E+15	DT2 (M)	1.270E-02				

DS=DA (M)	DP1 (PA)	DP2 (PA)	DP3 (PA)	DP4 (PA)	DP5 (PA)	DP6 (PA)	DP7 (PA)	DP8 (PA)	DP9 (PA)
6.000E-03	-9.765E+03	-4.240E+03	-3.326E+03	-1.626E+03	-5.139E+02	4.828E+03	6.246E+03	7.654E+03	9.065E+03
8.000E-03	-6.798E+03	-6.189E+03	-5.453E+03	-1.236E+03	-1.212E+02	2.594E+03	3.667E+03	7.728E+03	8.798E+03
1.000E-02	-6.616E+03	-7.491E+03	-7.044E+03	-6.265E+02	5.037E+01	1.177E+03	1.785E+03	8.011E+03	8.618E+03
1.200E-02	-8.498E+03	-8.013E+03	-7.771E+03	-2.724E+02	5.836E+01	5.622E+02	8.641E+02	8.177E+03	8.498E+03

MD (KG/S)	T1 (K)	T2 (K)	T3 (K)	T4 (K)	T5 (K)	T6 (K)	T7 (K)	T8 (K)	T9 (K)
6.908E-03	2.331E+01	2.527E+01	2.527E+01	2.515E+01	2.515E+01	2.370E+01	2.370E+01	2.358E+01	2.358E+01
1.157E-02	2.405E+01	2.528E+01	2.528E+01	2.520E+01	2.520E+01	2.434E+01	2.434E+01	2.427E+01	2.427E+01
1.418E-02	2.456E+01	2.559E+01	2.559E+01	2.553E+01	2.553E+01	2.483E+01	2.483E+01	2.477E+01	2.477E+01
1.524E-02	2.491E+01	2.588E+01	2.588E+01	2.582E+01	2.582E+01	2.517E+01	2.517E+01	2.511E+01	2.511E+01

TS (K)	TA (K)	PSH (W)	QS (W)	FF	LS=LA (M)	LAMS	LAMA	REMIN	REMAX
2.324E+01	2.520E+01	6.099E+00	8.110E+01	2.677E-06	2.443E+00	3.333E+00	3.362E+00	1.412E+05	3.408E+05
2.385E+01	2.534E+01	1.021E+01	8.521E+01	1.090E-06	1.999E+00	1.959E+00	1.973E+00	2.365E+05	4.201E+05
2.419E+01	2.578E+01	1.252E+01	8.752E+01	1.015E-06	1.692E+00	1.334E+00	1.343E+00	2.879E+05	4.198E+05
2.434E+01	2.621E+01	1.346E+01	8.846E+01	2.719E-07	1.466E+00	9.853E-01	9.934E-01	3.076E+05	3.760E+05

OUTTS
DATE & TIME PRINTED: THURSDAY, NOVEMBER 7, 1985 @ 20:55:11.

TASK 2: TABLE 6.5 BLOCK 2

CIRCUIT: 70K FAN: BEHIND THE STAGE

CIRCUIT2OK?	FALSE	P (PA)	2.0[illegible]E+06	LS (M)	LS	N25	1
F	1	CP (J/KG K)	1.2E+03	DS (M)	DS	N45	1
QA (W)	125	DHF (M)	45	DSC (M)	3.12	N67	1
QT1 (W)	15	FF	1.5[illegible]	LA (M)	LA	N89	2
QT2 (W)	10	M (KG/MOL)	4.003E-03	DA (M)	DA	L25 (M)	3.36
QFC (W)	5	R (J/MOL K)	8.314	DAC (M)	3.12	L45 (M)	3.36
		G (M/S**2)	9.81	LT (M)	7.0	L67 (M)	3.36
		SM	1.[illegible]E-05	DT1 (M)	1.27[illegible]E-02	L89 (M)	3.36
		SP	1.[illegible]E+05	DT2 (M)	1.27[illegible]E-02		

ZE23	0.6
ZE45	0.8
ZE67	0.8
ZE89	0.8
LACT	0.07

DS=DA (M)	DP1 (PA)	DP2 (PA)	DP3 (PA)	DP4 (PA)	DP5 (PA)	DP6 (PA)	DP7 (PA)	DP8 (PA)	DP9 (PA)
6.000E-03	-3.142E+03	-1.473E+03	-1.044E+03	-6.755E+02	-1.706E+02	1.857E+03	2.290E+03	2.599E+03	3.142E+03
8.000E-03	-3.152E+03	-2.096E+03	-1.735E+03	-4.555E+02	-6.512E+01	1.837E+03	1.469E+03	2.634E+03	3.132E+03
1.000E-02	-3.113E+03	-2.646E+03	-2.420E+03	-2.562E+02	5.379E+00	5.111E+02	7.520E+02	2.705E+03	3.113E+03
1.200E-02	-3.096E+03	-2.895E+03	-2.773E+03	-9.748E+01	4.451E+01	2.519E+02	5.849E+02	2.892E+03	3.096E+03

MD (KG/S)	T1 (K)	T2 (K)	T3 (K)	T4 (K)	T5 (K)	T6 (K)	T7 (K)	T8 (K)	T9 (K)
1.902E-03	6.730E+01	8.213E+01	8.213E+01	8.112E+01	8.112E+01	6.899E+01	6.899E+01	6.798E+01	6.798E+01
3.648E-03	6.764E+01	7.546E+01	7.546E+01	7.493E+01	7.493E+01	6.866E+01	6.866E+01	6.837E+01	6.807E+01
4.845E-03	6.809E+01	7.402E+01	7.402E+01	7.362E+01	7.362E+01	6.836E+01	6.836E+01	6.640E+01	6.640E+01
5.390E-03	6.862E+01	7.396E+01	7.396E+01	7.360E+01	7.360E+01	6.932E+01	6.932E+01	6.696E+01	6.696E+01

TS (K)	TA (K)	PSH (W)	QS (W)	FF	LS=LA (M)	LAMS	LAMA	REMIN	REMAX
6.728E+01	6.113E+01	1.679E+00	1.467E+02	3.895E-06	2.952E+00	6.713E+00	6.853E+00	2.035E+04	9.368E+04
6.747E+01	7.506E+01	3.221E+00	1.482E+02	2.429E-08	2.399E+00	3.832E+00	3.877E+00	4.036E+04	1.348E+05
6.760E+01	7.401E+01	4.278E+00	1.493E+02	4.560E-07	2.030E+00	2.563E+00	2.589E+00	5.486E+04	1.432E+05
6.765E+01	7.436E+01	4.758E+00	1.494E+02	2.223E-09	1.759E+00	1.879E+00	1.899E+00	6.134E+04	1.327E+05

OUTTS
DATE & TIME PRINTED: THURSDAY, NOVEMBER 14, 1985 @ 12:05:00.

CIRCUIT: 20K FAN: BEHIND THE STAGE

CIRCUIT20K??TRUE		P (PA)	4.000E+06	LS (M)	LS	N23 1	ZE23 0.8
F	1	CP (J/KG K)	6.0E+03	DS (M)	DS	N45 1	ZE45 0.8
QA (W)	60	DHF (M)	20	DSC (M)	0.10	N67 1	ZE67 0.8
QT1 (W)	5	EF	0.50	LA (M)	LA	N89 1	ZE89 0.8
QT2 (W)	5	M (KG/MOL)	4.003E-03	DA (M)	DA	L23 (M) 0.16	LACT 0.07
QFC (W)	5	R (J/MOL K)	8.314	DAC (M)	0.10	L45 (M) 0.50	
		G (M/S**2)	9.81	LT (M)	7.0	L67 (M) 0.50	
		SM	1.000E-03	DT1 (M)	1.270E-02	L89 (M) 0.50	
		SP	1.000E+05	DT2 (M)	1.27LE-02		

DS=DA (M)	DP1 (PA)	DP2 (PA)	DP3 (PA)	DP4 (PA)	DP5 (PA)	DP6 (PA)	DP7 (PA)	DP8 (PA)	DP9 (PA)
6.000E-03	-8.210E+03	-3.345E+03	-2.622E+03	-1.405E+03	-2.278E+02	4.821E+03	5.940E+03	7.096E+03	8.210E+03
8.000E-03	-8.058E+03	-5.057E+03	-4.461E+03	-9.847E+02	-9.821E+01	2.965E+03	3.826E+03	7.200E+03	8.058E+03
1.000E-02	-7.943E+03	-6.452E+03	-6.081E+03	-5.343E+02	-1.115E+01	1.504E+03	2.015E+03	7.433E+03	7.943E+03
1.200E-02	-7.860E+03	-7.157E+03	-6.947E+03	-2.518E+02	3.374E+01	7.469E+02	1.026E+03	7.560E+03	7.860E+03

MD (KG/S)	T1 (K)	T2 (K)	T3 (K)	T4 (K)	T5 (K)	T6 (K)	T7 (K)	T8 (K)	T9 (K)
8.947E-03	2.293E+01	2.440E+01	2.440E+01	2.430E+01	2.430E+01	2.318E+01	2.318E+01	2.309E+01	2.309E+01
1.516E-02	2.339E+01	2.428E+01	2.428E+01	2.422E+01	2.422E+01	2.356E+01	2.356E+01	2.351E+01	2.351E+01
1.907E-02	2.373E+01	2.445E+01	2.445E+01	2.441E+01	2.441E+01	2.388E+01	2.388E+01	2.384E+01	2.384E+01
2.087E-02	2.399E+01	2.465E+01	2.465E+01	2.461E+01	2.461E+01	2.413E+01	2.413E+01	2.409E+01	2.409E+01

TS (K)	TA (K)	PSH (W)	QS (W)	FF	LS=LA (M)	LAMS	LAMA	REMIN	REMAX
2.287E+01	2.435E+01	3.511E+00	7.851E+01	6.631E-08	2.443E+00	3.159E+00	3.181E+00	1.865E+05	3.011E+05
2.322E+01	2.434E+01	5.947E+00	8.095E+01	5.079E-06	1.999E+00	1.851E+00	1.861E+00	3.168E+05	3.825E+05
2.344E+01	2.462E+01	7.483E+00	8.248E+01	5.727E-09	1.692E+00	1.253E+00	1.259E+00	3.970E+05	3.851E+05
2.355E+01	2.492E+01	8.189E+00	8.319E+01	3.349E-06	1.466E+00	9.219E-01	9.277E-01	4.325E+05	3.511E+05

OUTTS
DATE & TIME PRINTED: THURSDAY, NOVEMBER 14, 1985 @ 12:19:04.

CIRCUIT: 70K FAN: BEHIND THE STAGE

CIRCUIT20K?	FALSE	P (PA)	4.000E+06	LS (M)	LS	N23	1	ZE23	0.8
F	1	CP (J/KG K)	5.2E+03	DS (M)	DS	N45	1	ZE45	0.8
QA (W)	120	DHF (M)	20	DSC (M)	0.12	N67	1	ZE67	0.8
QT1 (W)	10	EF	0.50	LA (M)	LA	N89	2	ZE89	0.8
QT2 (W)	10	M (KG/MOL)	4.003E-03	DA (M)	DA	L23 (M)	0.38	LACT	0.07
QFC (W)	5	R (J/MOL K)	8.314	DAC (M)	0.12	L45 (M)	0.50		
		G (M/S**2)	9.81	LT (M)	7.0	L67 (M)	0.50		
		SM	1.000E-03	DT1 (M)	1.270E-02	L89 (M)	0.50		
		SP	1.000E+05	DT2 (M)	1.270E-02				

DS=DA (M)	DP1 (PA)	DP2 (PA)	DP3 (PA)	DP4 (PA)	DP5 (PA)	DP6 (PA)	DP7 (PA)	DP8 (PA)	DP9 (PA)
6.000E-03	-2.801E+03	-1.259E+03	-8.949E+02	-5.619E+02	-1.319E+02	1.639E+03	2.016E+03	2.308E+03	2.801E+03
8.000E-03	-2.794E+03	-1.831E+03	-1.525E+03	-4.189E+02	-6.361E+01	9.712E+02	1.302E+03	2.331E+03	2.794E+03
1.000E-02	-2.781E+03	-2.327E+03	-2.135E+03	-2.311E+02	-1.189E+01	4.673E+02	6.750E+02	2.478E+03	2.781E+03
1.200E-02	-2.765E+03	-2.567E+03	-2.460E+03	-9.917E+01	2.143E+01	2.290E+02	3.439E+02	2.592E+03	2.765E+03

MD (KG/S)	T1 (K)	T2 (K)	T3 (K)	T4 (K)	T5 (K)	T6 (K)	T7 (K)	T8 (K)	T9 (K)
2.622E-03	6.722E+01	7.793E+01	7.793E+01	7.720E+01	7.720E+01	6.840E+01	6.840E+01	6.767E+01	6.767E+01
4.926E-03	6.747E+01	7.321E+01	7.321E+01	7.282E+01	7.282E+01	6.813E+01	6.813E+01	6.774E+01	6.774E+01
6.508E-03	6.782E+01	7.218E+01	7.218E+01	7.188E+01	7.188E+01	6.833E+01	6.833E+01	6.804E+01	6.804E+01
7.248E-03	6.823E+01	7.215E+01	7.215E+01	7.189E+01	7.189E+01	6.870E+01	6.870E+01	6.844E+01	6.844E+01

TS (K)	TA (K)	PSH (W)	QS (W)	FF	LS=LA (M)	LAMS	LAMA	REMIN	REMAX
6.720E+01	7.721E+01	1.029E+00	1.460E+02	5.874E-08	2.932E+00	6.294E+00	6.391E+00	2.886E+04	8.819E+04
6.731E+01	7.295E+01	1.933E+00	1.469E+02	8.830E-08	2.399E+00	3.607E+00	3.639E+00	5.610E+04	1.242E+05
6.739E+01	7.222E+01	2.554E+00	1.476E+02	3.112E-07	2.030E+00	2.415E+00	2.434E+00	7.471E+04	1.313E+05
6.742E+01	7.253E+01	2.844E+00	1.478E+02	6.146E-08	1.759E+00	1.771E+00	1.785E+00	8.321E+04	1.219E+05

Appendix 10.5 The stainless steel tubes in the measuring unit

In this appendix is shown how the dimensions of the stainless steel tubes inside the measuring unit were determined.
Usually there exists a temperature gradient over the tube wall ($T_{w1} \neq T_{w2}$, see Fig.A5.1).

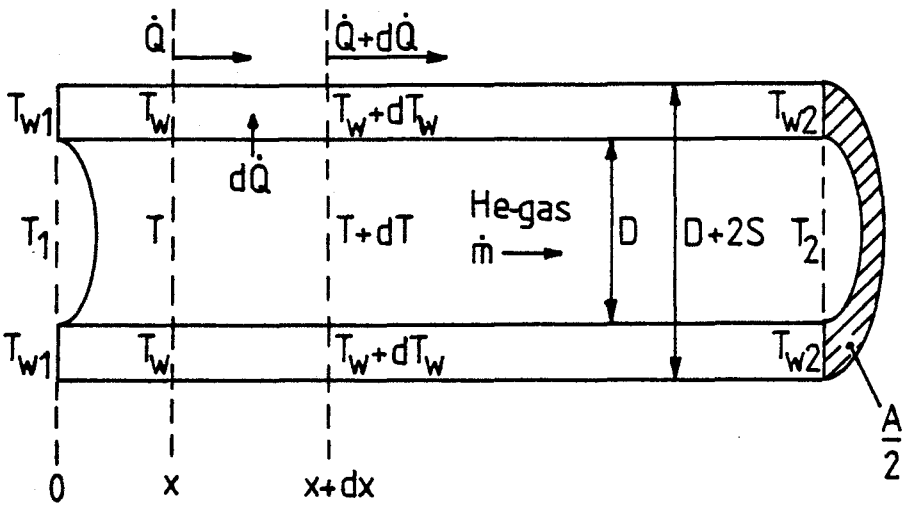

Fig.A5.1 Cross-sectional view of a stainless steel tube inside the measuring unit. The inner diameter D, the wall thickness S and the area A have been indicated, as well as the distance x, the gas temperature T, the wall temperature T_w, the conductive heat flow $\dot{Q}$ and the mass flow $\dot{m}$.

If the left end of the tube has been fixed to a heat exchanger ($T_{w1}=T_{he}$), then the dimensions of the tube should be such, that $T_{w2} \approx T_2$. In this way a thermometer, fixed on the outside at the right end of the tube wall, will measure the gas temperature T_2. Otherwise, if the right side of the tube has been fixed to a heat exchanger ($T_{w2}=T_{he}$), the tube design should be such that $T_{w1} \approx T_1$.
The heat conduction through the area A of the wall is given by

$$\dot{Q}(x) = -\lambda(T_w)\, A\, \frac{dT_w}{dx} ,$$

where λ is the thermal conductivity of the tube wall.

Differentiation with respect to x yields

$$d\dot{Q} = -A \frac{d}{dx}[\lambda(T_w) \frac{dT_w}{dx}] dx . \qquad (A5\text{-}1)$$

The conductive heat exchange between the gas and the tube wall is described by

$$d\dot{Q} = \alpha(T) (T-T_w) \pi D dx \qquad (A5\text{-}2)$$

and the first law of thermodynamics for an open system yields

$$d\dot{Q} = -\dot{m} dh = -\dot{m} c_p dT . \qquad (A5\text{-}3)$$

Eliminating $d\dot{Q}$ we find from (A5-1) and (A5-2)

$$-A \frac{d}{dx}[\lambda(T_w) \frac{dT_w}{dx}] = \alpha(T) \pi D (T-T_w), \qquad (A5\text{-}4)$$

from (A5-1) and (A5-3)

$$\frac{A}{\dot{m}c_p} \frac{d}{dx}[\lambda(T_w) \frac{dT_w}{dx}] = \frac{dT}{dx} \qquad (A5\text{-}5)$$

and from (A5-2) and (A5-3)

$$- \frac{\alpha(T) \pi D}{\dot{m} c_p} (T-T_w) = \frac{dT}{dx} . \qquad (A5\text{-}6)$$

The equations (A5-4) to (A5-6) describe the stationary state behaviour of T_w and T as functions of x. From now on $\lambda(T_w)$ and $\alpha(T)$ will be regarded as being temperature independent. This is allowed even at temperatures between 150K and 300K: $\lambda(150K<T<300K) \approx 14W/(m\ K)$ and $\alpha(T) \sim T^{0.11}$ (see appendix 10.2 and equation (A3-5) respectively).
Differentiation of (A5-6) with respect to x and substitution of the expression for dT_w/dx thus found in (A5-5) yields

$$\frac{A\lambda}{\alpha \pi D} \frac{d^3T}{dx^3} + \frac{A\lambda}{\dot{m} c_p} \frac{d^2T}{dx^2} - \frac{dT}{dx} = 0. \qquad (A5\text{-}7)$$

Differentiation of (A5-4) with respect to x and substitution of (A5-5) results in a differential equation in T_w, which is identical with (A5-7).

Both differential equations suggest solutions of the form $e^{\pm x/L_{ch}}$ where L_{ch} represents a certain characteristic length, which should be small in comparison with the lengths of the stainless steel tubes (see Fig.A5.2).

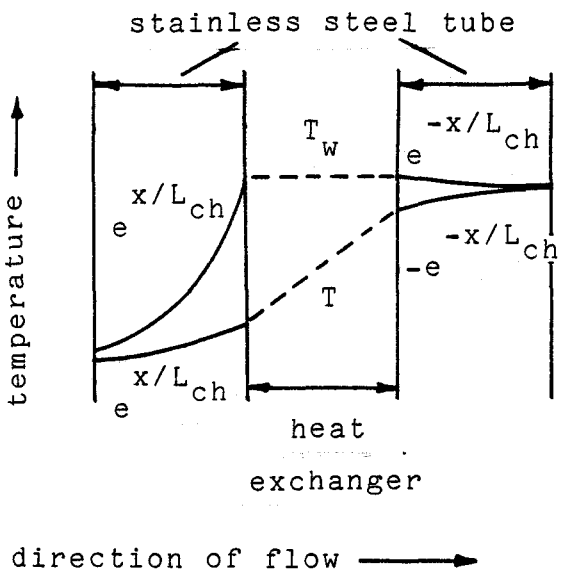

Fig.A5.2 The way in which the wall temperature T_w of the stainless steel tubes and the gas temperature T vary in the direction of the flow

It is convenient to write (A5-7) in a dimensionless form via

$$T = t_o \tau \qquad \text{and} \qquad x = l_o \xi \; : \qquad \text{(A5-8)}$$

τ and ξ are the dimensionless temperature and distance respectively. When l_o is chosen to be

$$l_o := \frac{A\lambda}{\dot{m}\, c_p} \; , \qquad \text{(A5-9)}$$

(A5-7) is reduced to

$$C \frac{d^3\tau}{d\xi^3} + \frac{d^2\tau}{d\xi^2} - \frac{d\tau}{d\xi} = 0 \qquad \text{where} \qquad \text{(A5-10)}$$

$$C = \frac{(\dot{m}c_p)^2}{\alpha \pi D\, A\lambda} \approx \frac{\dot{m}^{1.2}\, c_p^{\,2}\, D^{0.8}}{11.4\, T^{0.11}\, \pi^2\, S(D+S)} \quad \text{(see (A3-5))}.$$

Substitution of $\tau = e^{a\xi}$ in (A5-10) yields

$$a_{1,2} = \frac{-1 \pm (1 + 4C)^{1/2}}{2C} \; . \qquad \text{(A5-11)}$$

With $\dot{m}$=0.1g/s, c_p=5.2kJ/(kg K), T=300K, λ=14W/(m K), D=8mm and S=1mm it can be shown that C>3.4 10^2.
The characteristic length L_{ch} is found by equating $e^{\pm x/L_{ch}}$ and $e^{a\xi} \approx e^{\pm\xi/\sqrt{C}}$:

$$L_{ch} = \frac{x}{\xi}\sqrt{C} = l_o\sqrt{C} = \left(\frac{A\lambda}{\alpha\,\pi D}\right)^{1/2} \qquad \text{(A5-12)}$$

$$\approx \left(\frac{\lambda\, S(S+D)\, D^{0.8}}{11.4\, T^{0.11}\, \dot{m}^{0.8}}\right)^{1/2}.$$

Stainless steel tubes have been used with S=0.3mm, D=7.4mm and a length of 0.1m.
With T=20K, $\dot{m}$=12g/s and λ=2W/(m K) it is found that L_{ch}=0.4mm.
Taking T=150K, $\dot{m}$=0.5g/s and λ=14W/(m K) we find L_{ch}=4mm.
A tube length of 0.1m should therefore be sufficient in protecting gas temperature measurements against influences from a heat exchanger.